WE-Heraeus Physics School

QCD – Old Challenges and New Opportunities

Bad Honnef, Sept 24–30, 2017

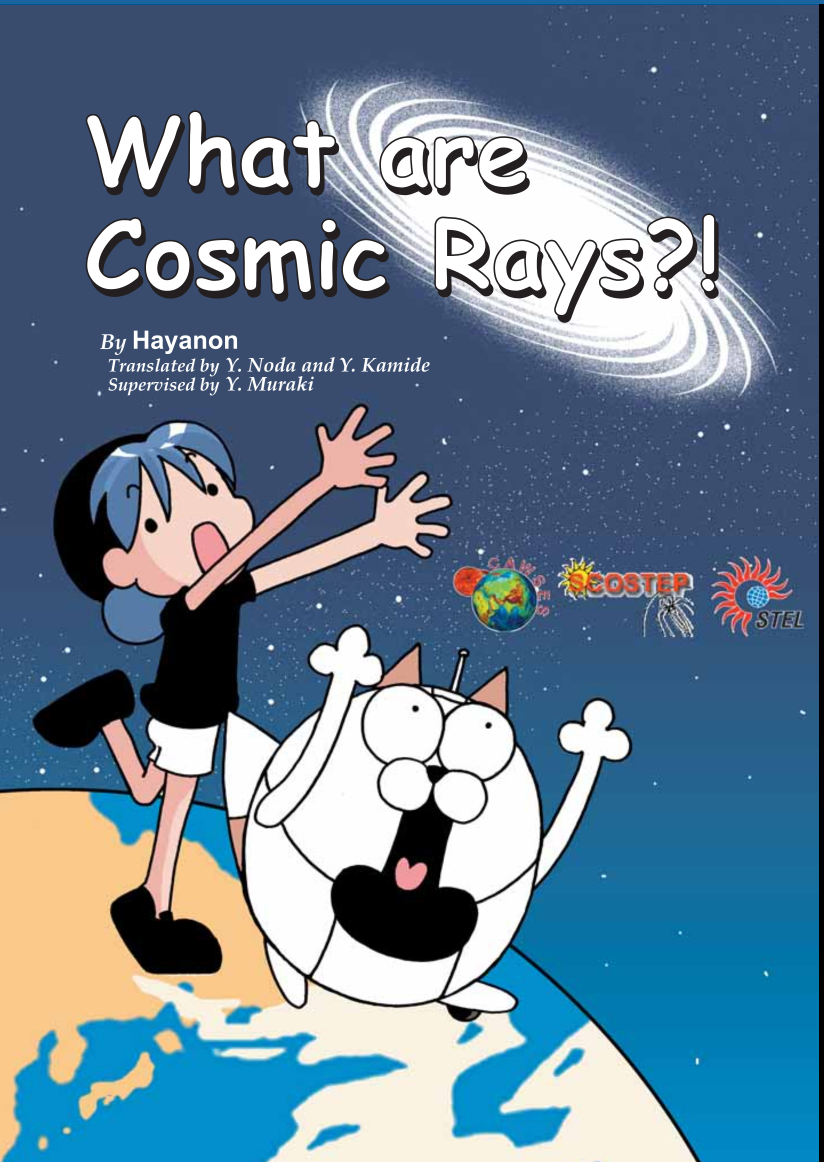

QCD processes in Cosmic Rays air showers

Alessia Tricomi
University and INFN Catania, Italy

- Cosmic Rays
- Extensive air showers
- Interplay between CR Physics and accelerators
- The LHCf experiments

What are Cosmics Rays

Electromagnetic radiation: Radio
IR
Visible
UV
X
γ

Astronomy
Astrophysics

Charged particles: p
e^-
e^+
$\bar{p}$
Nuclei
Antinuclei?
???

Subjects of this talk

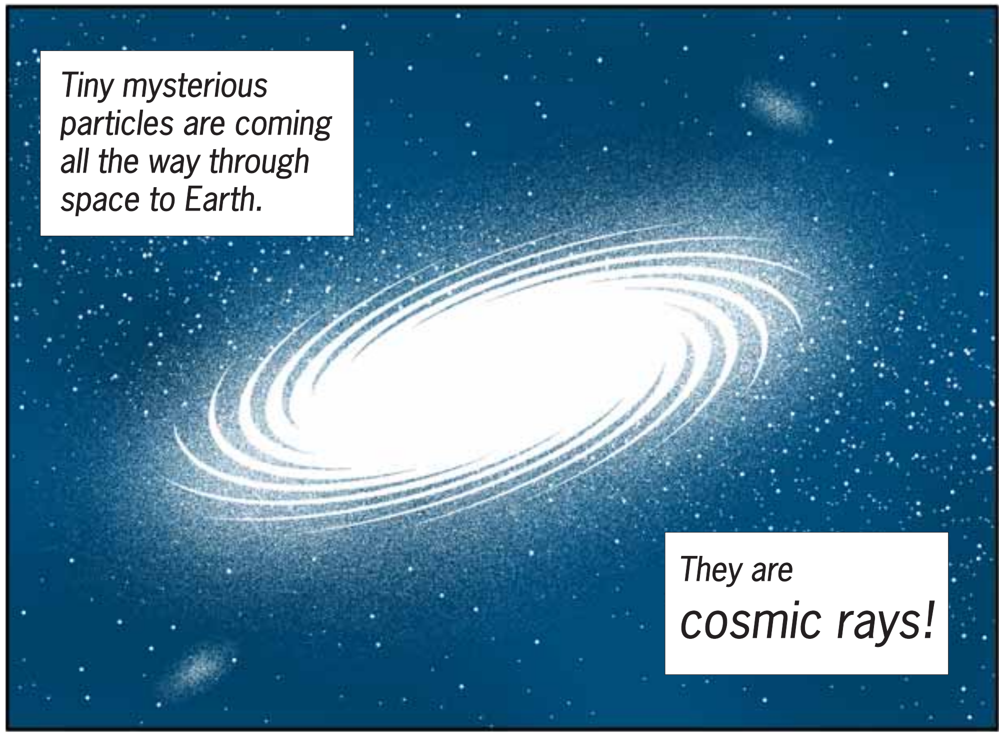

Neutral particles: ν
???

Brief history of Cosmic Rays Detecton

1912 Hess discovers cosmic rays

1925 Quasi-isotropy

1938 Auger discover
extensive air show
(E = 10^{15} eV!)

1946 First experiment
to detect EAS

Nowadays Giant EAS array detectors
based on hybrid tecnique

Primary cosmic rays

$$\Phi \propto E^{-2.7}$$

Deviations from this power law

- knee (4.10^{15} eV)
- ankle (5.10^{18} eV)

Very different techniques are necessary to cover these huge differences of:

- Fluxes
- Energies

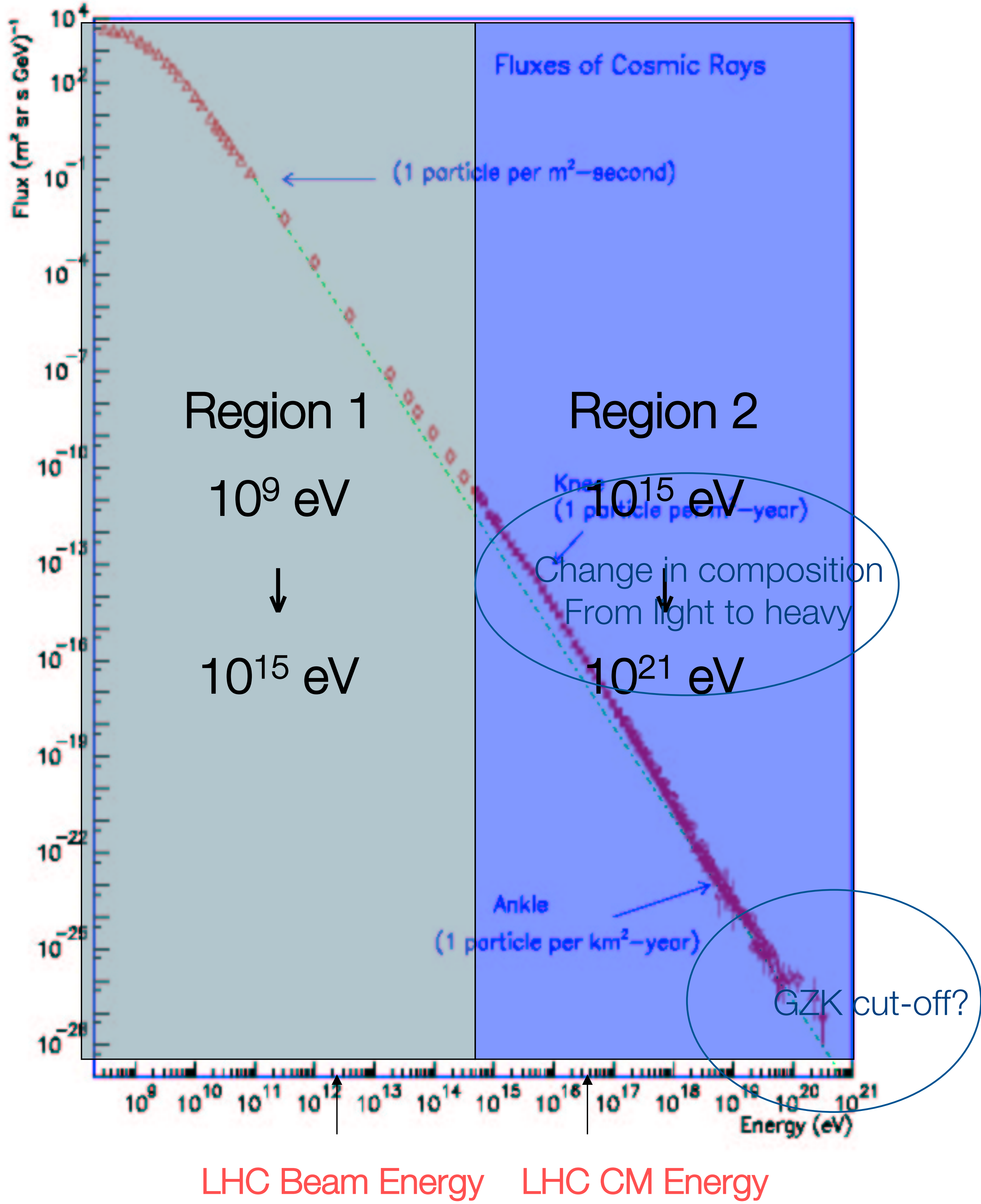

CR Detection

Direct measurements

Indirect measurements

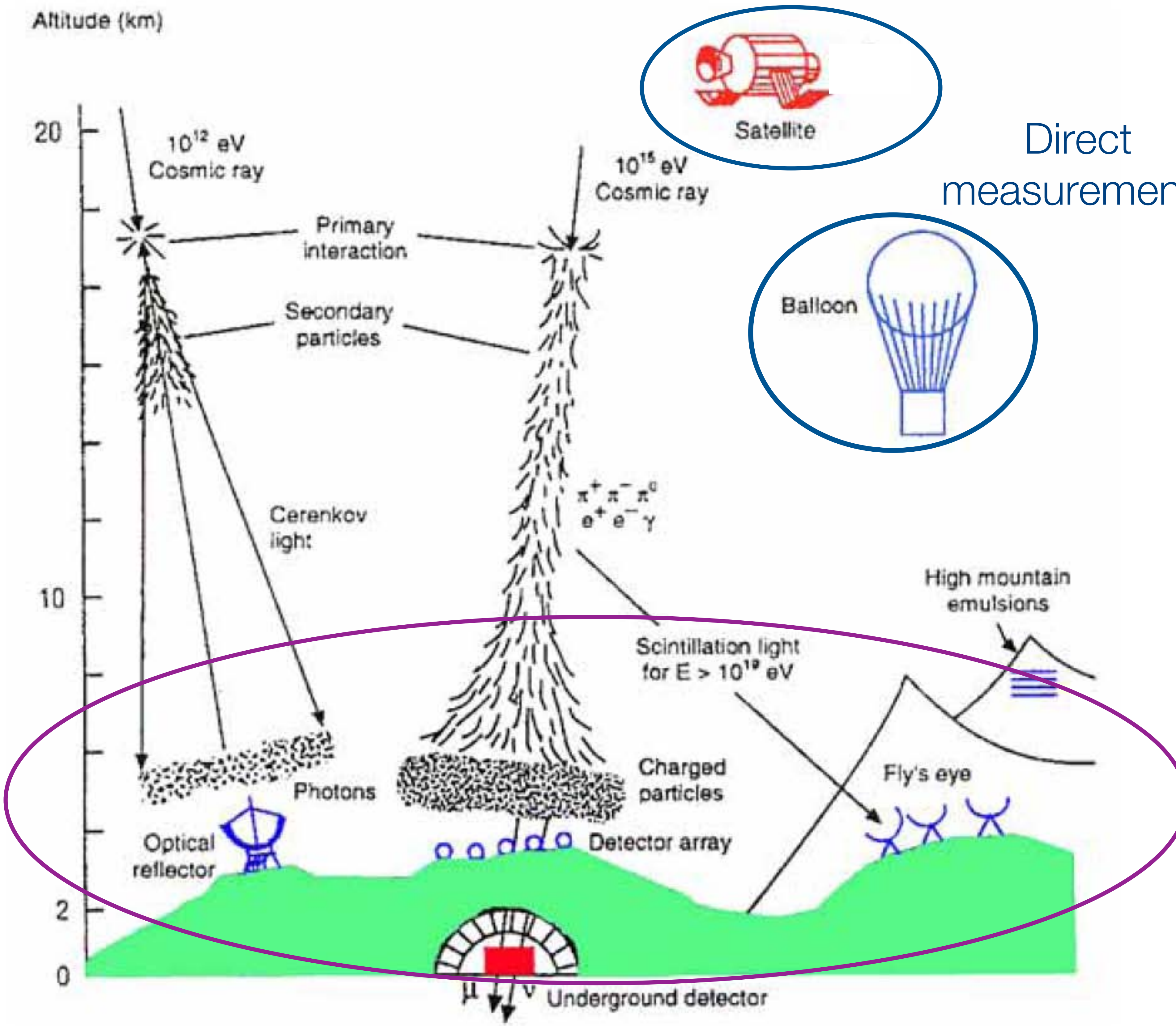

HE-UHECR

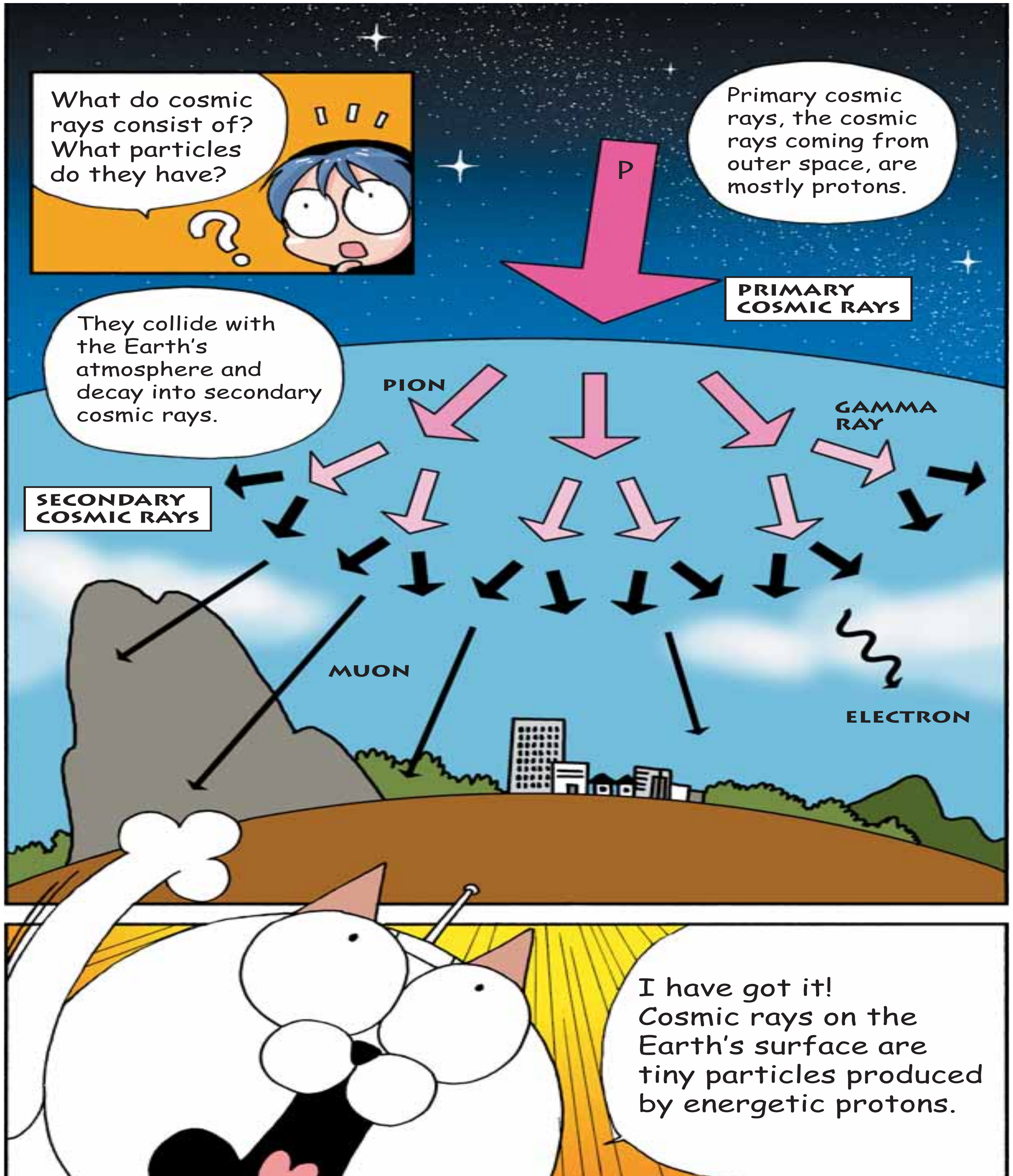

What do cosmic rays consist of? What particles do they have?
P
Primary cosmic rays, the cosmic rays coming from outer space, are mostly protons.
PRIMARY COSMIC RAYS
They collide with the Earth's atmosphere and decay into secondary cosmic rays.
PION
GAMMA RAY
SECONDARY COSMIC RAYS
MUON
ELECTRON
I have got it! Cosmic rays on the Earth's surface are tiny particles produced by energetic protons.

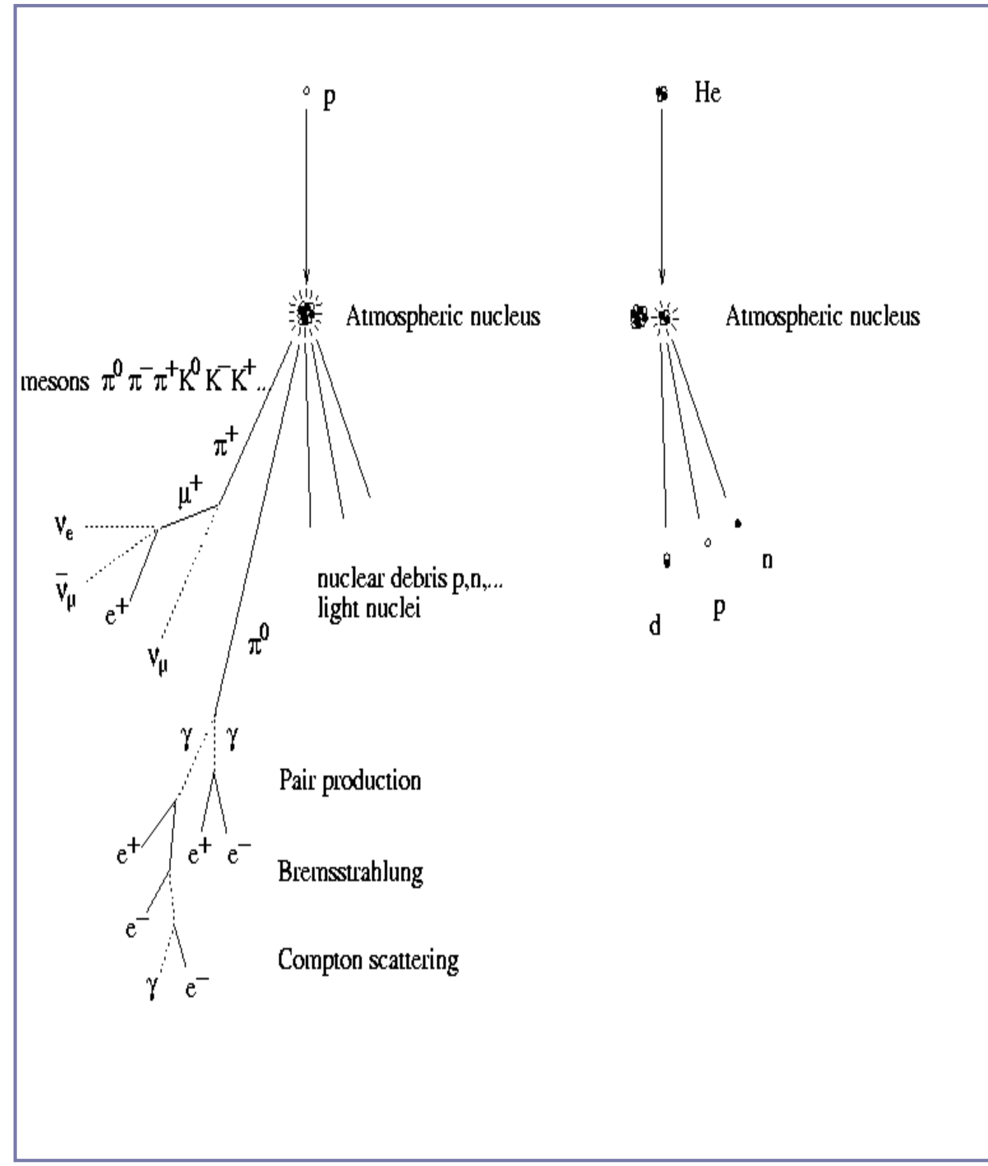

p
He
Atmospheric nucleus
Atmospheric nucleus
mesons $\pi^0 \pi^- \pi^+ K^0 K^- K^+$...
π^+
μ^+
ν_e
$\bar{\nu}_\mu$
e^+
ν_μ
π^0
nuclear debris p,n,... light nuclei
n
d
p
γ γ
Pair production
e^+ e^+ e^-
Bremsstrahlung
e^-
Compton scattering
γ e^-

Air Shower simulation

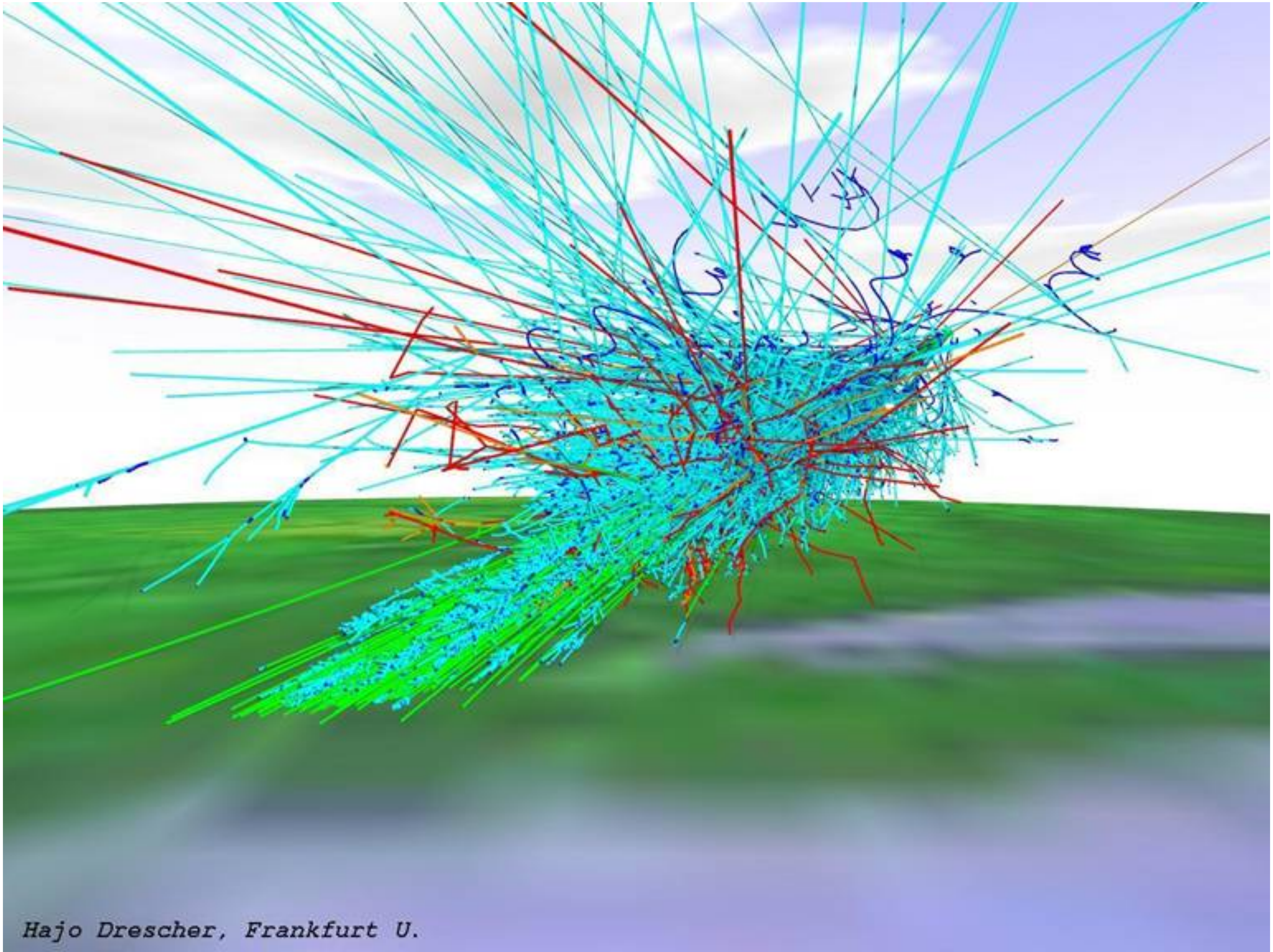

Air Shower simulation

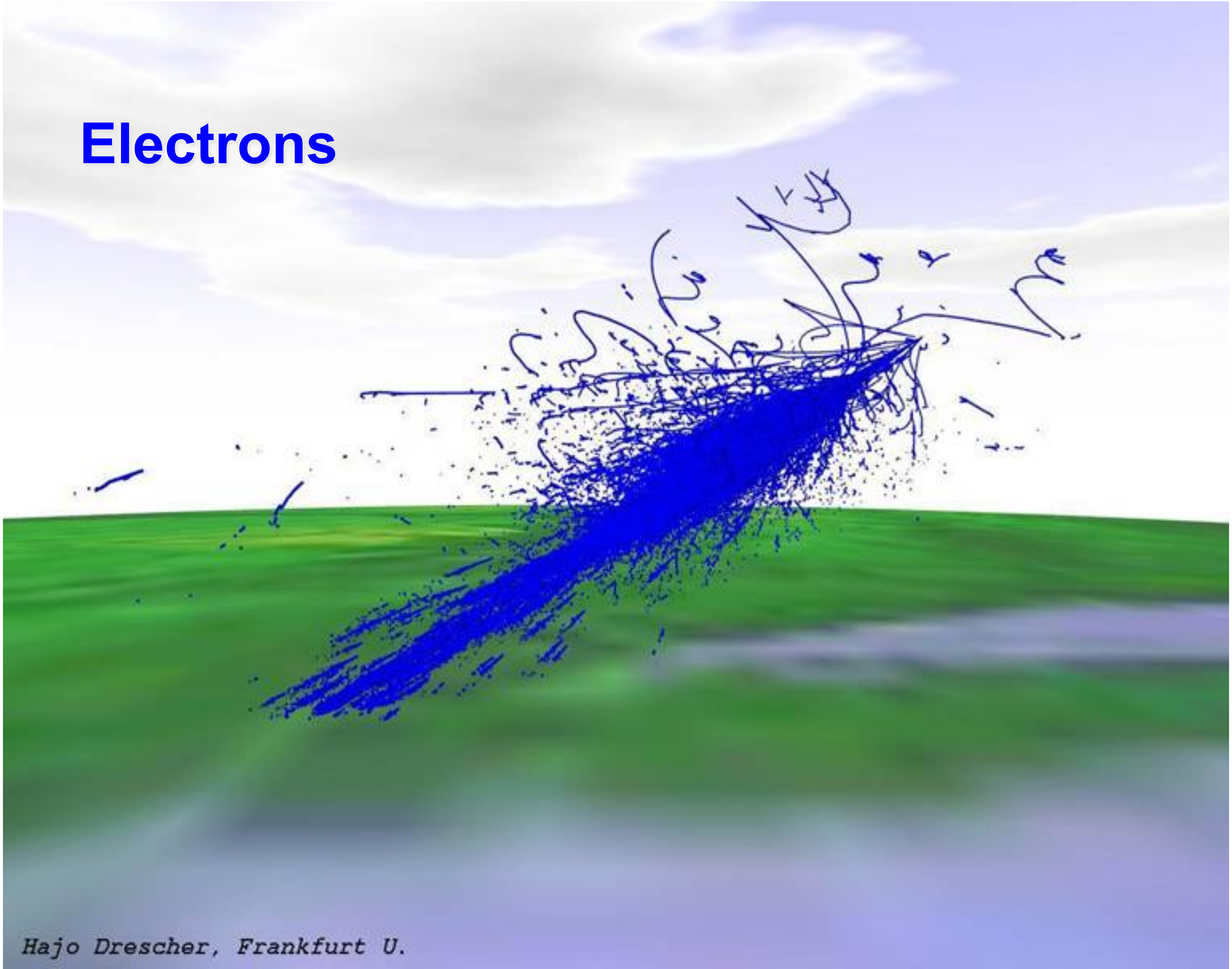

Air Shower simulation

Air Shower simulation

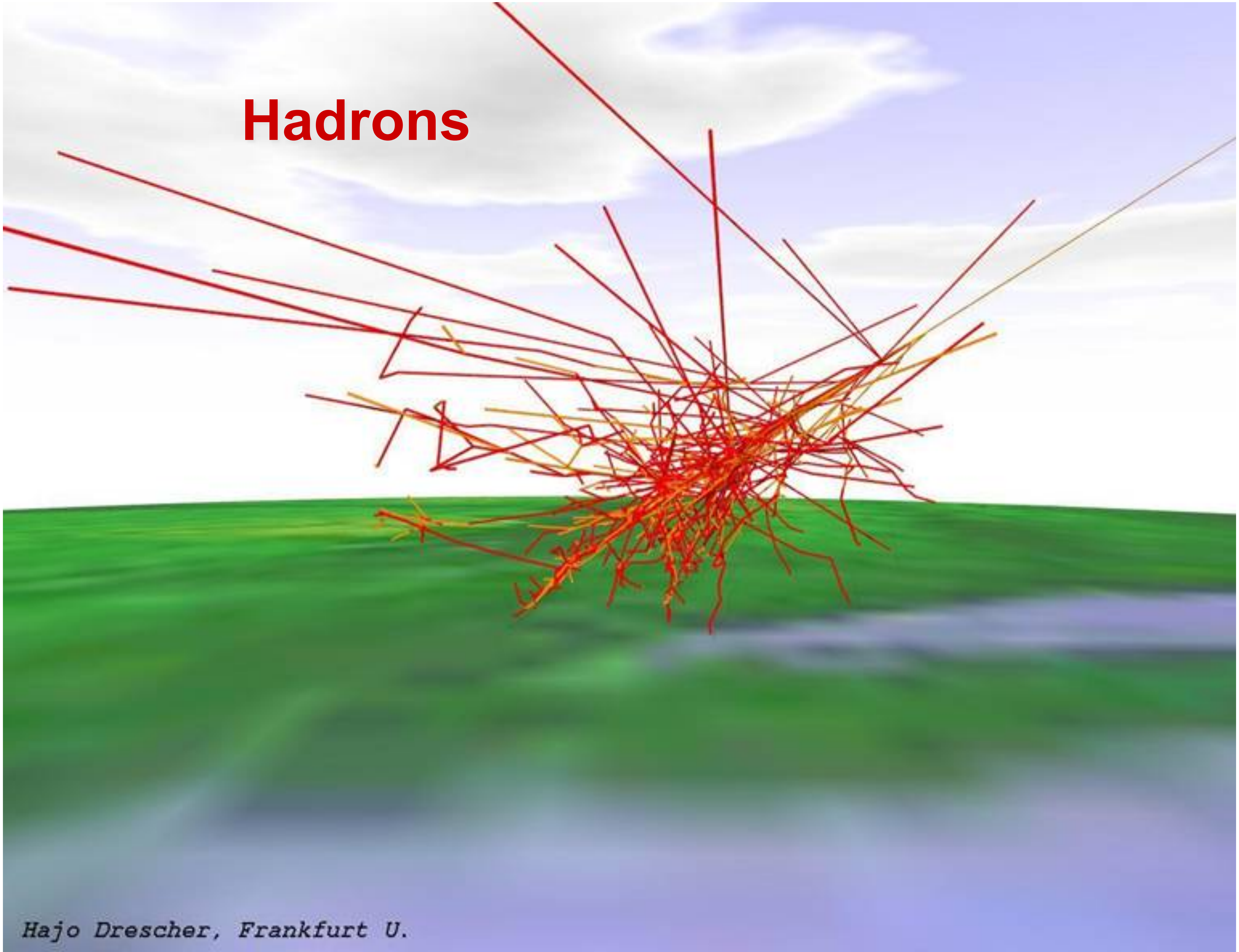

Indirect measurements

If the energy of the CR is too big to be directly measured, indirect measurements are necessary.

The atmosphere is used as 'PASSIVE CALORIMETER'

Object of the measurements:

1. Charged particles: μ±, e±, p (Extended Air Shower detectors, EAS)
2. Cherenkov light
3. Fluorescence light

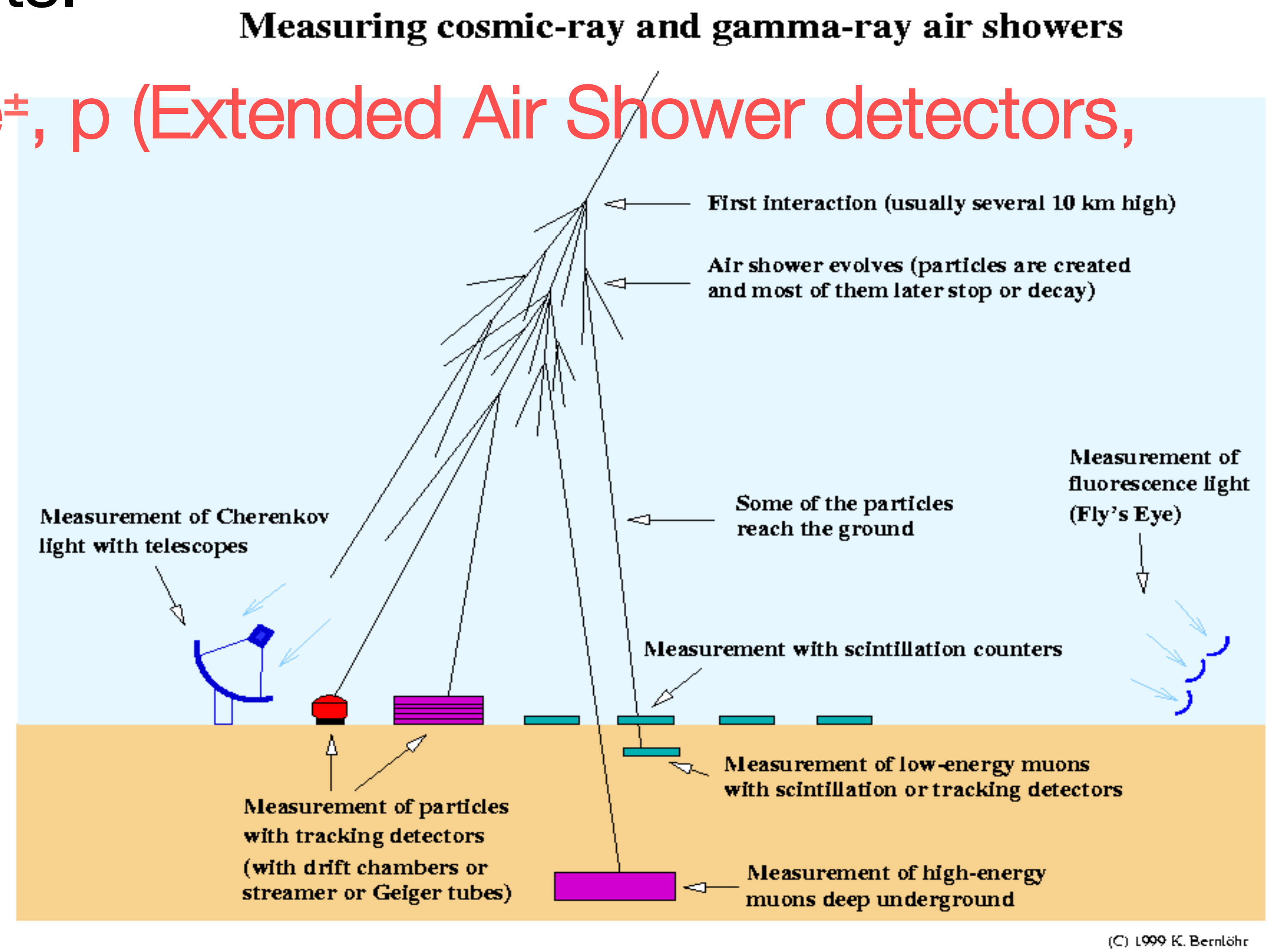

Charged component: EAS vs Atmospheric Depth

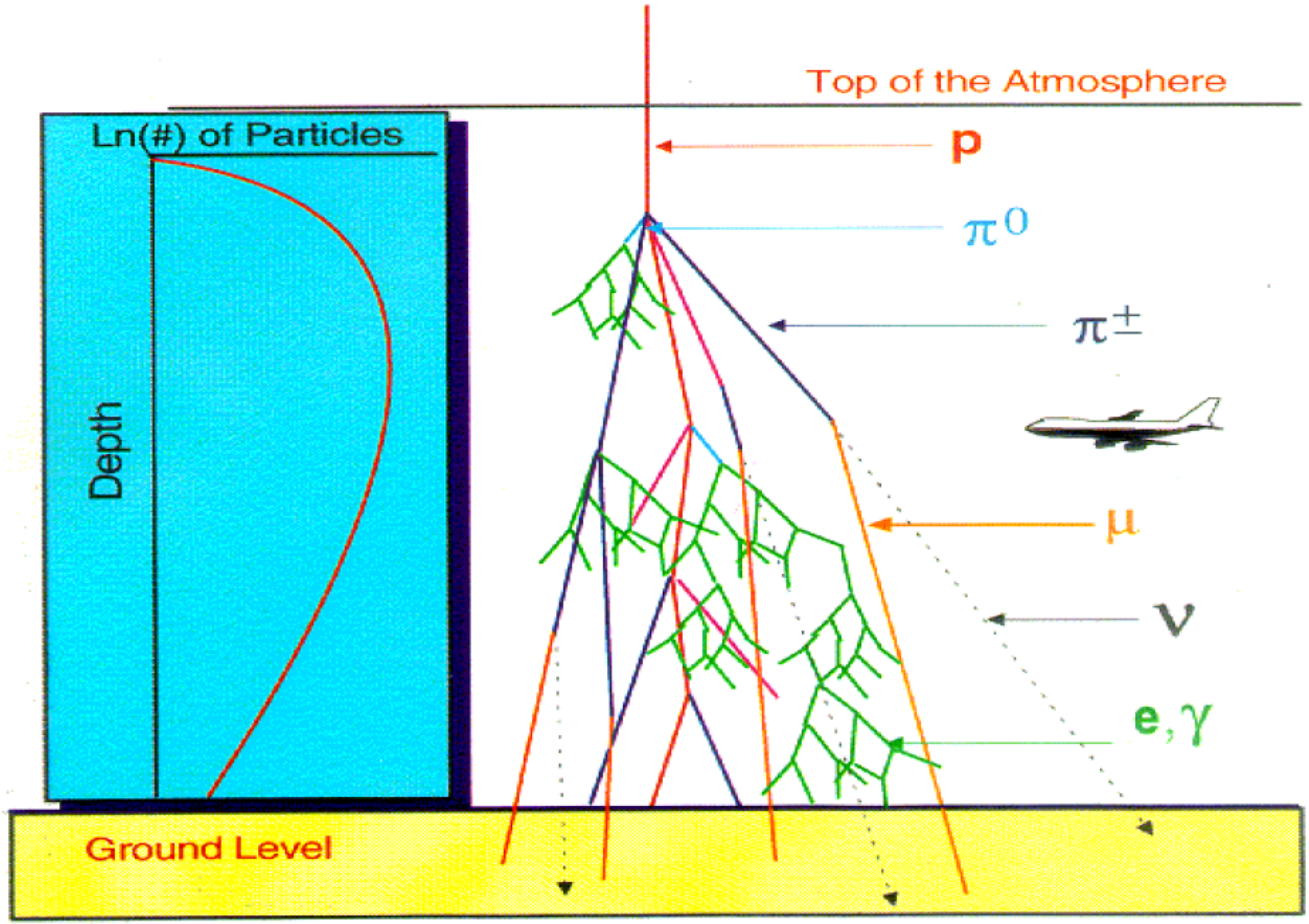

Analytic Shower Model – EM Showers

Simplified model [Heitler]:
shower development governed by X_0
e- loses [1 - 1/e] = 63% of energy in 1 X_0 (Brems.)

Assume:
$E > E_c$: no energy loss by ionization/excitation
$E < E_c$: energy loss only via ionization/excitation

Simple shower model:
- $2^{X/\lambda}$ particles after $t=X/\lambda$ splittings
- each with energy $E_0/2^t$
- stops if $E < E_C$
- number of particles $N_{max} = E_0/E_C$
- Maximum at $X_{max}=\lambda \ln_2(E_0/E_C)$

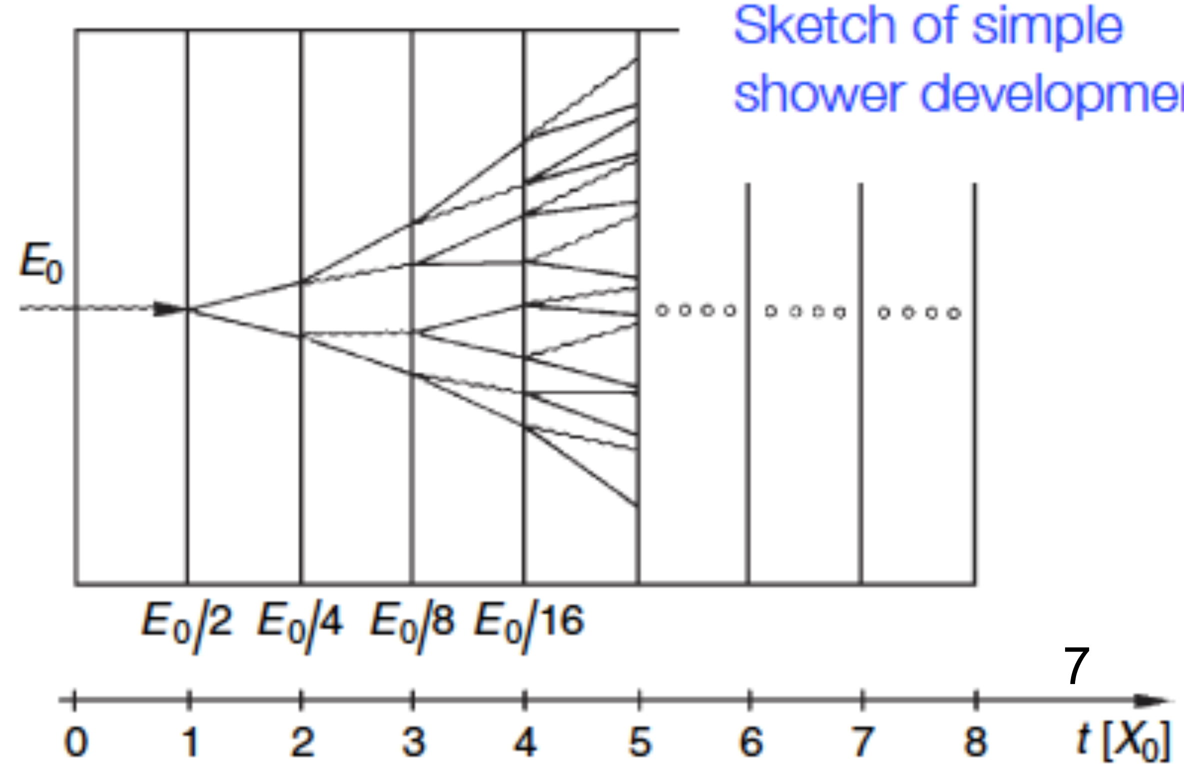

Sketch of simple shower development

This model is reasonably valid for EM showers
~ roughly valid for Hadronic showers

Analytic Shower Model – Hadronic Showers

Heitler model is reasonably valid for EM showers and only roughly valid for hadronic showers

Assume:

- Only the first interaction contribute to shower size

$$X_{max} = X_0 \ln\left[\frac{2(1-K_{el})E_0}{(\langle m\rangle/3)\varepsilon_0}\right] + \lambda_N(E_0) ,$$

$$N_e^{max} = \frac{1}{2}\frac{\langle m\rangle}{3}\frac{(1-K_{el})E_0}{\varepsilon_0} ,$$

m is the effective meson multiplicity
K_{el} is the elasticity coefficient of the first interaction (roughly ½)
$\varepsilon_0 = E_c$ of the electrons in air (81 MeV)

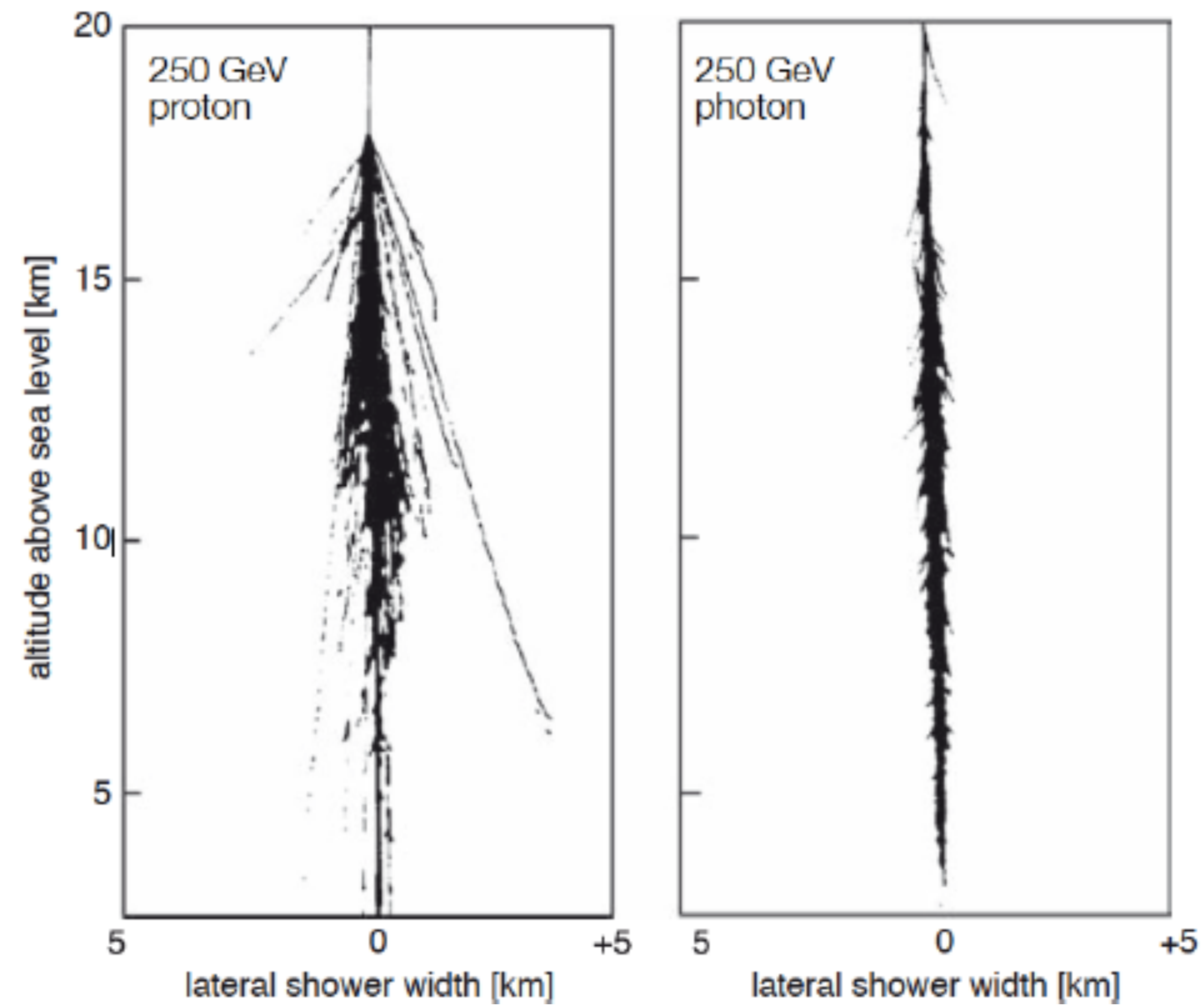

Analytic Shower Model – Hadronic Showers

Heitler model is reasonably valid for EM showers and only roughly valid for hadronic showers

Assume:

- Only the first interaction contribute to shower size
- Superposition principle is valid → Nucleus with mass A and energy E_0 is equivalent to A nucleons with energy E_0/A

$$X_{max} = X^p_{max} - X_0 \ln A$$

$$N_\mu/N_e = A^{1-\beta}(N\mu/N_e)^p$$

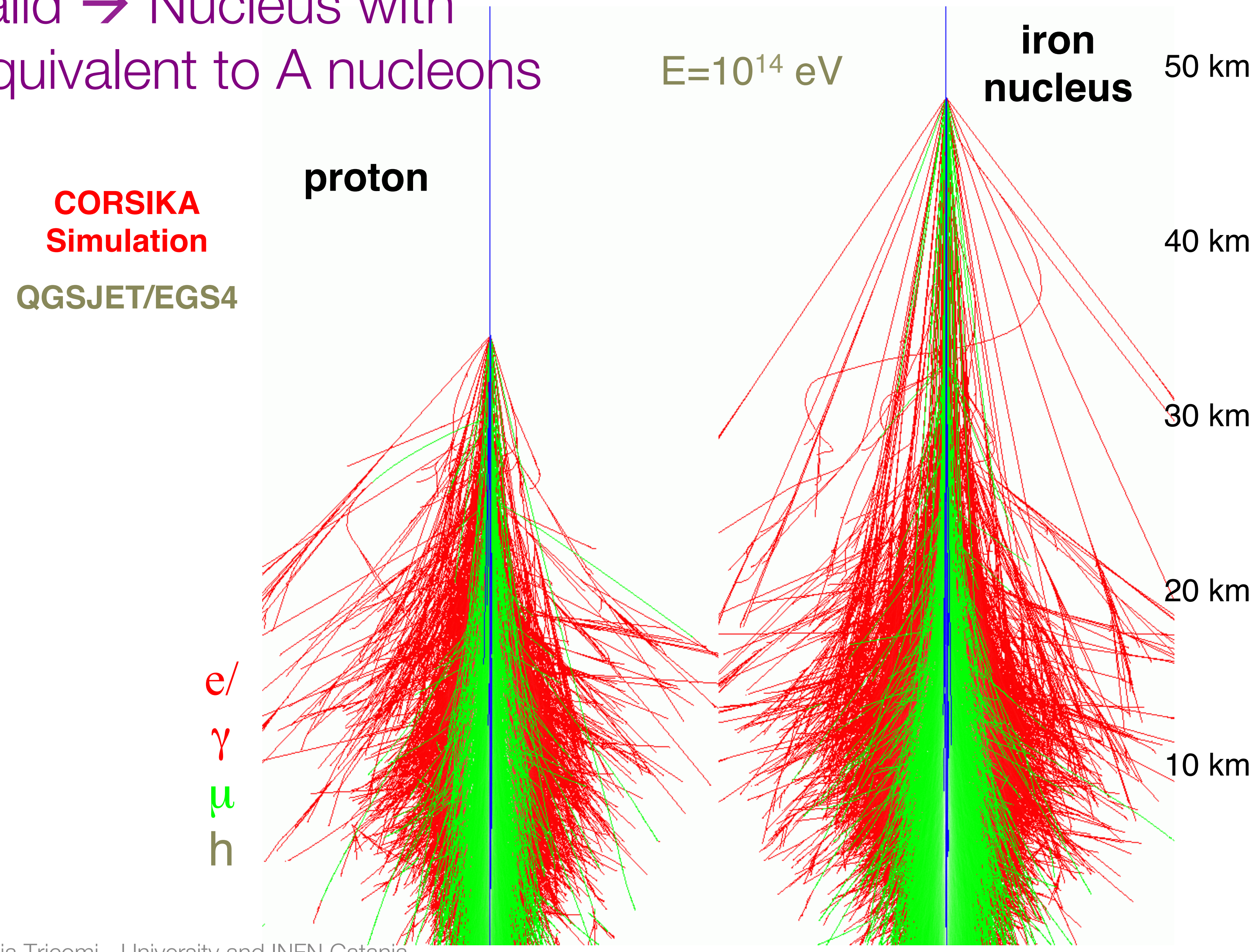

Hadronic showers: life is more complicated

Hadronic interaction:

Elastic:

$$p + \mathrm{Nucleus} \rightarrow p + \mathrm{Nucleus}$$

Inelastic:

$$p + \mathrm{Nucleus} \rightarrow \pi^{+} + \pi^{-} + \pi^{0} + \ldots + \mathrm{Nucleus}^{*}$$

$$\left[\begin{array}{ll} \mathrm{Nucleus}^{*} & \rightarrow \mathrm{Nucleus\ A} + n, p, \alpha, \ldots \\ & \rightarrow \mathrm{Nucleus\ B} + 5p, n, \pi, \ldots \\ & \rightarrow \mathrm{Nuclear\ fission} \end{array}\right]$$

1st stage:
- hard collision
- particle multplication (i.e. string model)

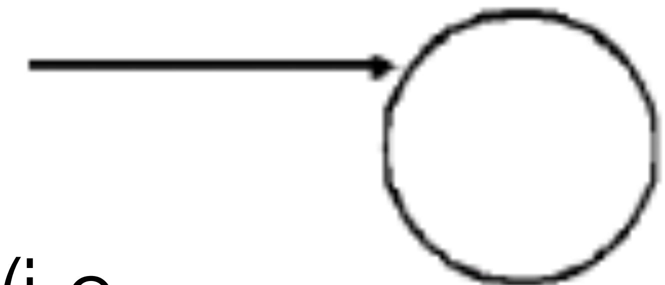

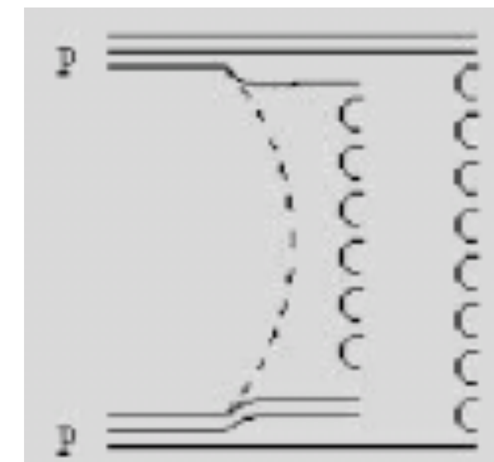

2nd stage: spallation
- Inter and intra-nuclear cascade
- Nuclear de-excitation

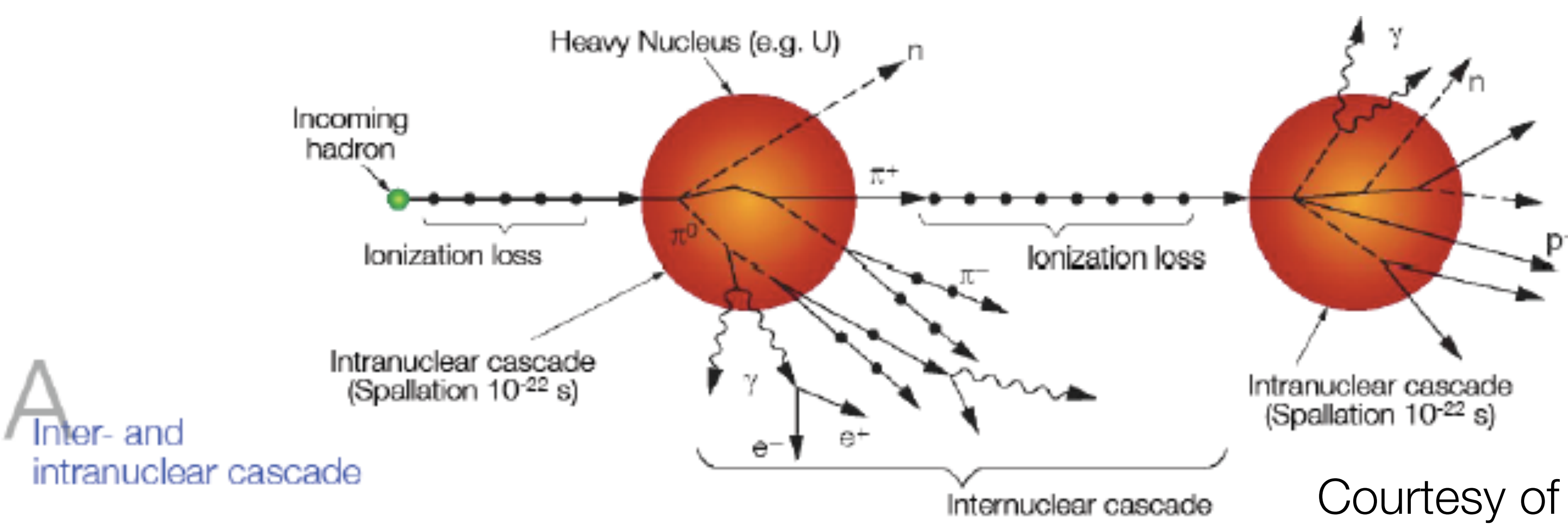

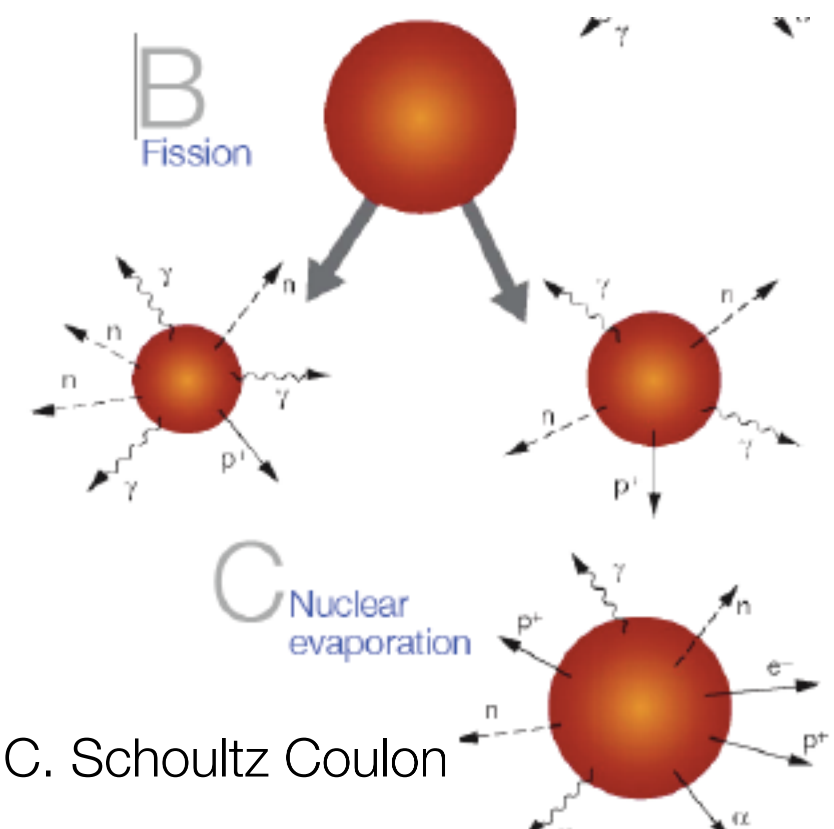

Courtesy of H. C. Schoultz Coulon

Charged component of EAS

Density Sampling

the particle density is observed in an array of detectors (sampling), and it is used to identify the shower core and the total number of particles in the shower → reconstruction of the energy of the primary CR

Fast Timing

by measuring the different arrival times of the particles on the different detectors of the array → the arrival direction of the primary CR (shower's axis)

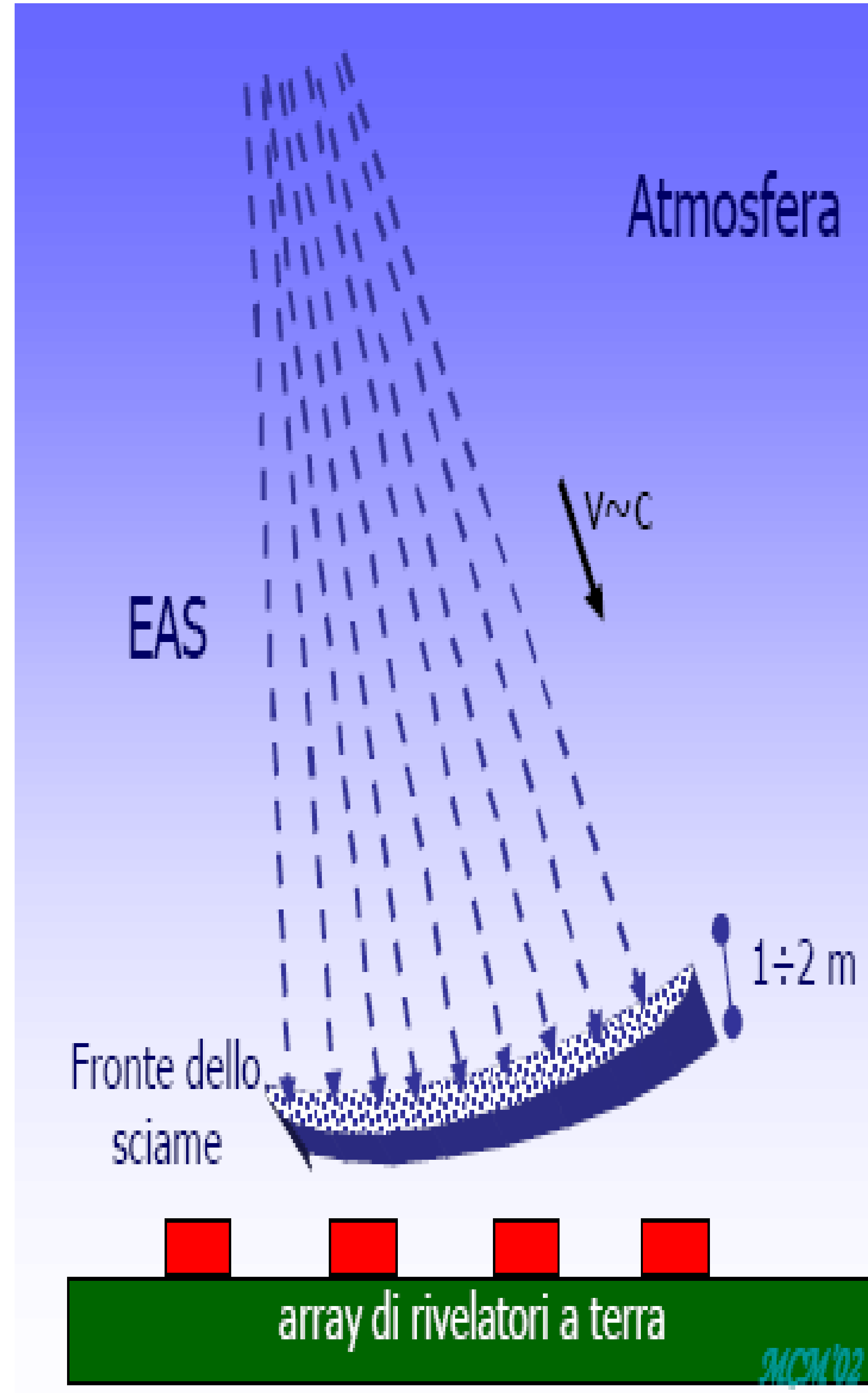

‘Complete’ EAS detection

Fluorescence detector to reconstruct the longitudinal development

Array of Cherenkov detectors for the lateral distribution measurement ($\alpha \cong 6^0$).

Array of charged particle detectors to sample the shower

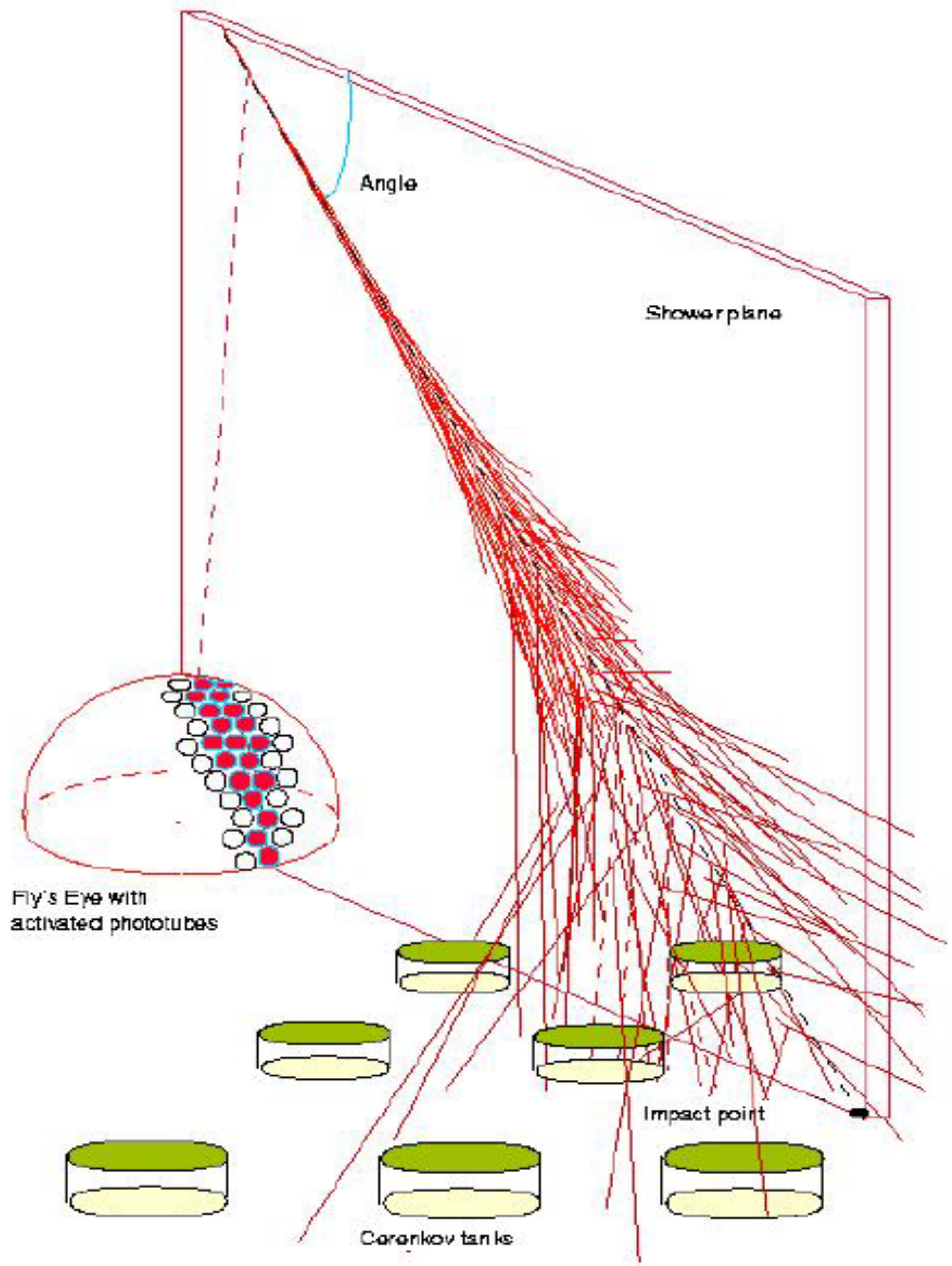

Hybrid Technique

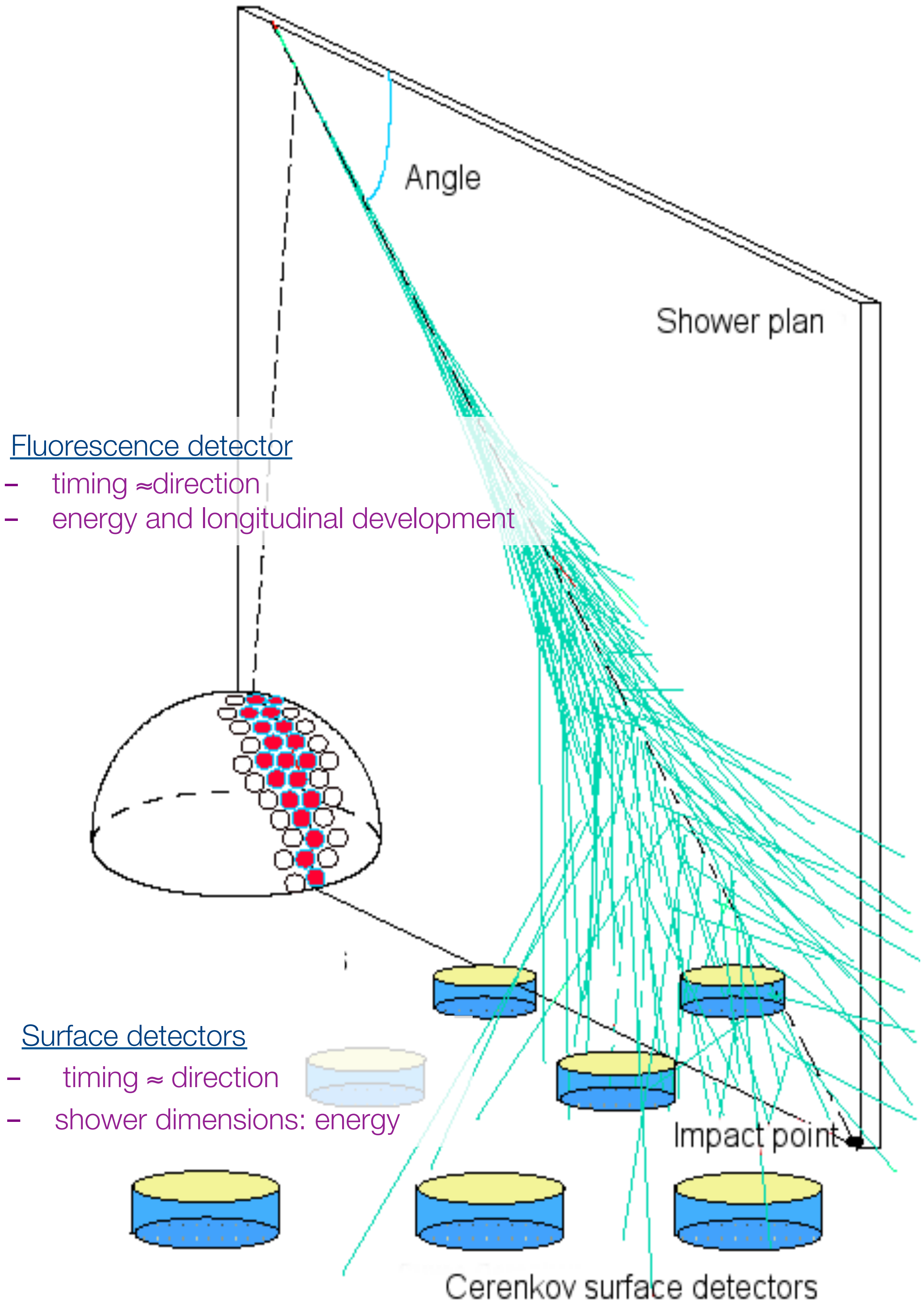

3-D image of the shower:
- ✓ Longitudinal profile from FD
- ✓ Lateral profile from SD
- ✓ Stereo detection

Cross calibration:
- ✓ Two complementary and independent methods for the EAS detection

Better data quality:
- ✓ Systematics are reduced
- ✓ Geometrical and energetic resolutions are improved
- ✓ Better determination of the shower axis (simultaneous measurement of the event with different detectors)
- ✓ Smaller model dependance

Uniform sky coverage:
- ✓ SD: 100% duty cycle
- ✓ FD: 10% duty cycle

A typical hybrid event

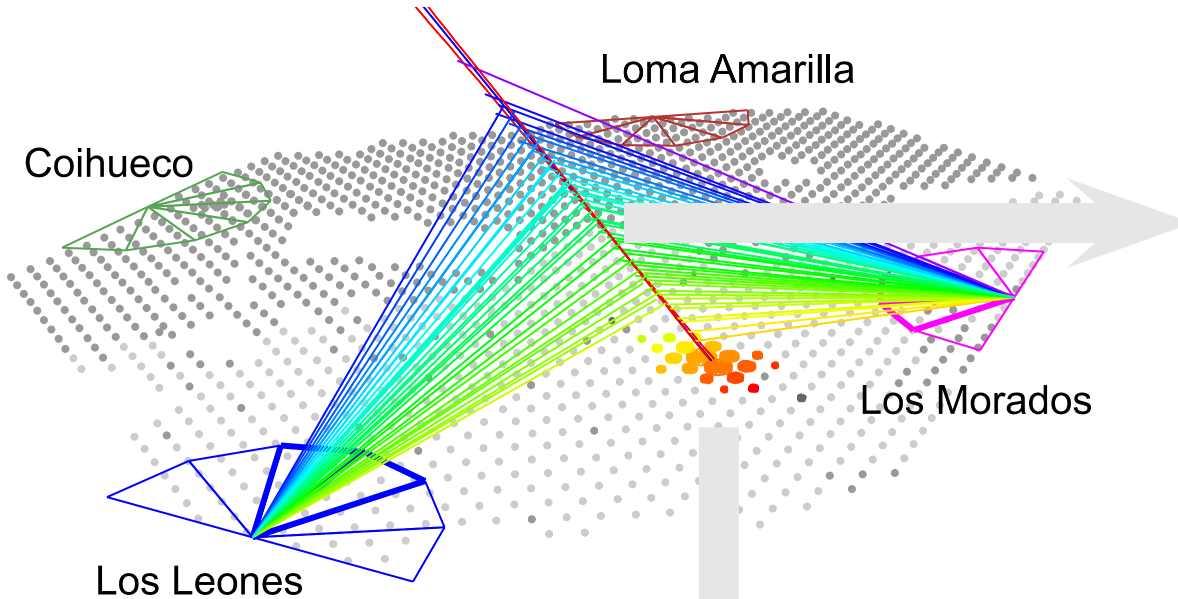

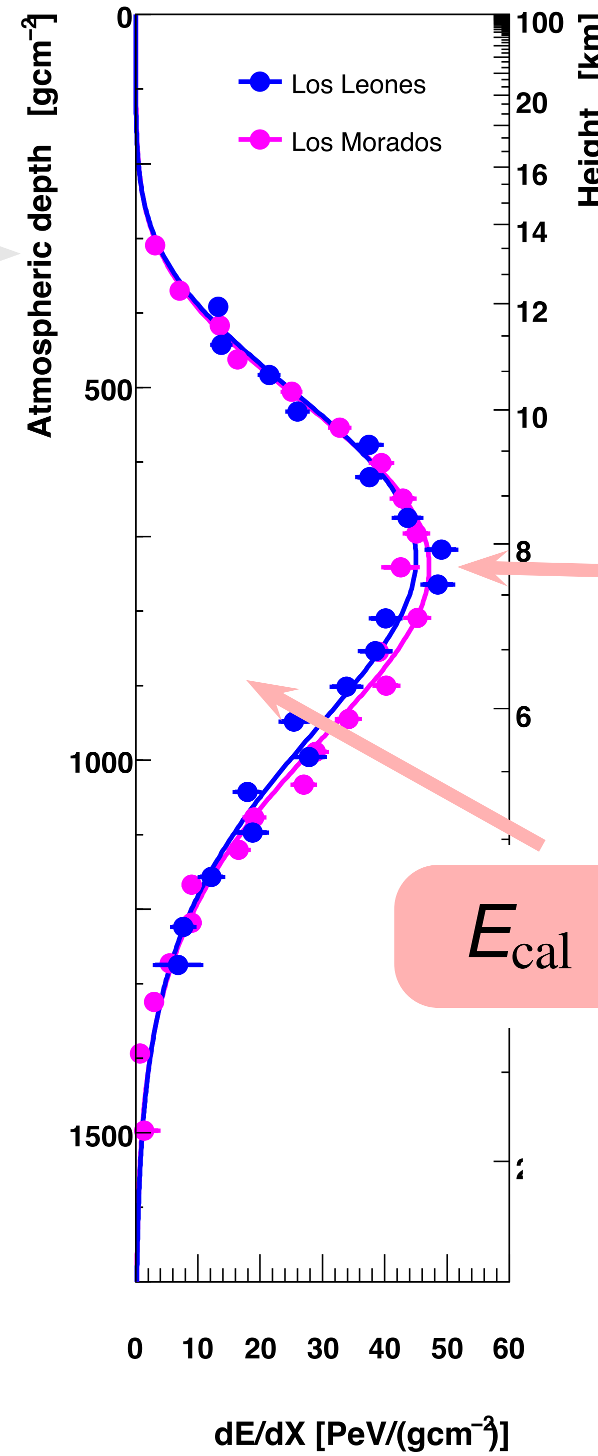

$\sigma X_{\max} \leq 20\,\mathrm{g/cm^2}$
$\Delta_{\mathrm{sys}} \leq 10\,\mathrm{g/cm^2}$

$X_{\max}$

$E_{\mathrm{cal}} = \int \frac{\mathrm{d}E}{\mathrm{d}X}\,\mathrm{d}X$

$\sigma_E/E \sim 8\,\%$
$\Delta_{\mathrm{sys}} \approx 15\,\%$

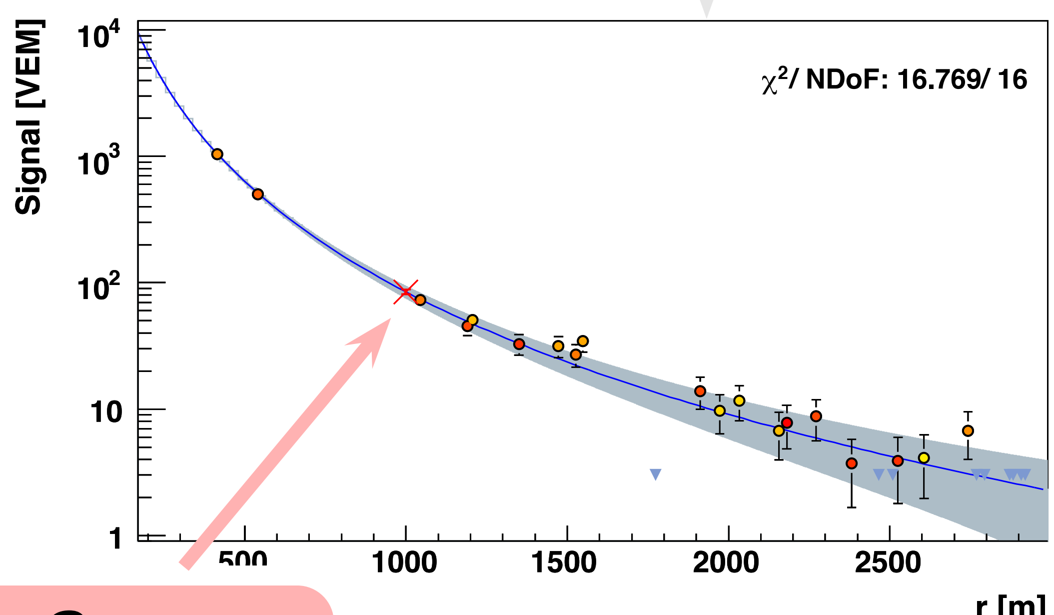

S_{1000}

$E_{\mathrm{surface}} = f(S_{1000},\,\theta)$

M. Unger, Pierre Auger Collaboration, ICRC 2017

Hadronic Interaction Models

Several models available: QGSJET DPMJET, EPOS, SYBILL, PYTHIA

- Theoretical concepts similar (multiple scattering of Gribov-Regge type, strings), but the practical implementation quite different
- Prediction significantly different

EPOS, QGSJET

Multiple scattering of Gribov-Regge type

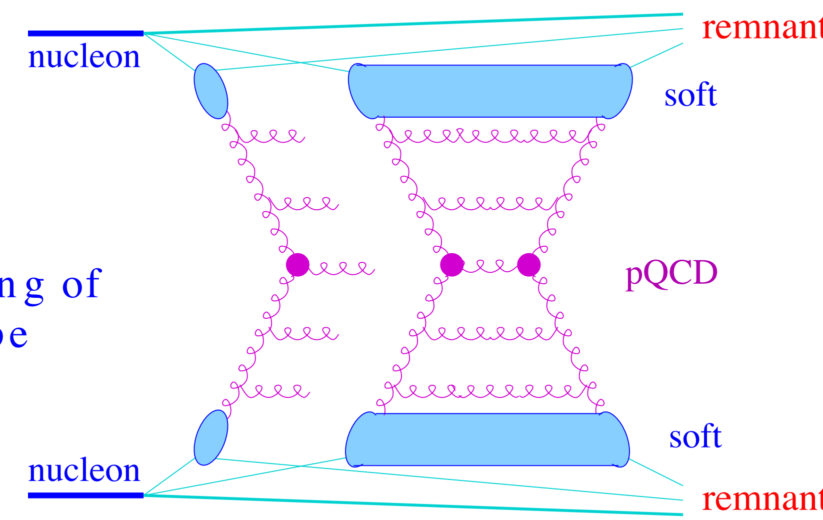

SIBYLL

as well multiple scattering of Gribov-Regge type

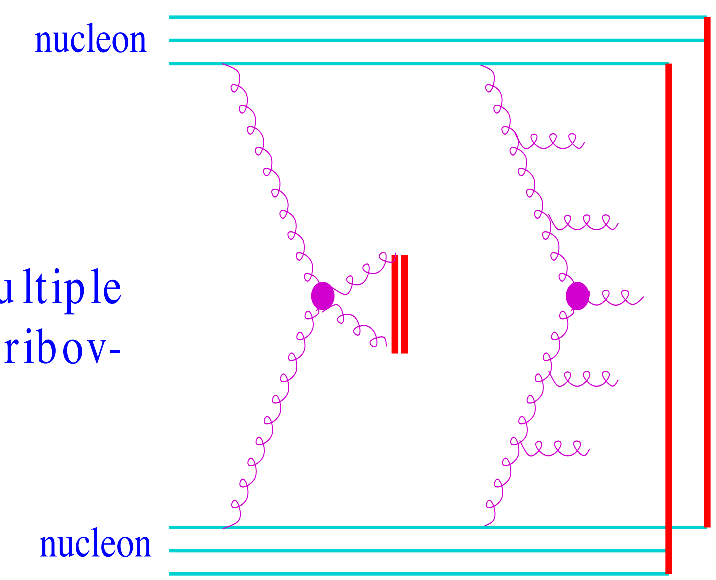

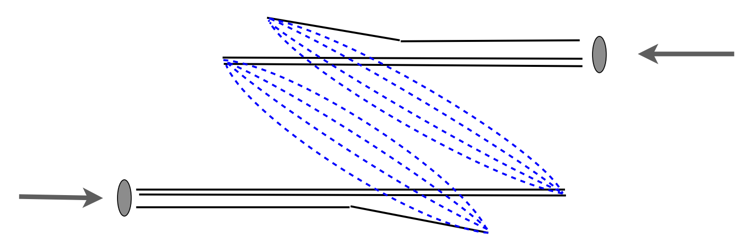

SIBYLL 2.1, DPMJET III:
strings connected to valence quarks;
first fragmentation step with harder fragmentation function

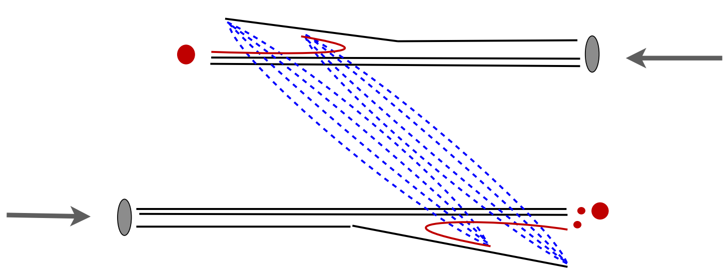

QGSJET II, SIBYLL 2.3:
fixed probability of strings connected to valence quarks or sea quarks;
explicit construction of remnant hadron

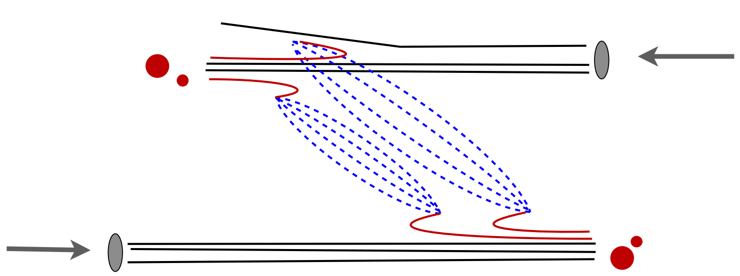

EPOS:
strings always connected to sea quarks;
bags of sea and valence quarks fragmented statistically

Courtesy of R. Engel

Additional complications due to nuclei

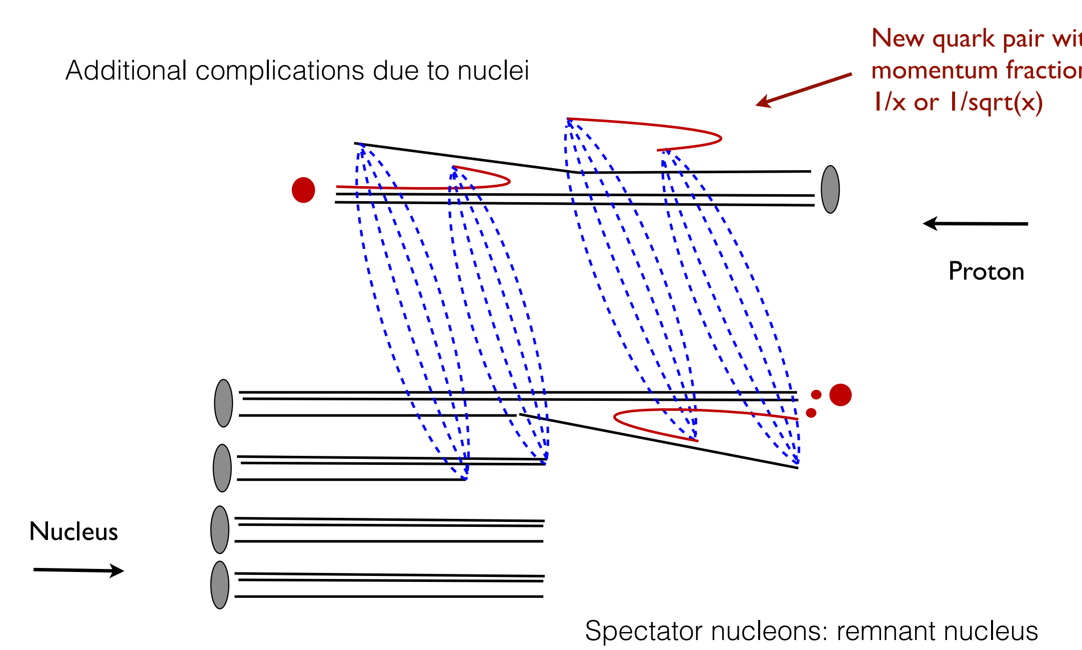

Ultra High Energy Cosmic Rays

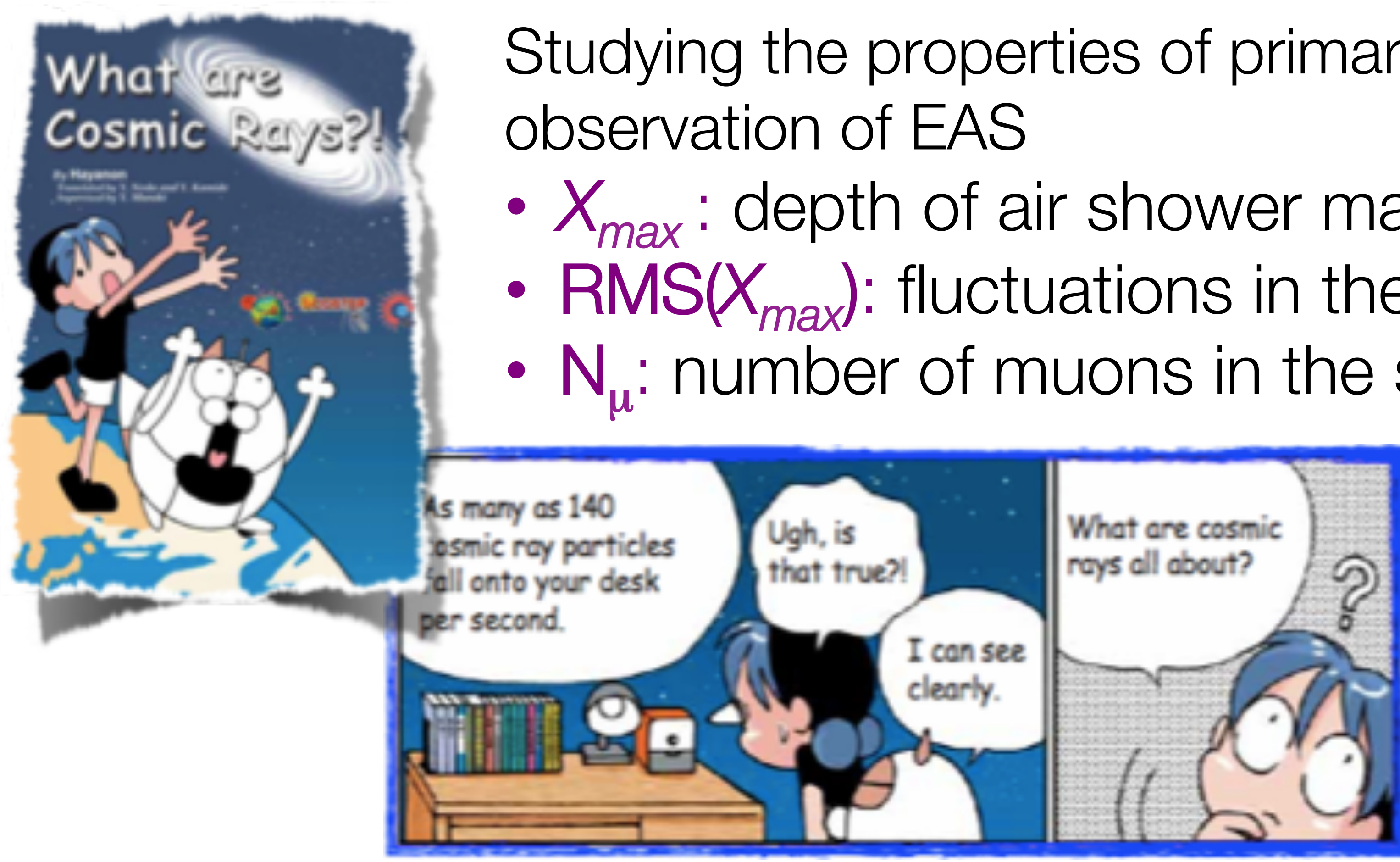

Studying the properties of primary High Energy Cosmic Rays based on observation of EAS

- X_{max} : depth of air shower maximum in the atmosphere
- RMS(X_{max}): fluctuations in the position of the shower maximum
- N_{μ}: number of muons in the shower at the detector level

\+

MC Simulation to describe hadronic interaction with atmosphere

Energy, mass composition, direction
—> source of primary cosmic rays
—> origin of the universe (final goal)

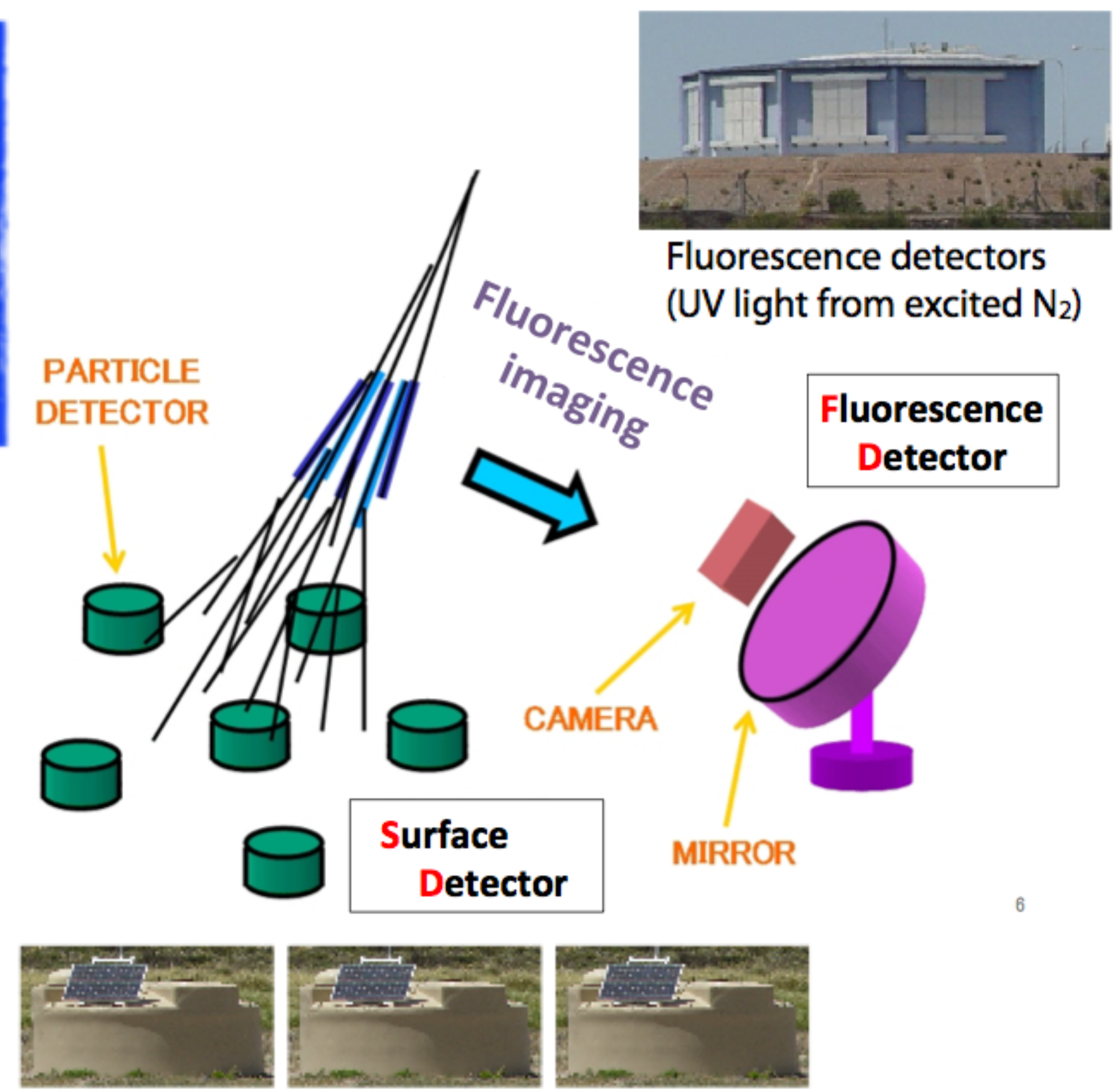

Surface detectors (charged+photon)

Hadronic Interactions

Cascade equations (1d !)

H. Drescher, G. Farrar
Phys.Rev.D67:116001,2003

$$\frac{\partial h_n(E,X)}{\partial X} = -h_n(E,X)\left(\frac{1}{\lambda_n(E)} + \frac{B_n}{E X}\right)$$

$$+\sum_m \int_{E_{\min}}^{E_{\max}} h_m(E',X)\left(\frac{W_{mn}(E',E)}{\lambda_m(E')} + \frac{B_m D_{mn}(E',E)}{E' X}\right) \mathrm{d}E$$

Mean free path → σ_{tot}(h+air → X)
See TOTEM's talk

Energy distribution of secondaries → dN/dx$_F$ (pt integrated !)

h_n:number of hadrons n per dE
E: Energy   X: slant depth
B_n: decay constant
λ_n:interaction length
W_{mn}: collision function
D_{mn}: decay function
initial condition:
$h_n(E,X)=\delta(E-E_0)$ for a given particle

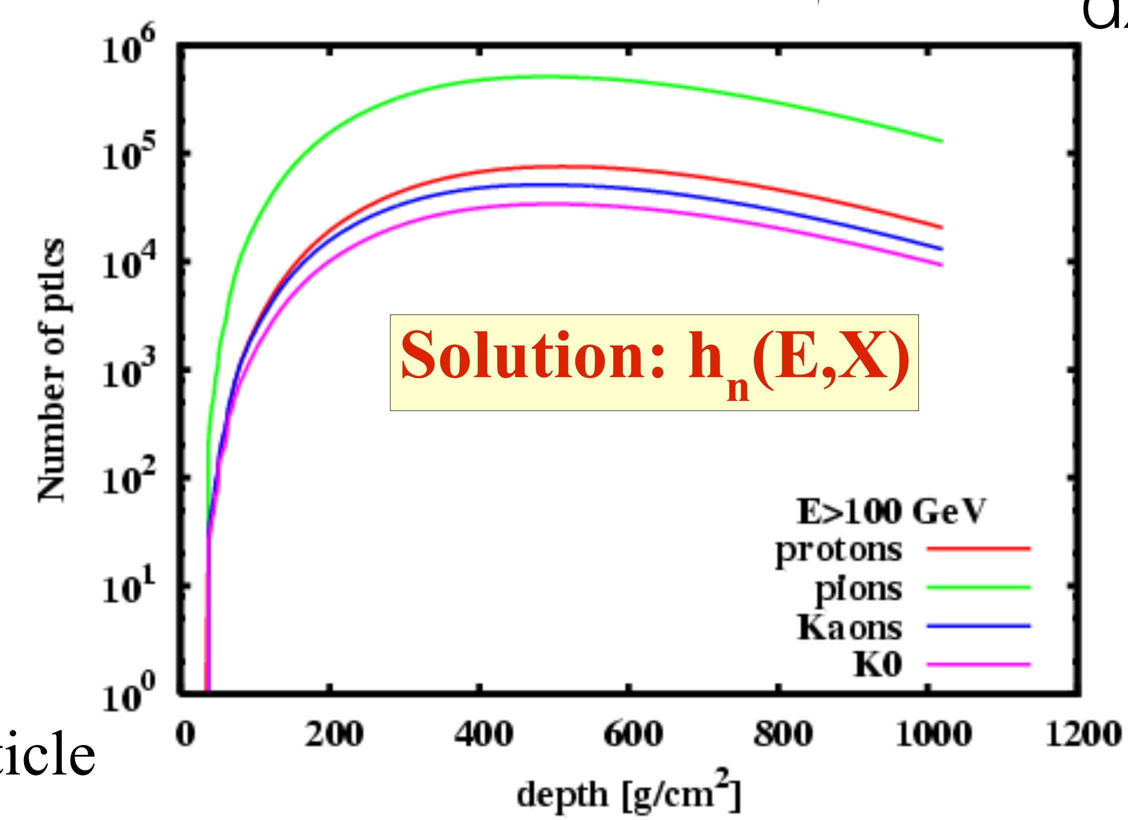

HECR Spectrum: more than ten years of debates…

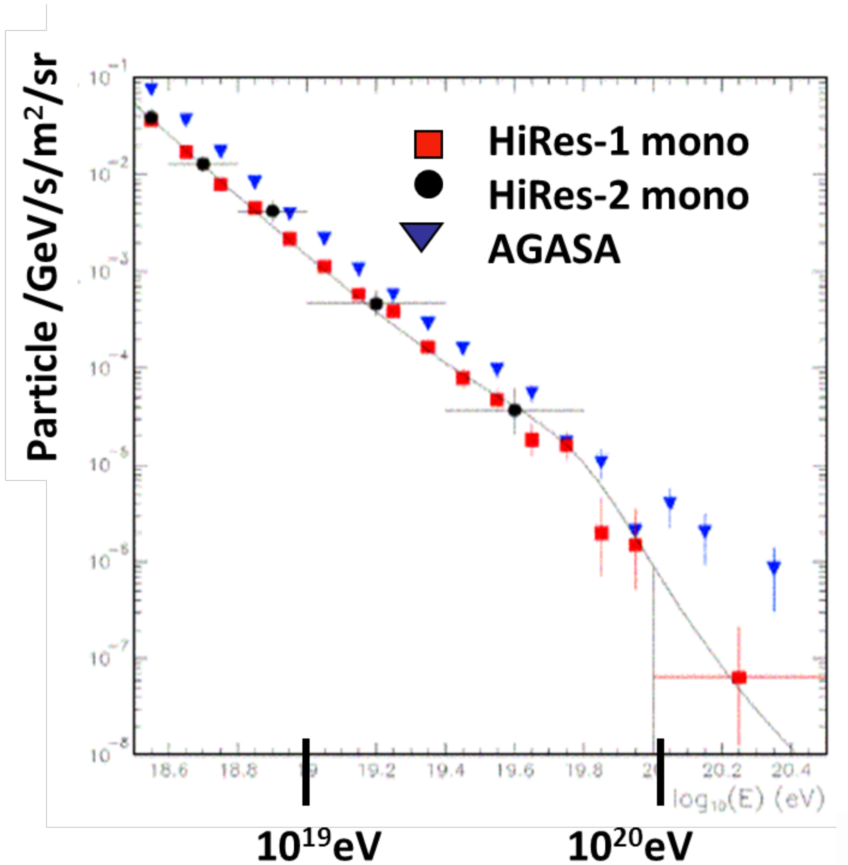

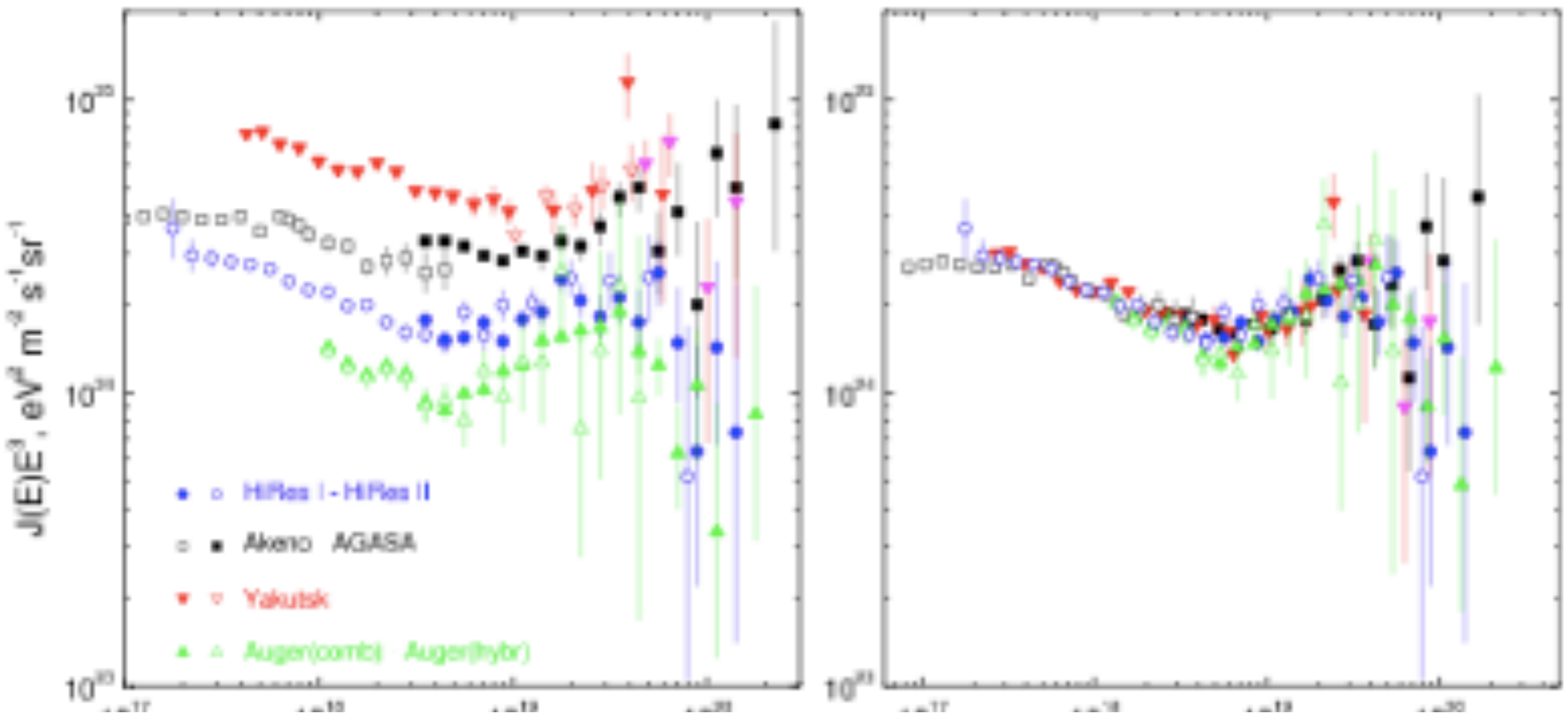

Flux systematic uncertainties

SD vertical: 5.8%

SD inclined: 5%

SD-750: 14% at 0.3 EeV

<7% at 3 EeV

Hybrid: 10% at 1 EeV

6% at 10 EeV

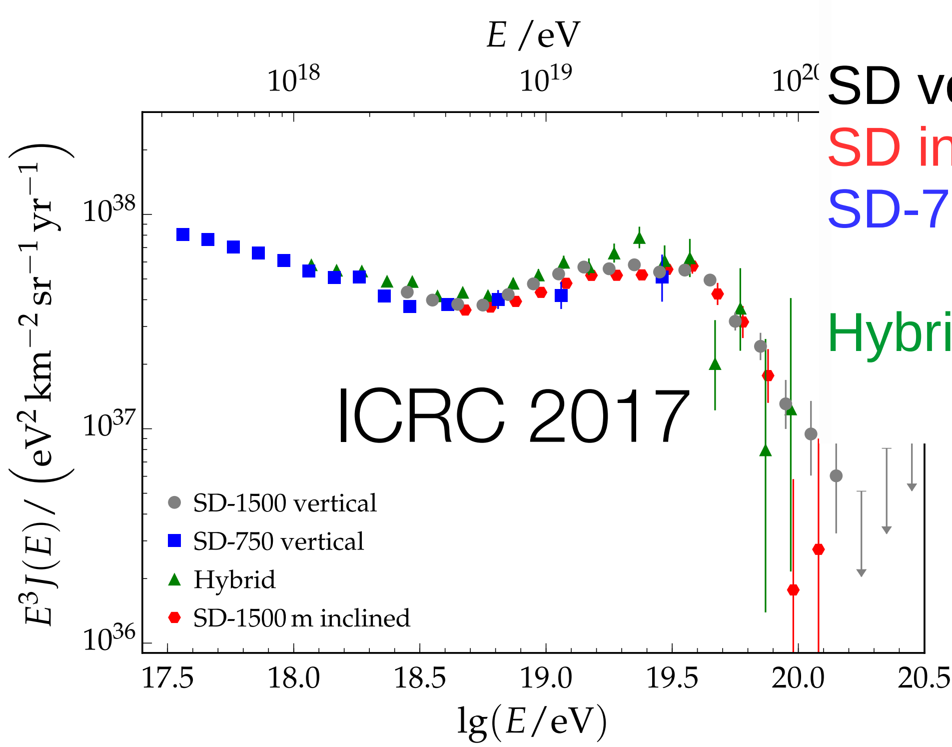

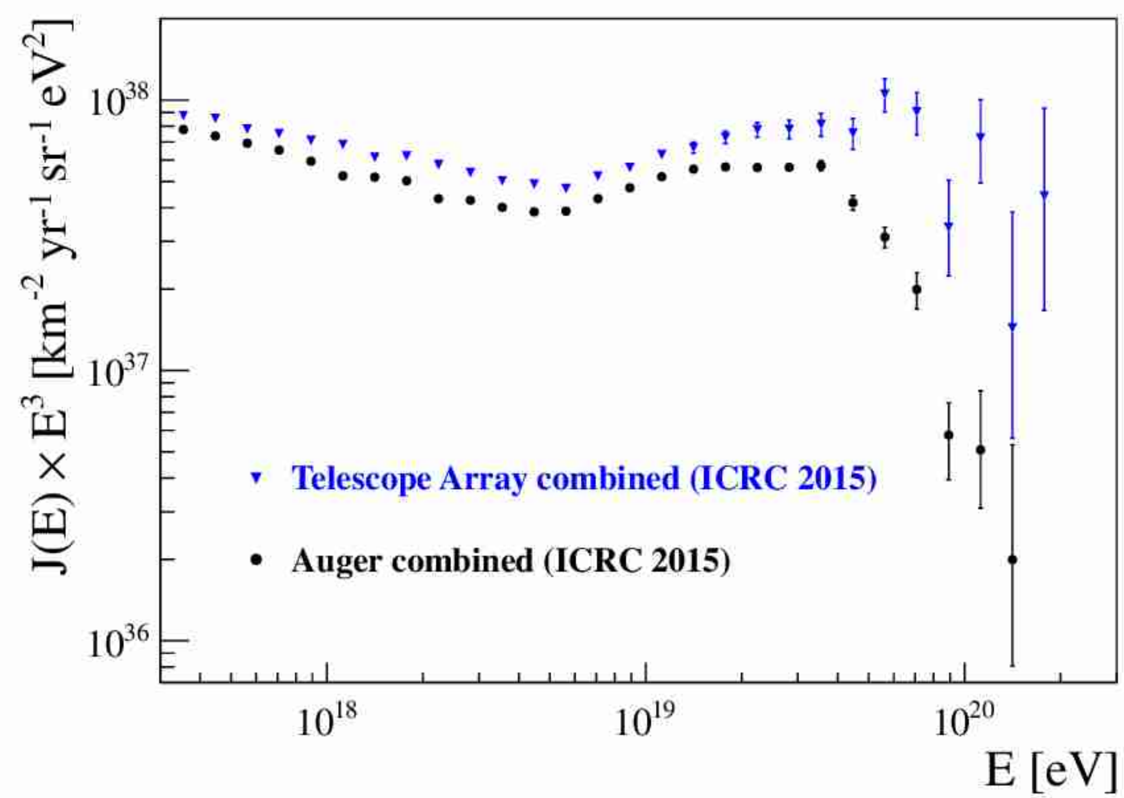

HECR Mass Composition

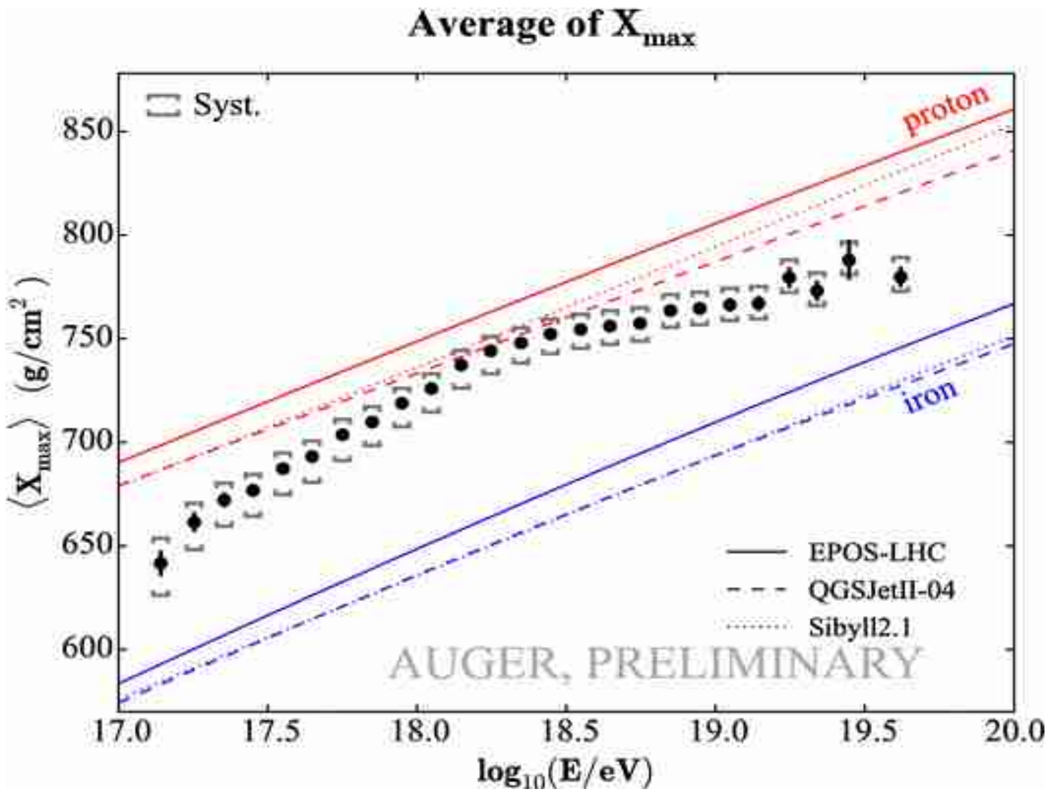

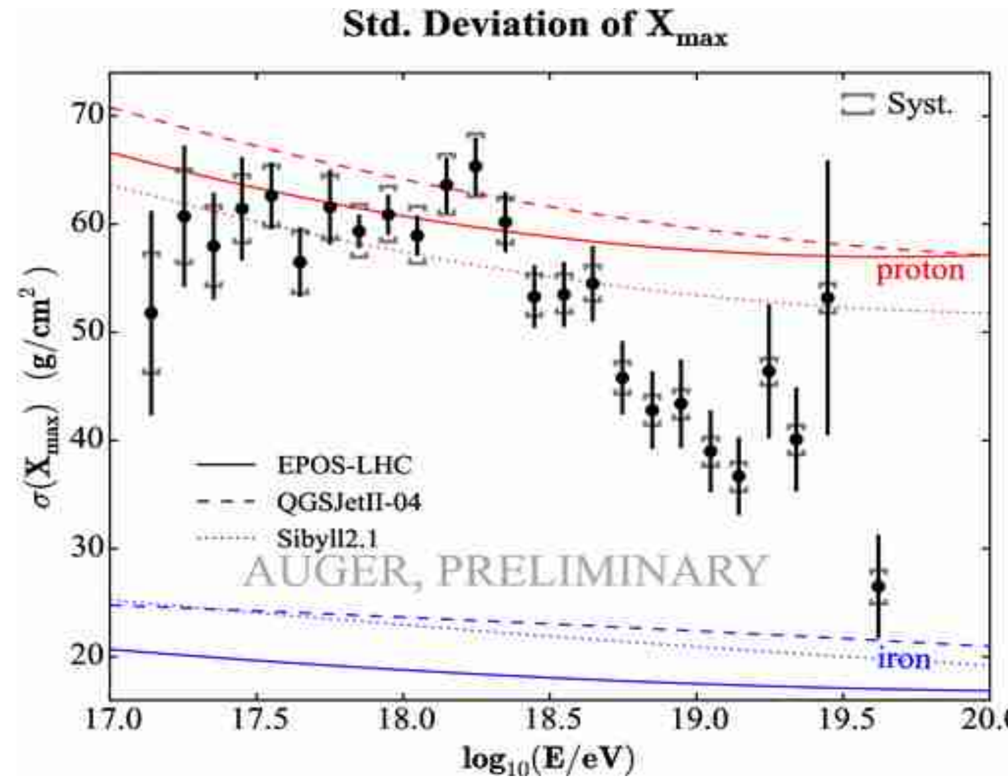

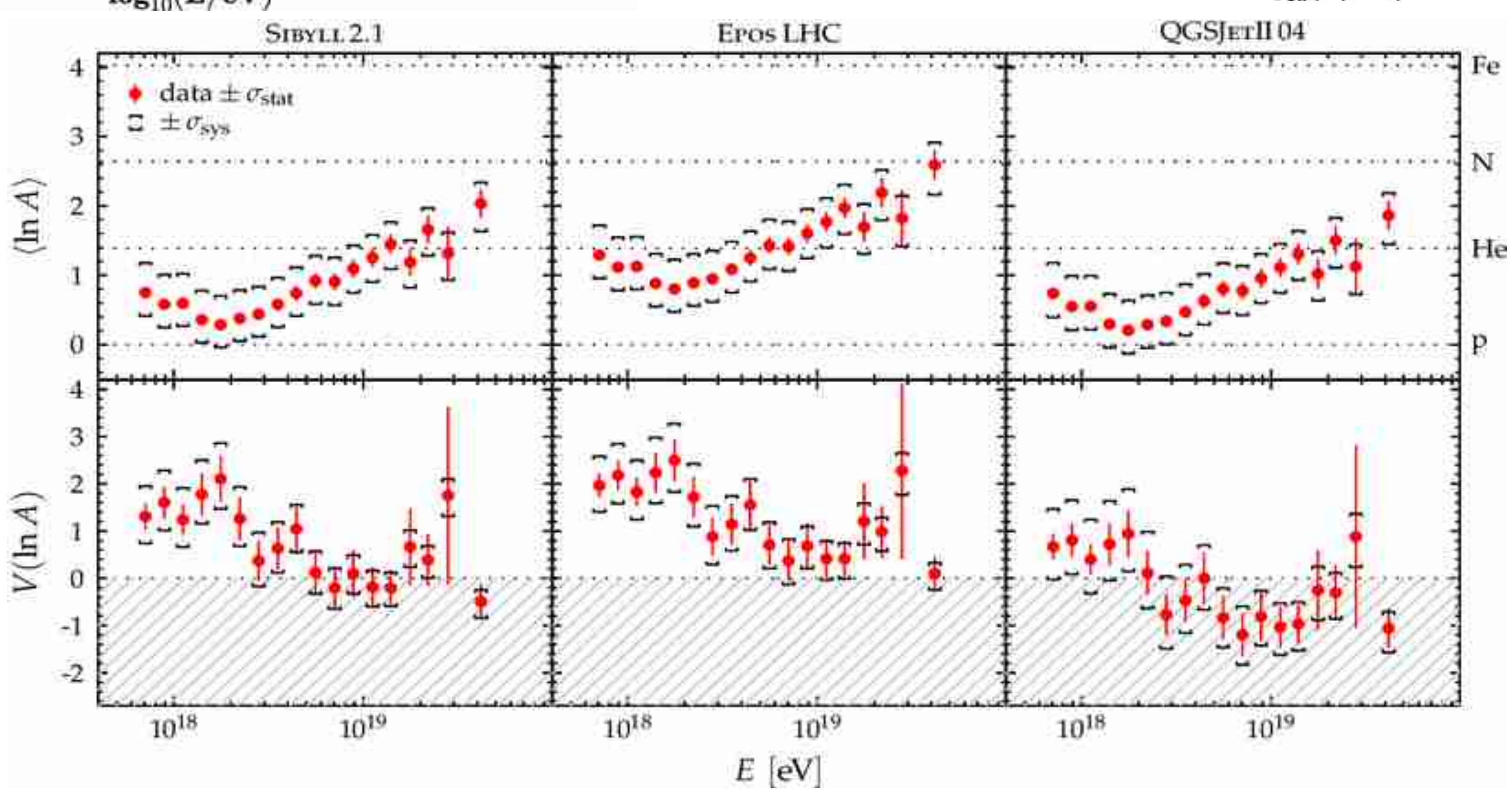

HECR Physics at LHC: LHCf Physics

Model-originated uncertainties or even discrepancies

- Energy
  - $E_{SD} > E_{FD}$: discrepancy
  - missing energy (μ,ν) in FD : uncertainty
- Mass
  - Mass vs. X_{max} in FD: uncertainty
  - Mass vs. e/μ or μ excess in SD : discrepancy

p-Pb

④ secondary interactions nucleon, π

⑤ Nuclear effects

p-p + p-Pb

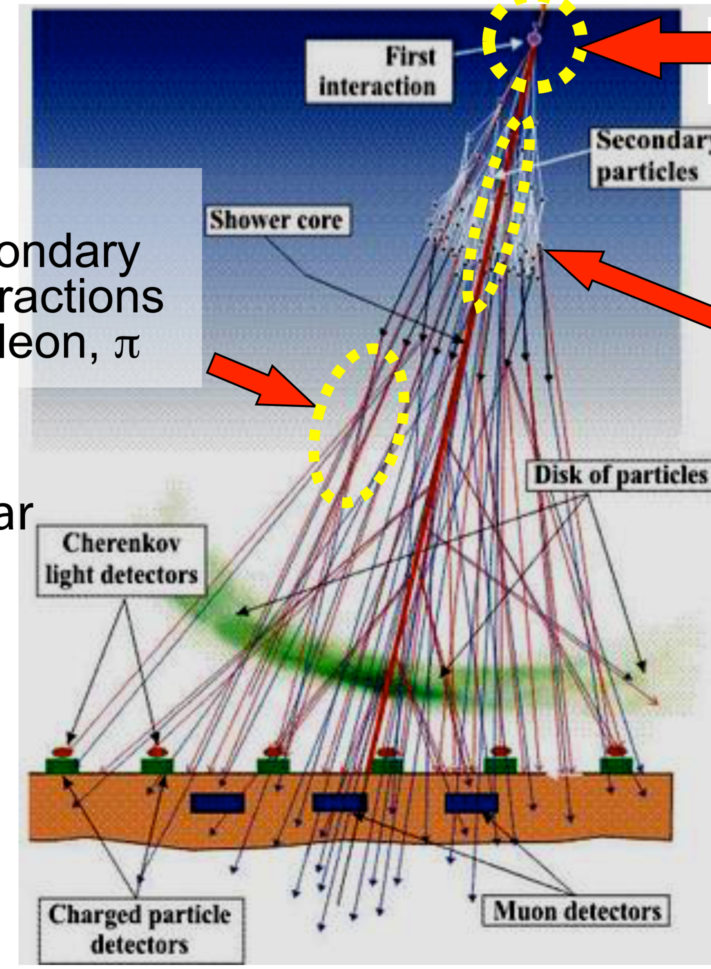

① Inelastic cross section

If large σ: rapid development
If small σ: deep penetrating

② **Forward energy spectrum**

If softer shallow development
If harder deep penetrating

③ **Inelasticity** **$k=1-E_{lead}/E_{avail}$**

If large k (π^0s carry more energy) rapid development
If small k (baryons carry more energy) deep penetrating

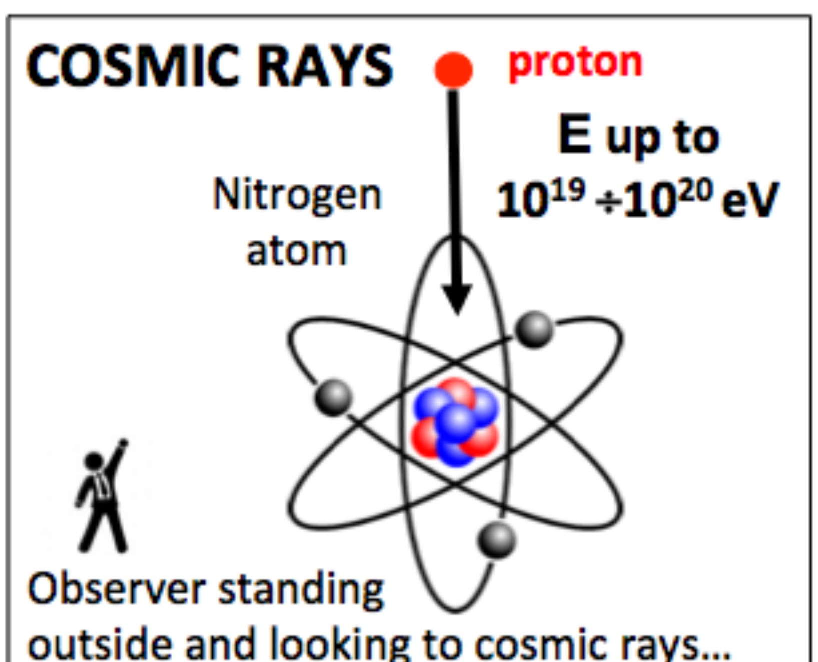

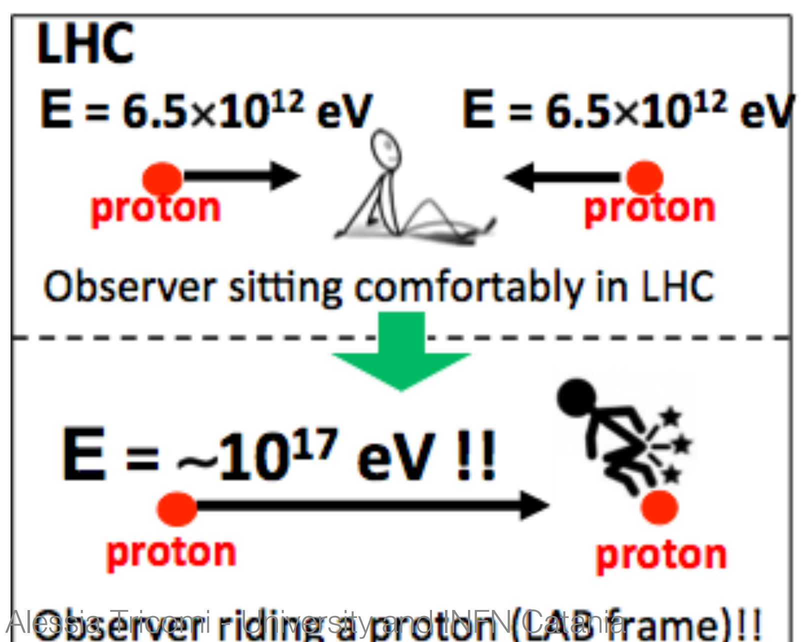

LHCf —>use LHC

6.5 TeV+6.5 TeV⇒$E_{lab}=9*10^{16}$ eV

3.5 TeV+3.5 TeV⇒$E_{lab}=2.6*10^{16}$ eV

450 GeV+450 GeV⇒$E_{lab}=2*10^{14}$ eV

to calibrate MCs

In addition: p-Pb collision at 5.02&8TeV to study nuclear effect

Alessia Tricomi University and INFN Catania

First models tuning after the first LHC data (EPOS and QGSJET)

Mean depth of shower maximum: Number of muons on ground:

(pre-LHC)

(post-LHC)

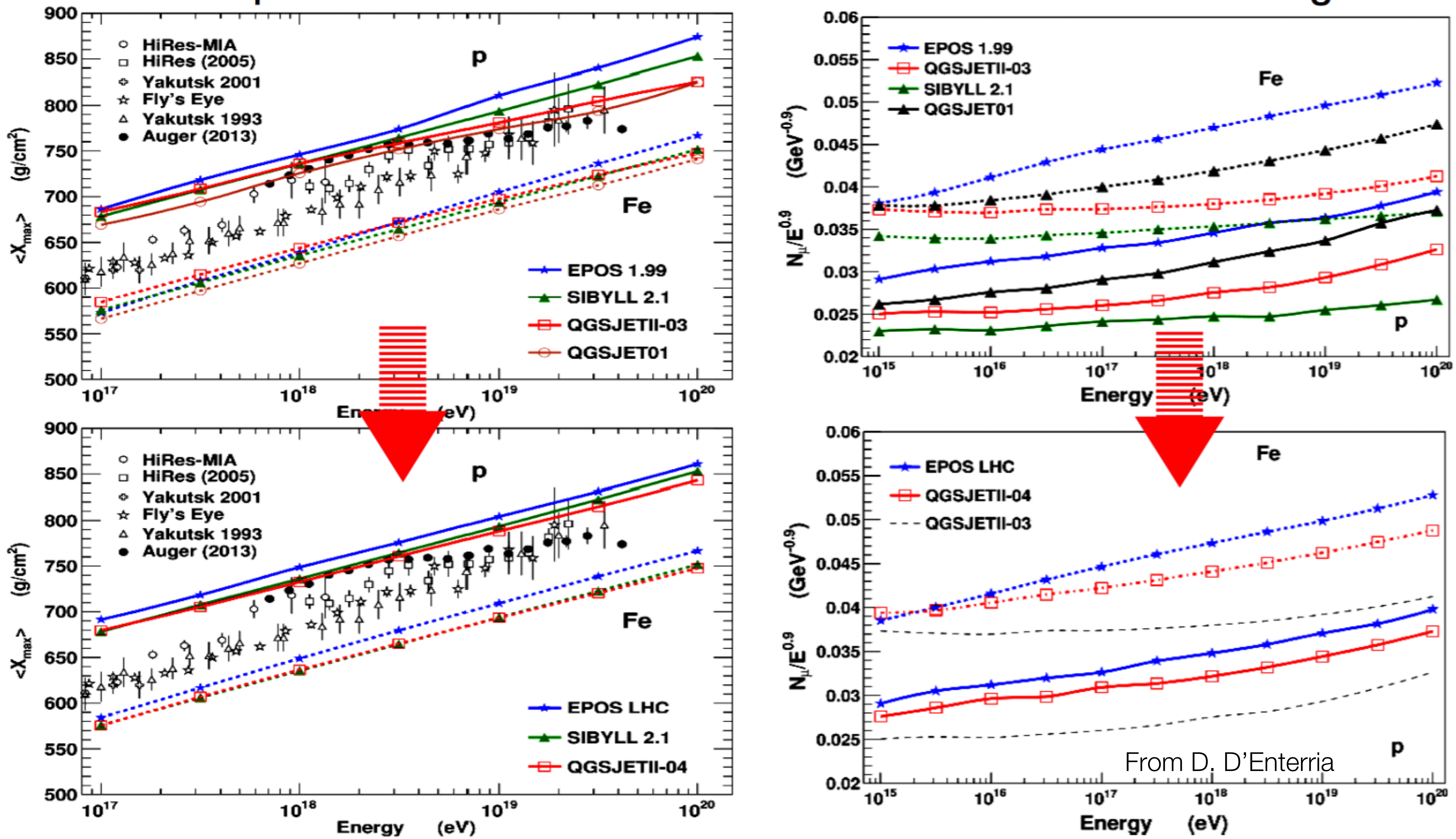

Significant reduction of differences btw different hadronic interaction models!!!

But not everything is perfect….

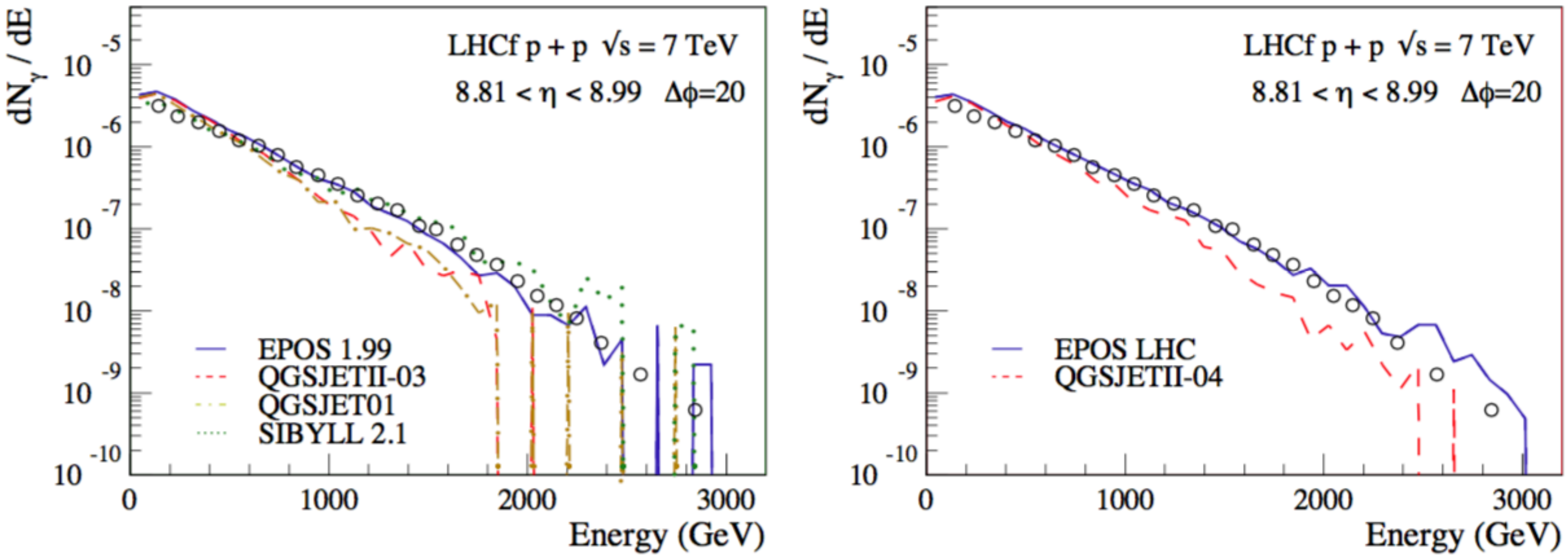

(Pierog 2014)

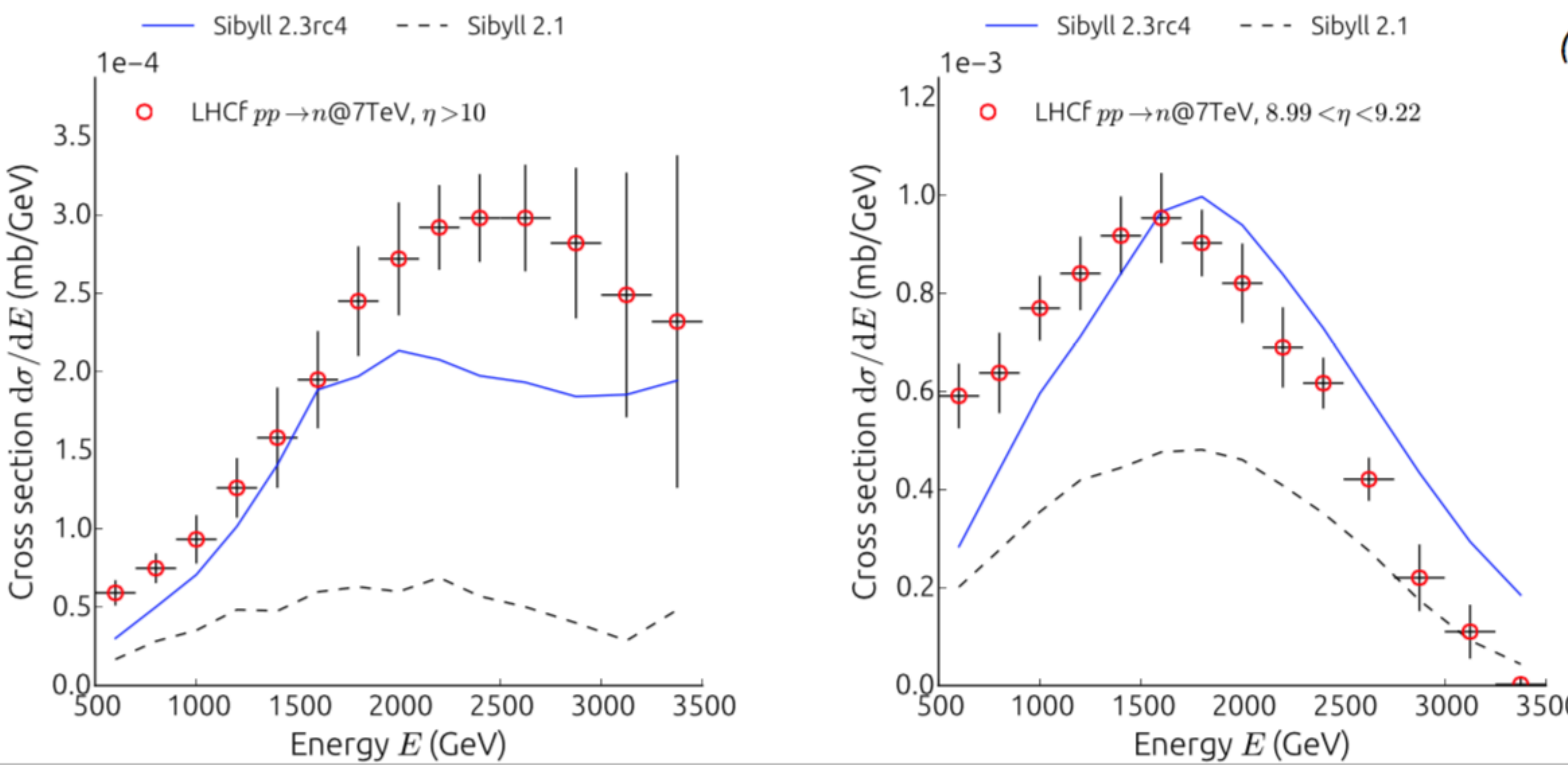

(Riehn 2015)

But…

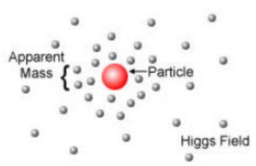

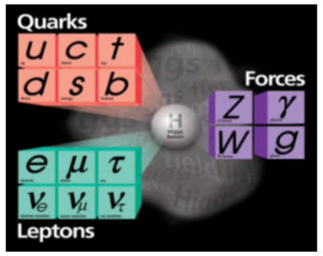

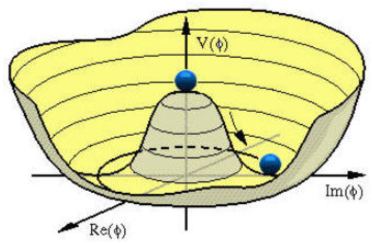

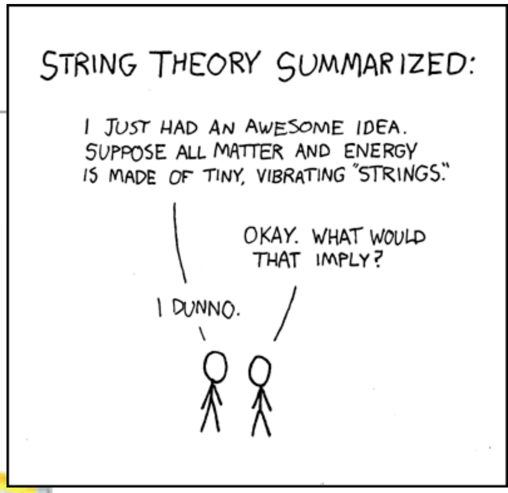

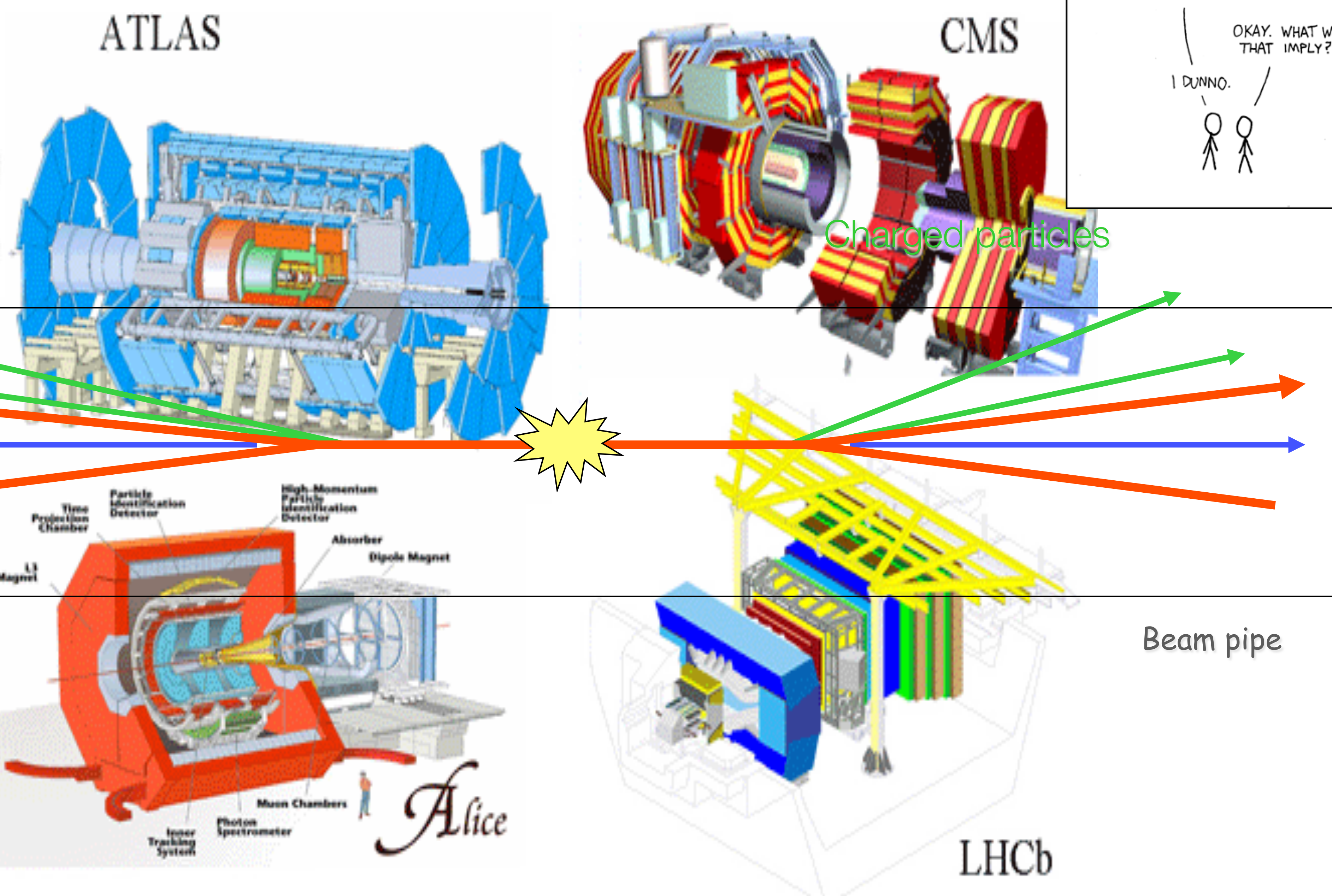

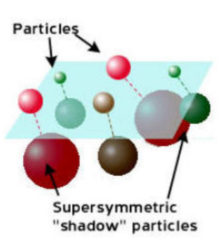

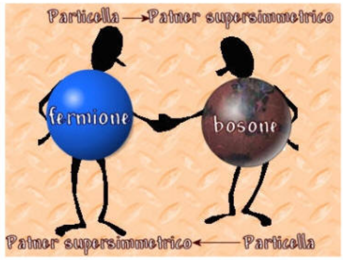

General purpose detectors (ATLAS, CMS,…) cover only the central region

Special detectors to access forward particles are necessary

How to access Very Forward Physics at LHC?

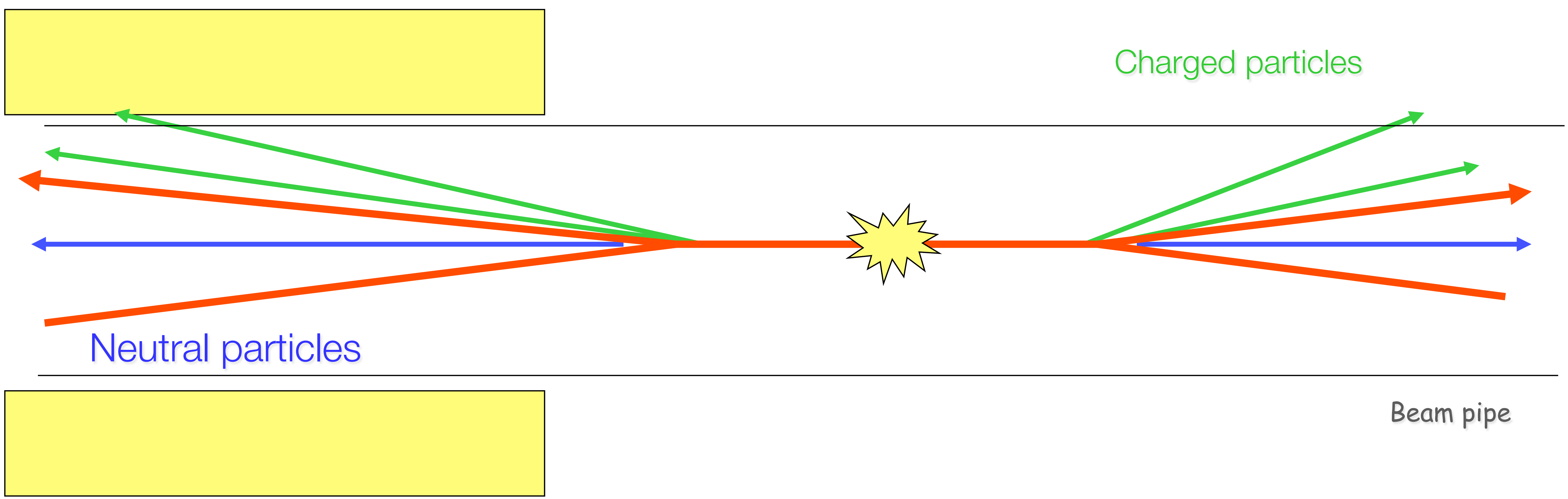

Surrounding the beam pipe with detectors
Simple way, but still miss very very forward particles

How to access Very Forward Physics at LHC?

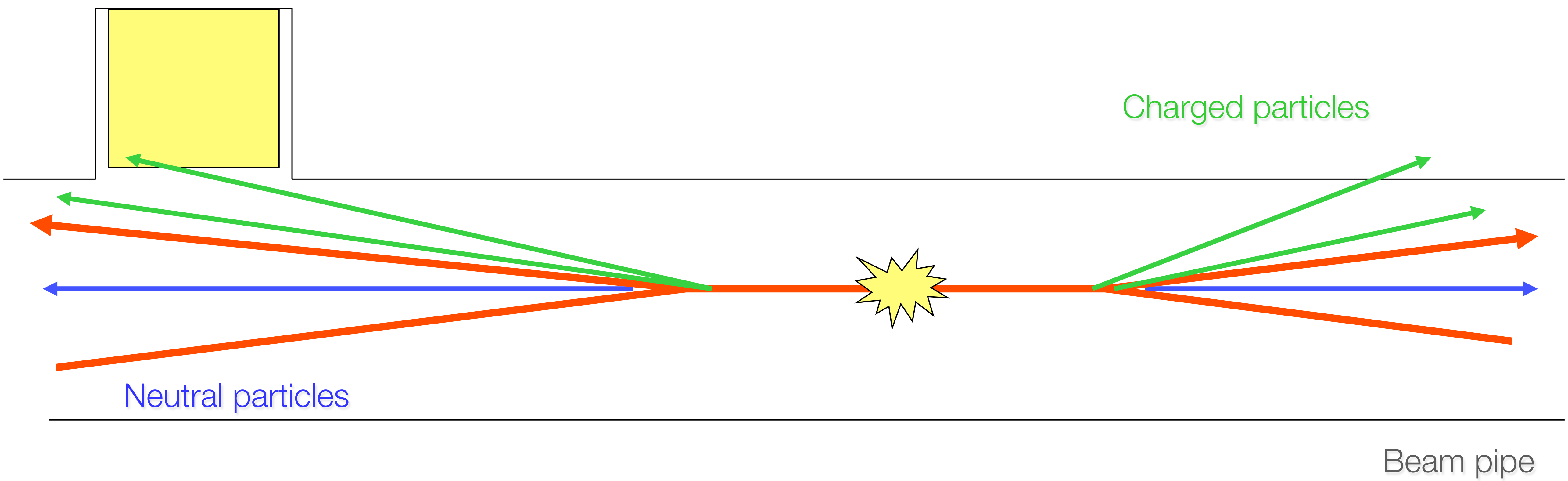

Install detectors inside the beam pipe
Challenging but ideal for charged particle
(TOTEM)

How to access Very Forward Physics at LHC?

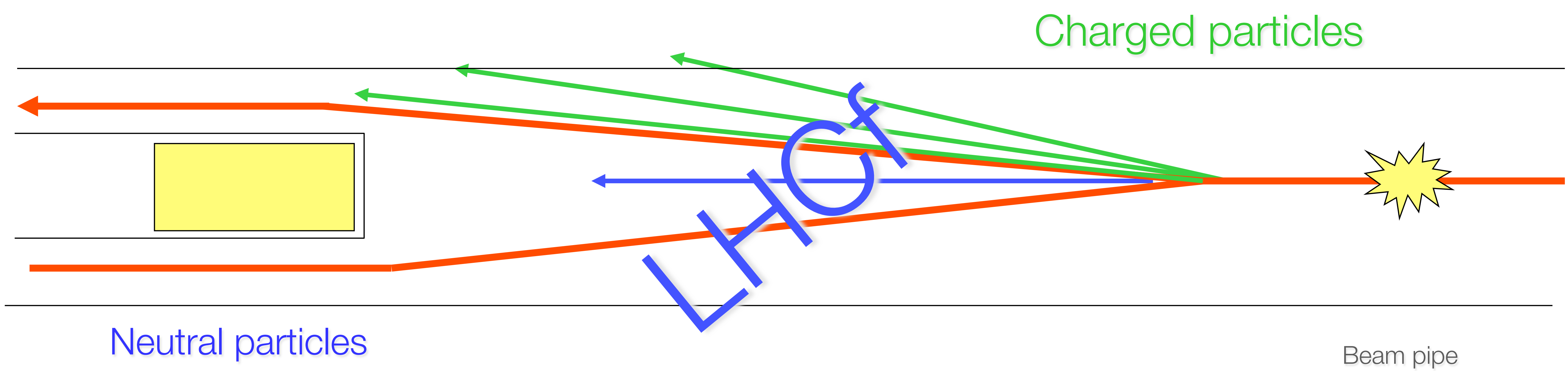

Y shape chamber enables us whole neutral measurements
Zero Degree Calorimeters

LHC phase space coverage

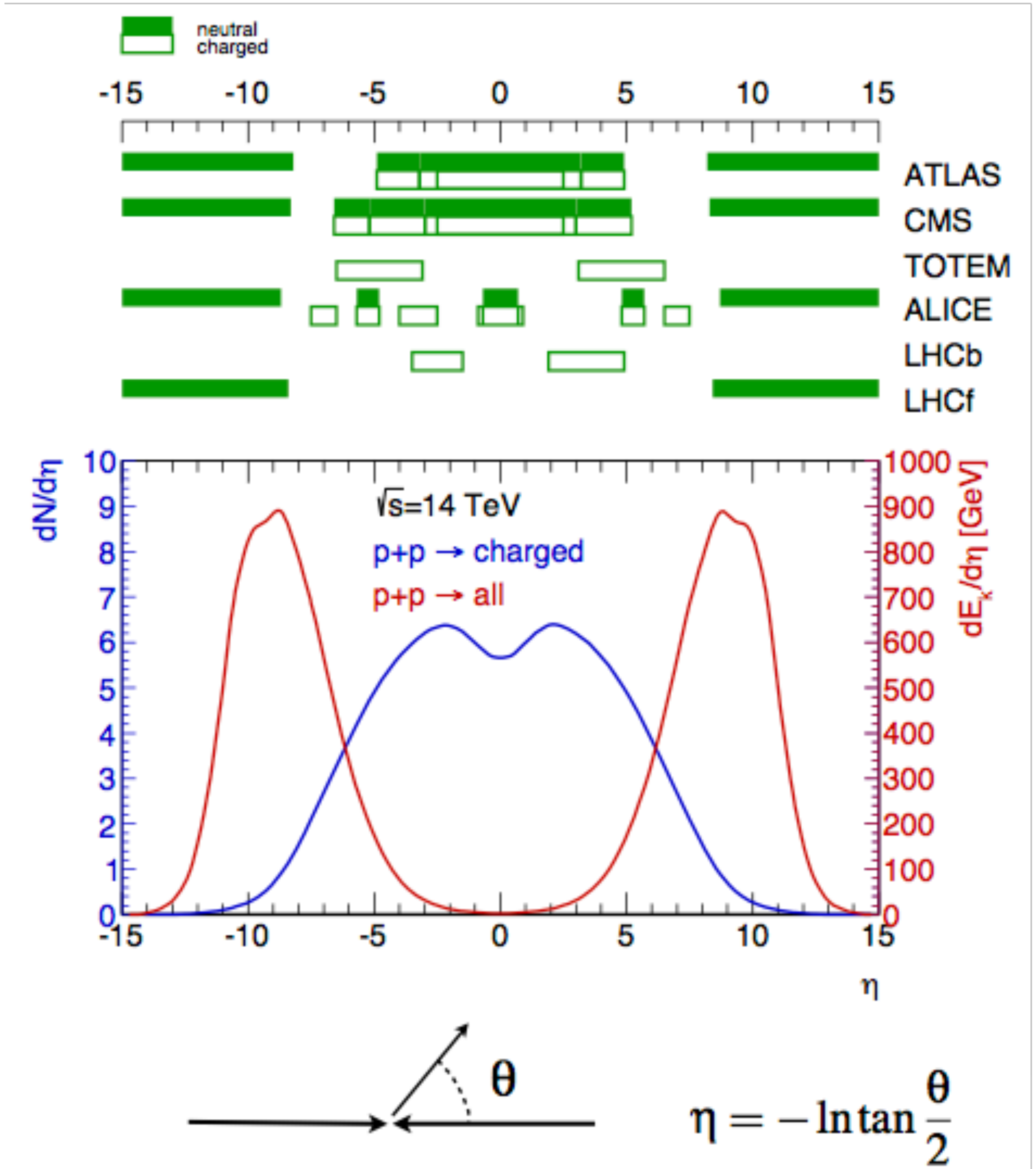

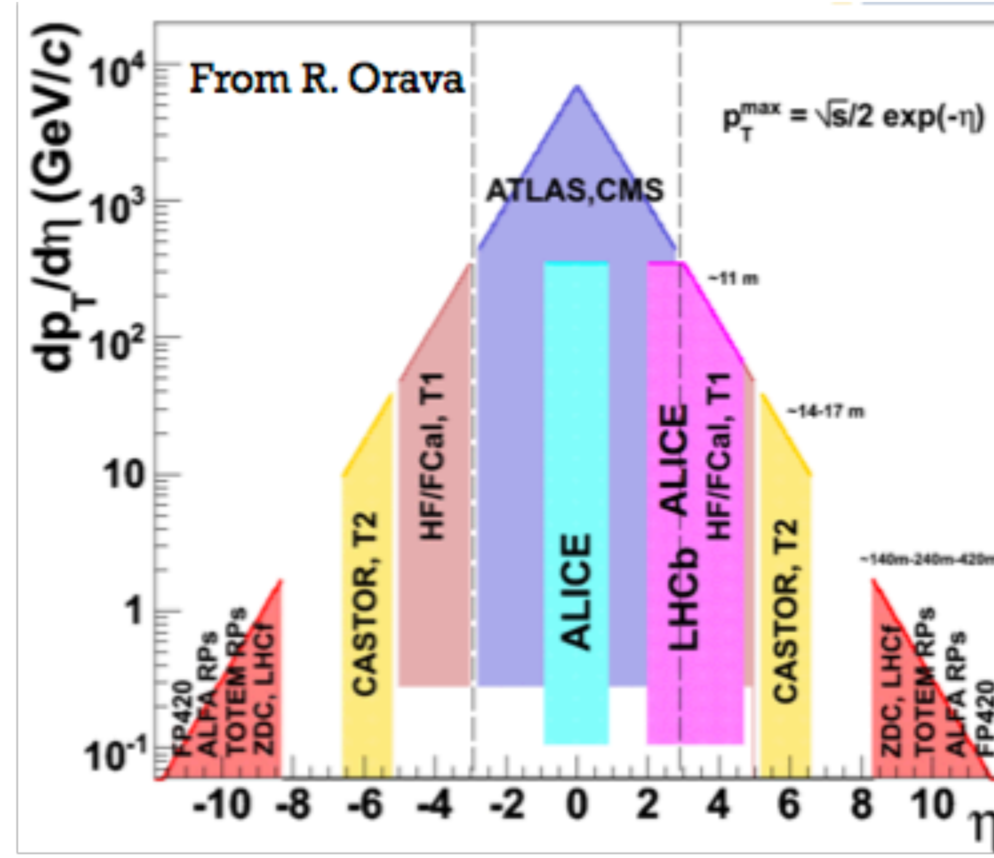

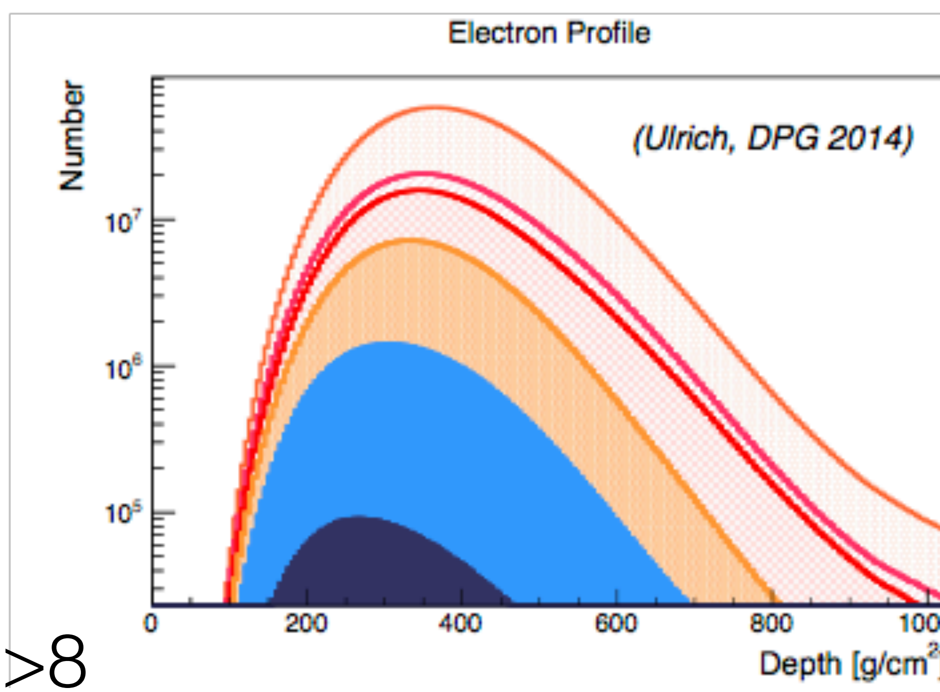

We are profiting of the broad coverage at LHC however more than 50% of the showers from η>8

→ Dedicated fwd experiments crucial!

LHCf: location and detector layout

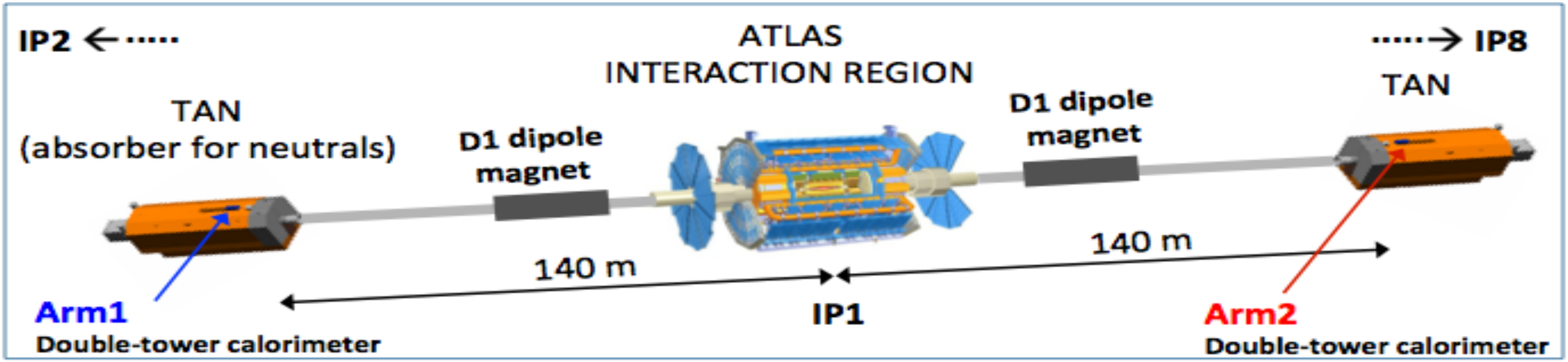

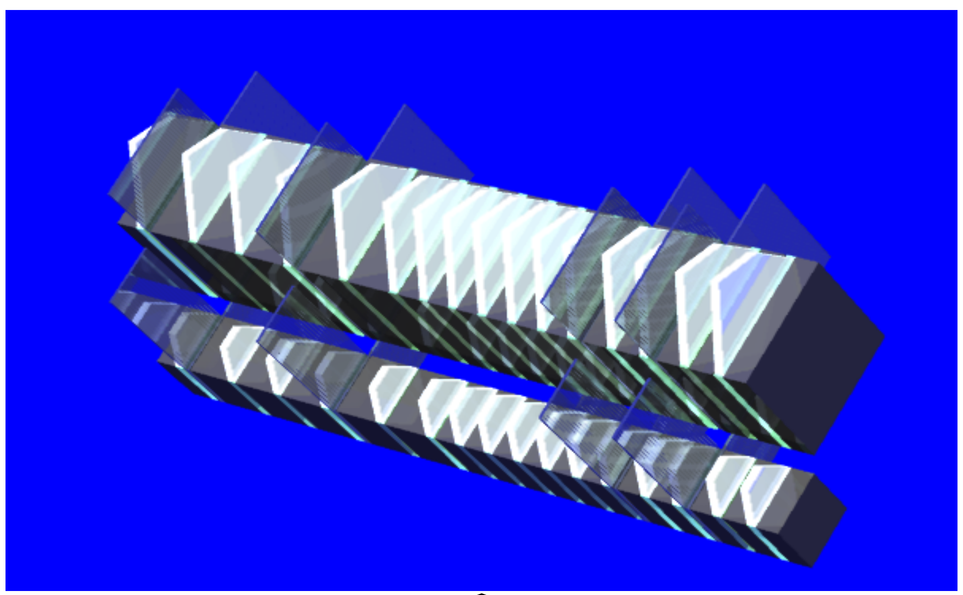

Arm#1 Detector
20mmx20mm+40mmx40mm
4 X-Y GSO Bars tracking layers

$44X_0$,
$1.6\ \lambda_{int}$

Energy resolution:
< 5% for photons
30% for neutrons
Position resolution:
< 200μm (Arm#1)
40μm (Arm#2)
Pseudo-rapidity range:
η > 8.7 @ zero Xing angle
η > 8.4 @ 140urad

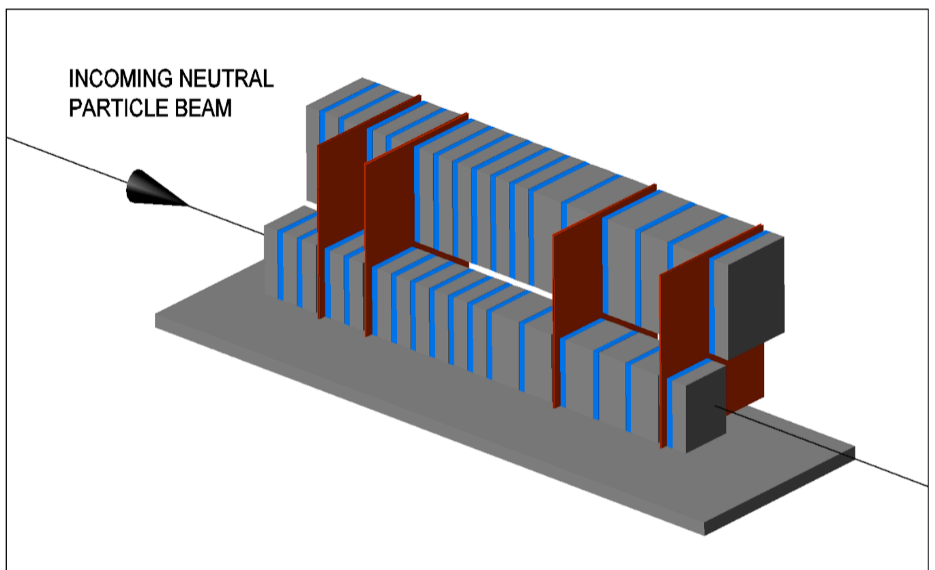

Arm#2 Detector
25mmx25mm+32mmx32mm
4 X-Y Silicon strip tracking layers

Event category in LHCf

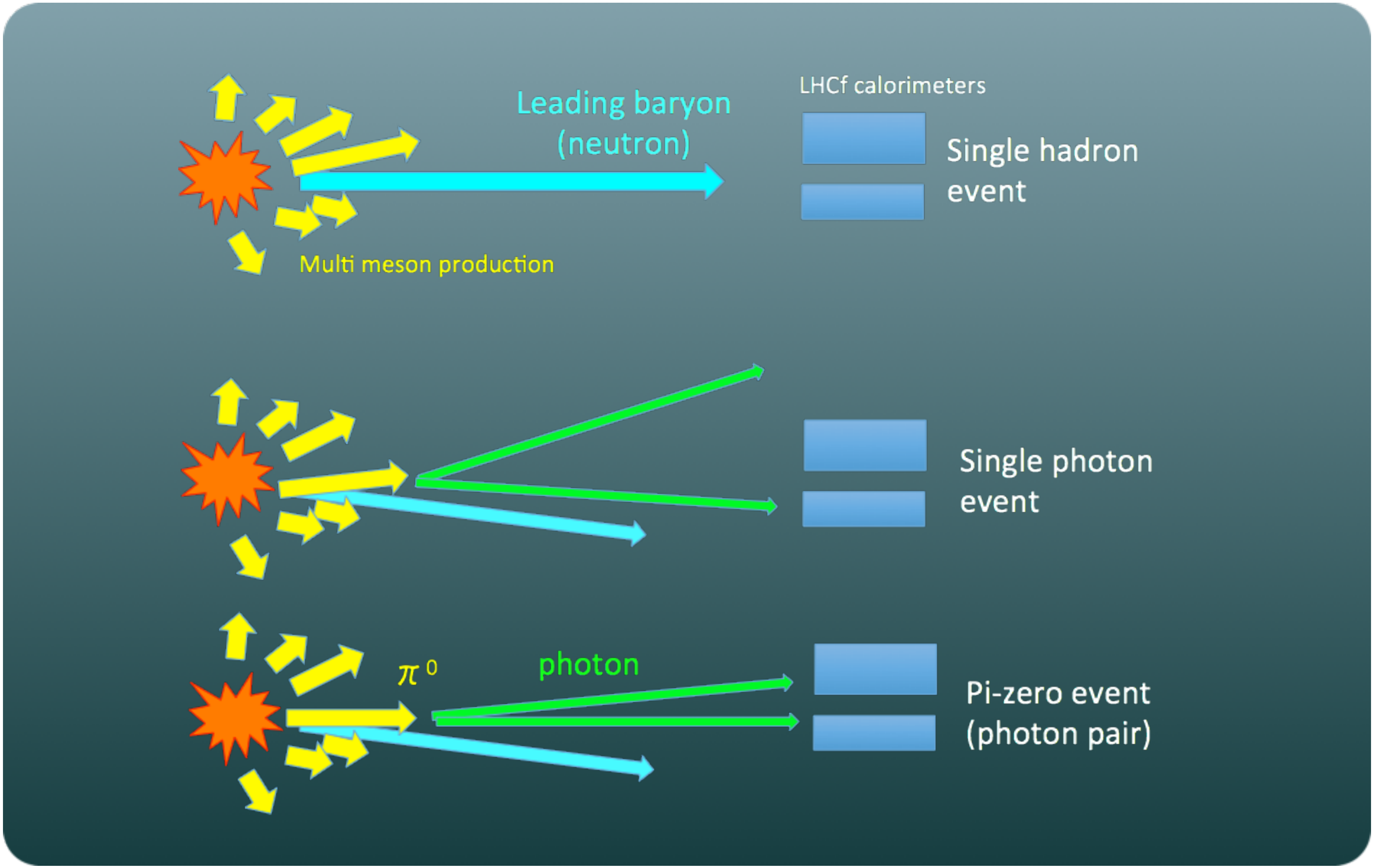

Event category in LHCf

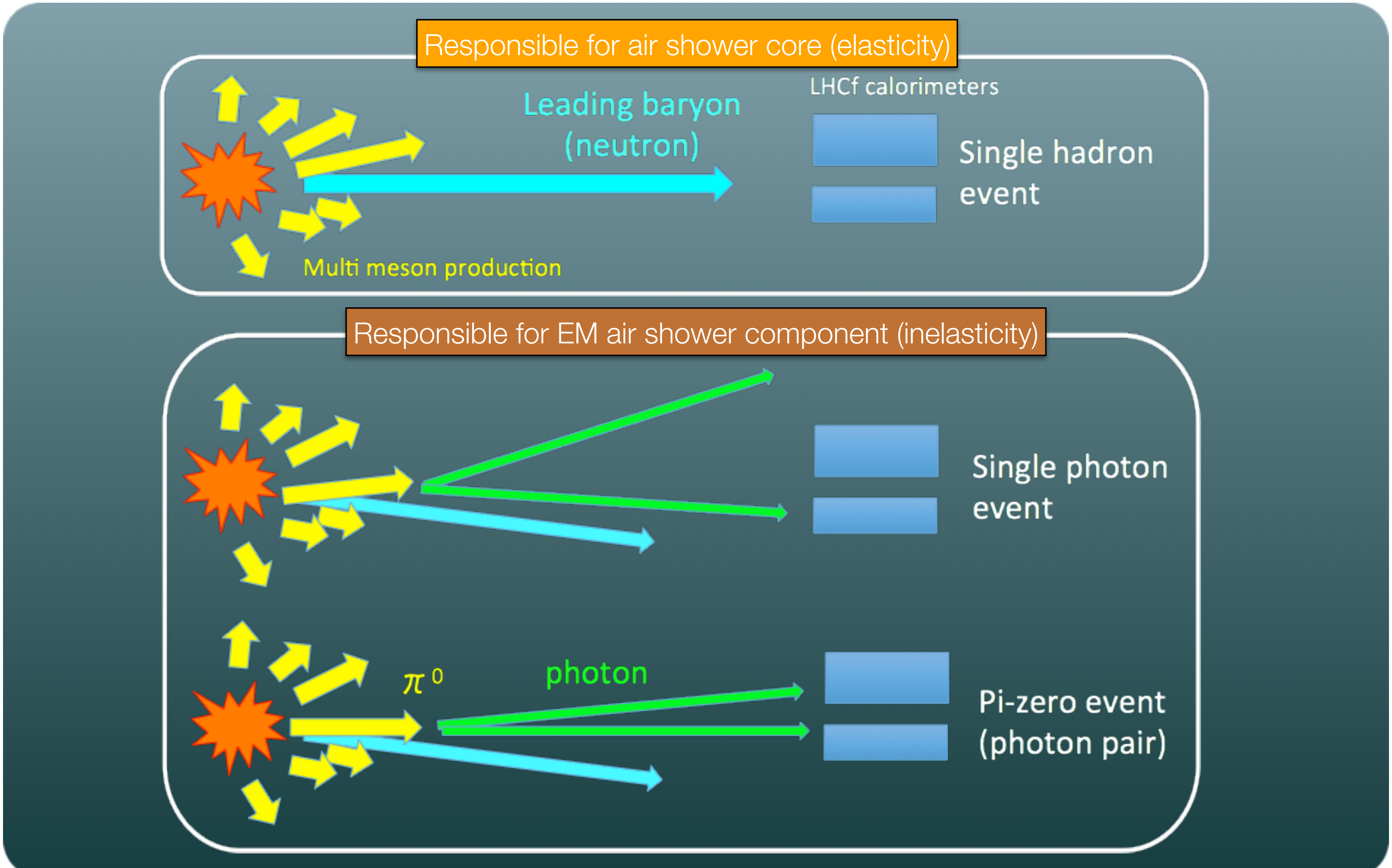

LHCf Data Taking and Analysis matrix

	Proton ELAB (Ev)	Photon (EM shower)	Neutron (hadron shower)	π^0 (EM shower)
Test beam at SPS		NIM. A 671, 129–136 (2012) JINST 12P03023(2017)	JINST 9 P03016 (2014) (2014)P03016	
p-p at 900GeV	4.3×10^{14}	Phys. Lett. B 715, 298-303 (2012)		
p-p at 7TeV	2.6×10^{16}	Phys. Lett. B 703, 128–134 (2011)	Phys. Lett. B 750, 360-366 (2015)	Phys. Rev. D 86, 092001 (2012)+ Phys. Rev. D 94, 032007(2016) Type II
p-p at 2.76TeV	4.1×10^{15}			Phys. Rev. C 89, 065209 (2014)+ Phys. Rev. D 94, 032007(2016) Type II
p-Pb at 5.02TeV	1.3×10^{16}			
p-p at 13TeV	9.0×10^{16}	Submitted to PLB	Preliiminary results	
p-Pb at 8.1 TeV	3.6×10^{16}	Run completed in November 2016		

Run1

Run2

Run3

Run4

γ energy spectra 7 vs 13 TeV

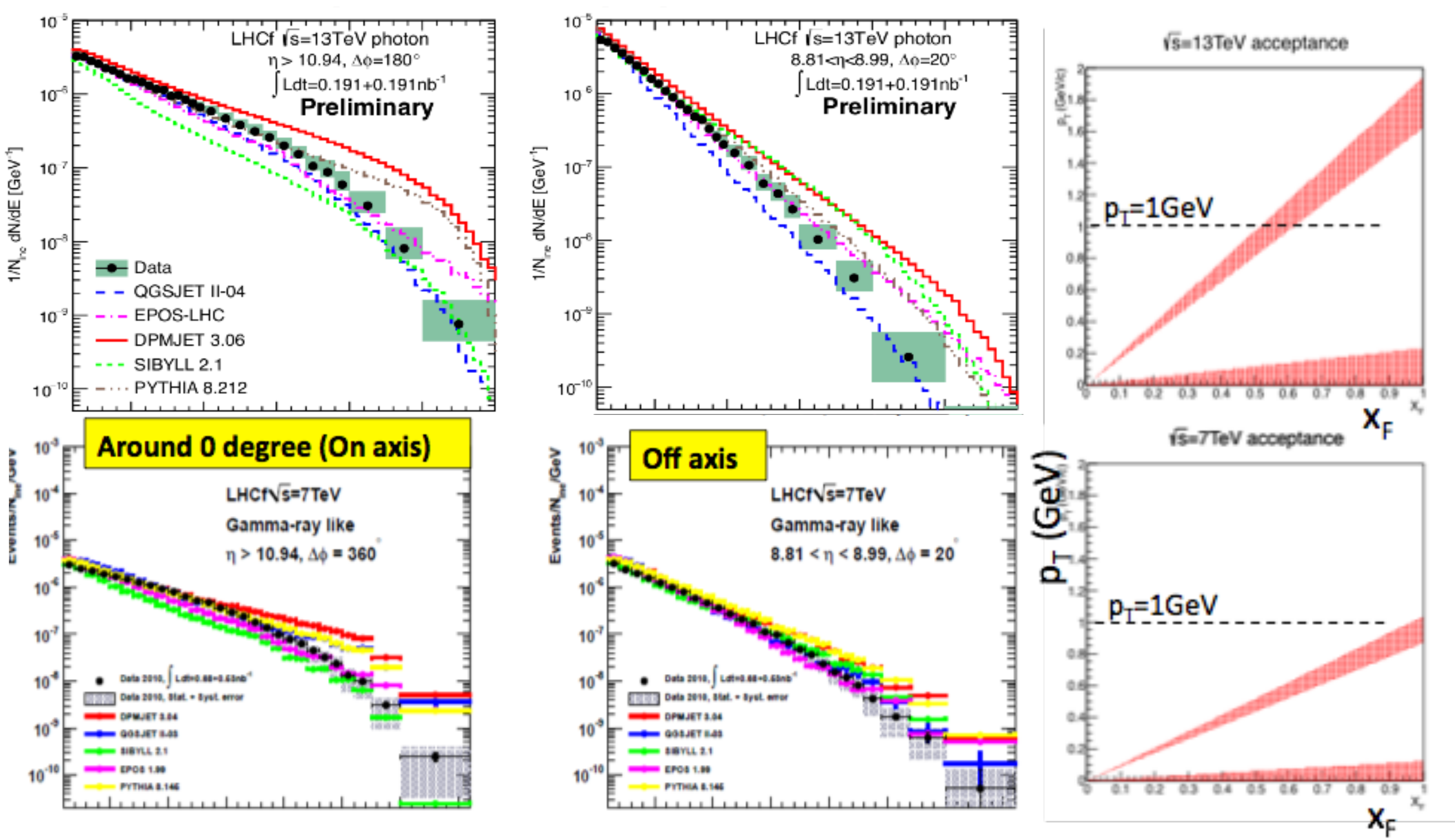

High energy data covers up to larger p_T

Similar trend in 7TeV and 13TeV, but differences look enhanced in 13TeV results

Photon spectra – Feynman Scaling

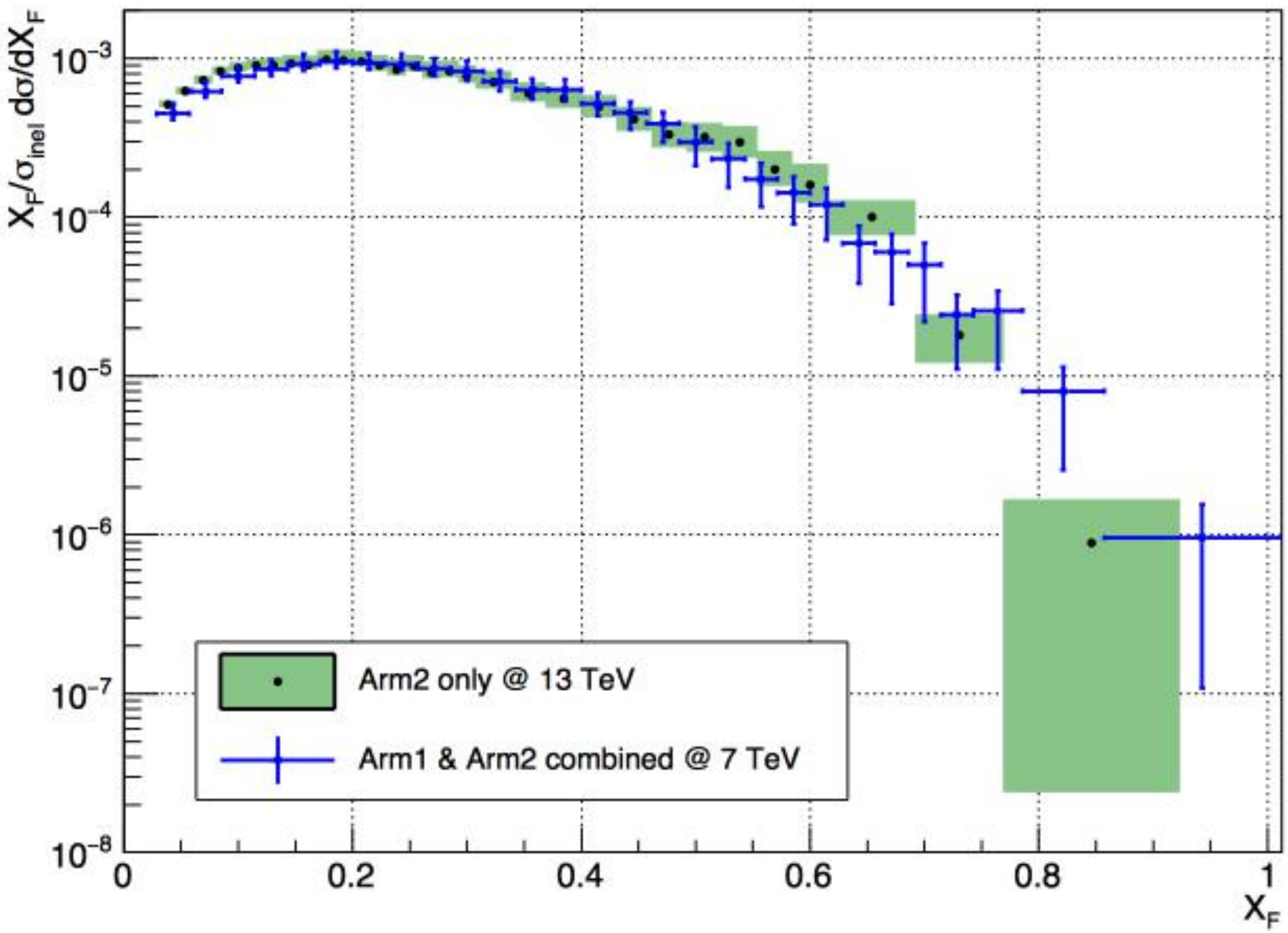

Feynman scaling: differential cross section as a function of X_F independent of $\sqrt{s}$ for X_F

Feynman scaling holds within systematic uncertainties

LHCf Type I and Type II π^0analysis

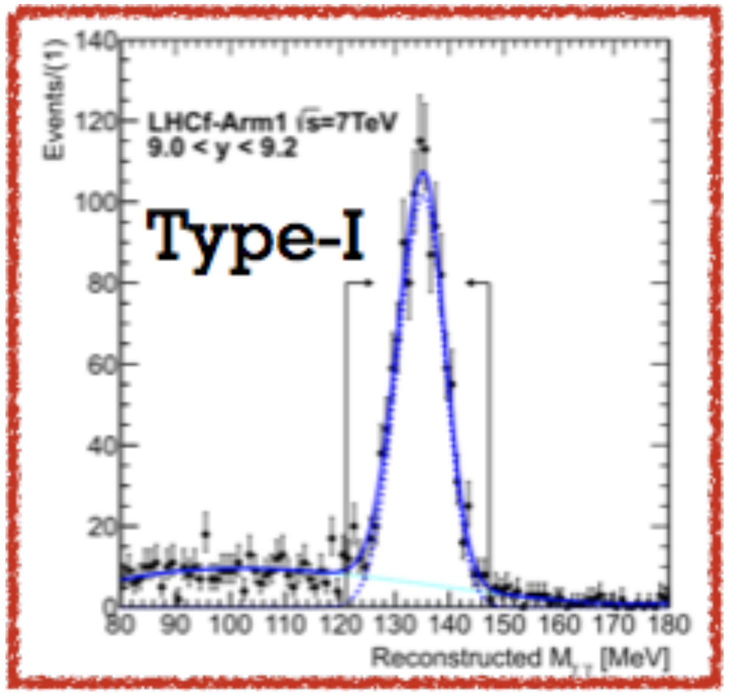

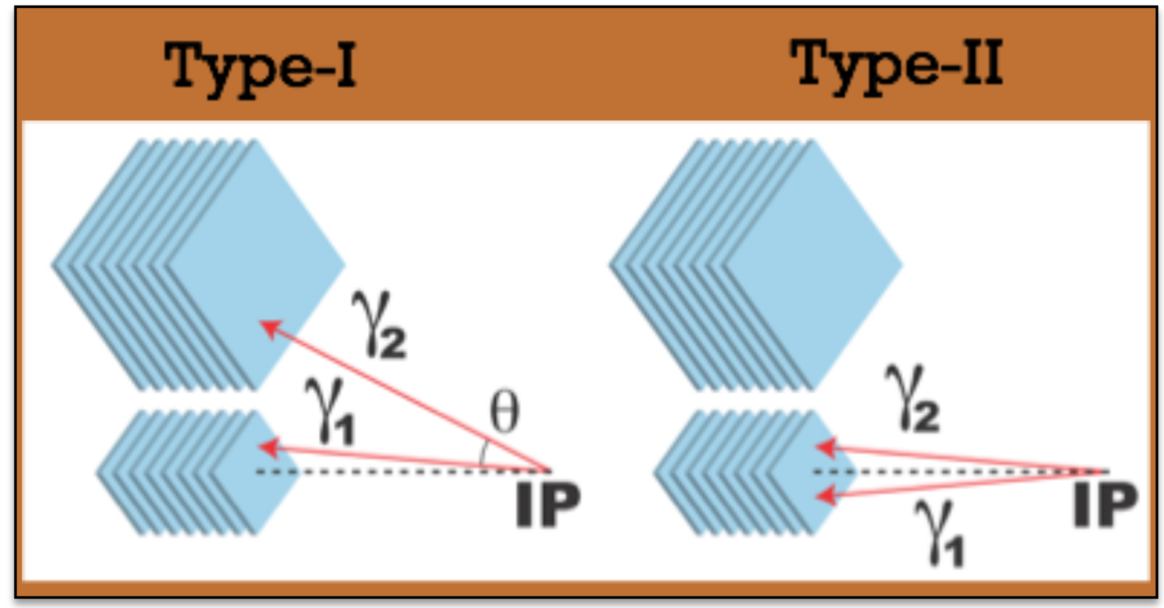

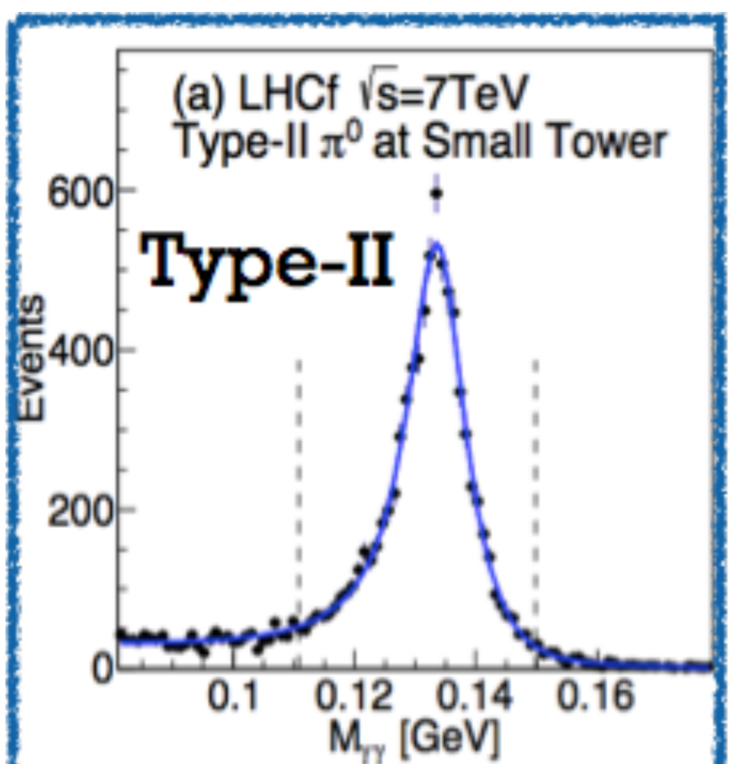

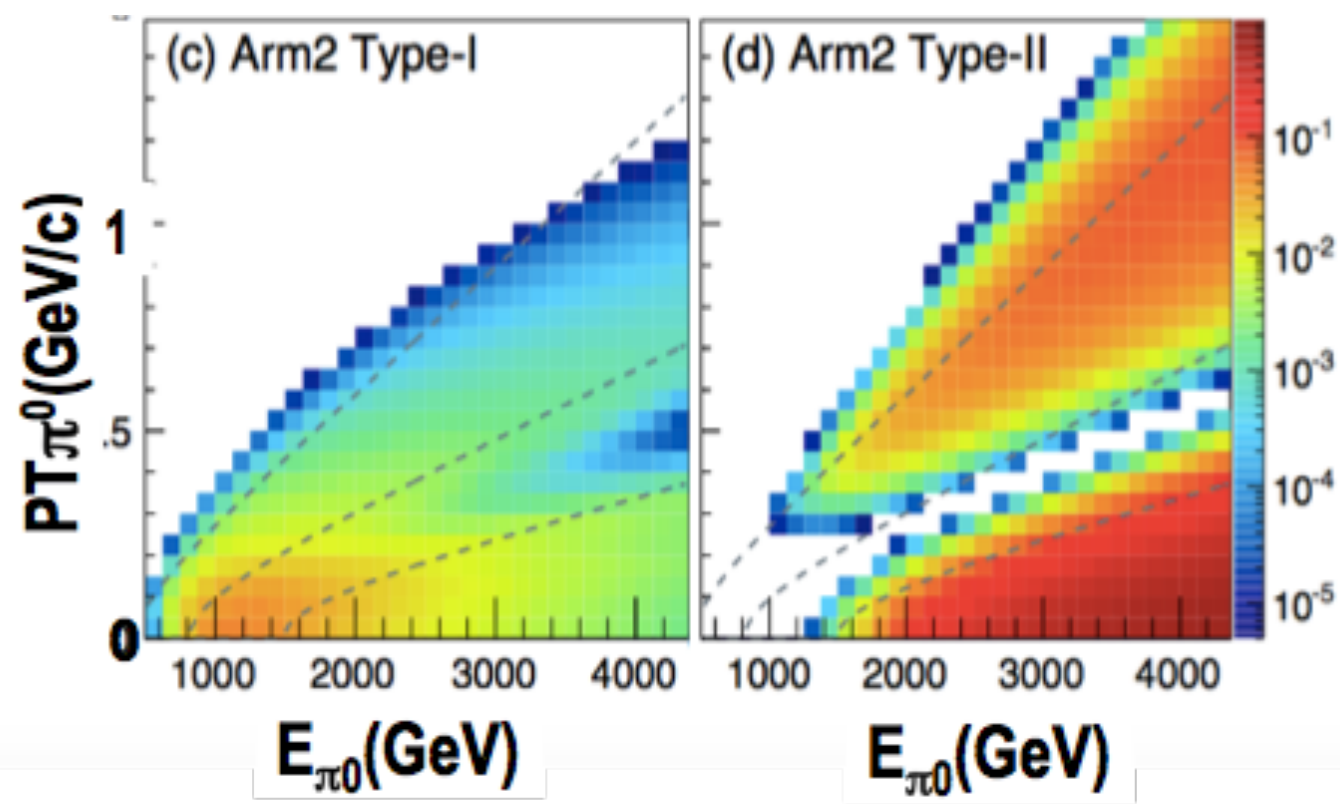

LHCf @ pp 7 TeV: π^0 p_T spectra

PRD 94 (2016) 032007

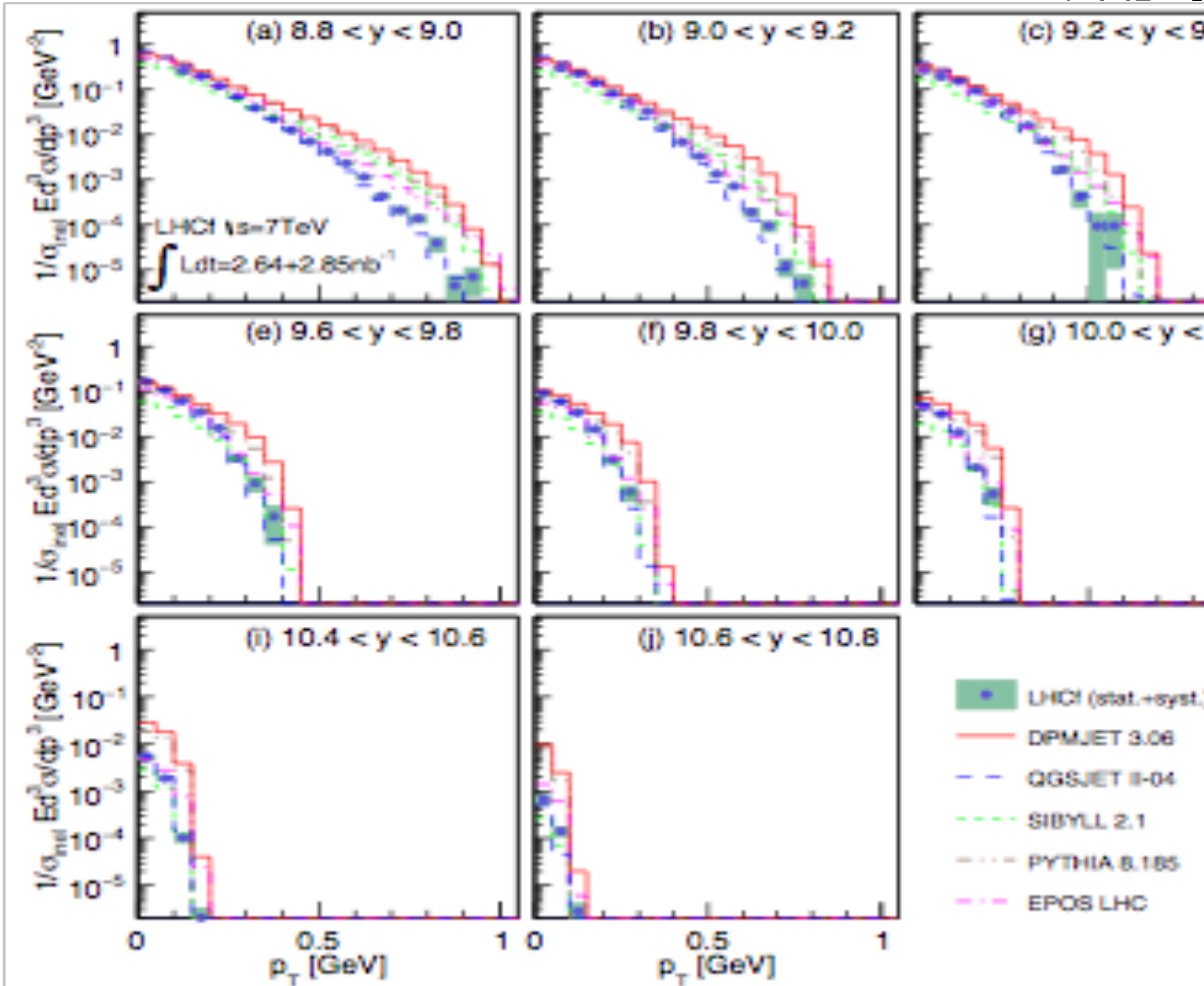

- QGSJETII-04: best agreement
- EPOS-LHC: harder than data for large p_T
- SYBILL: good agreement only for small y

LHCf @ pp 7 TeV: π^0 p_Z spectra

PRD 94 (2016) 032007

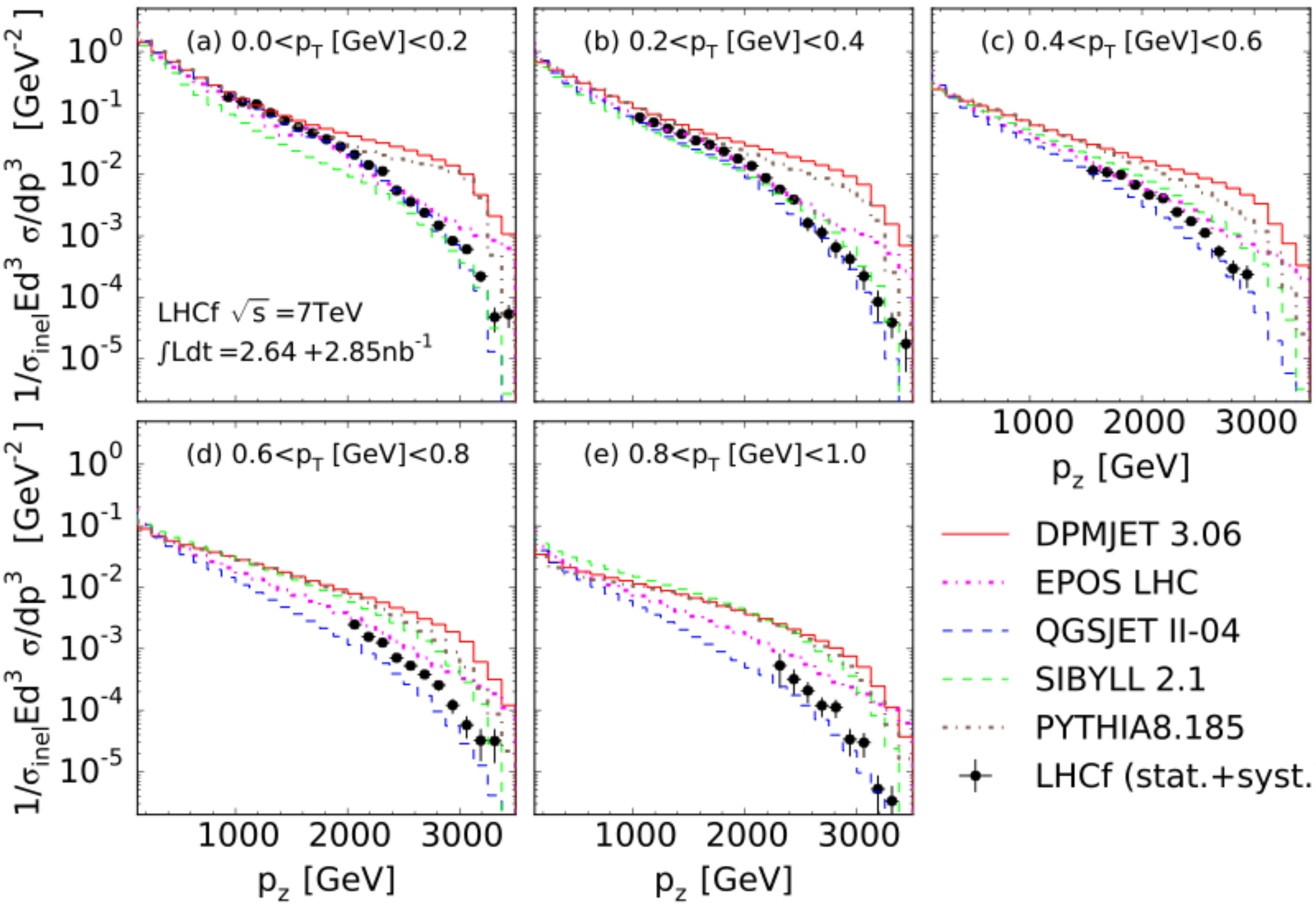

DPMJET and Pythia overestimate over all E-p_T range

LHCf @ pp 7 TeV: π^0 p_Z spectra SiBYLL 2.1

PRD 94 (2016) 032007

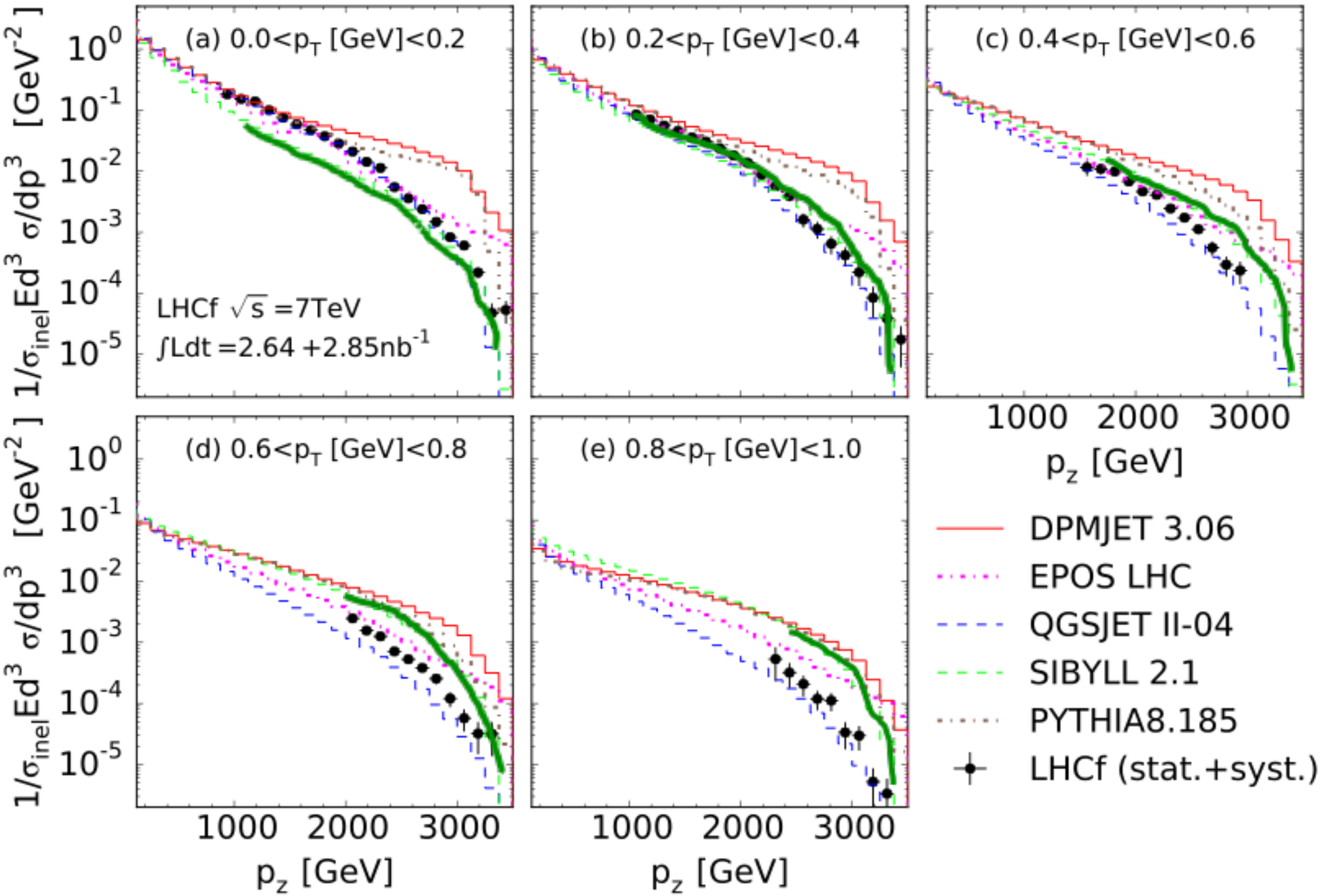

- Underestimate in low p_T, overestimate in high p_T
- Totally overestimate because of larger phase space in high p_T

LHCf @ pp 7 TeV: π^0 p_Z spectra EPOS-LHC

PRD 94 (2016) 032007

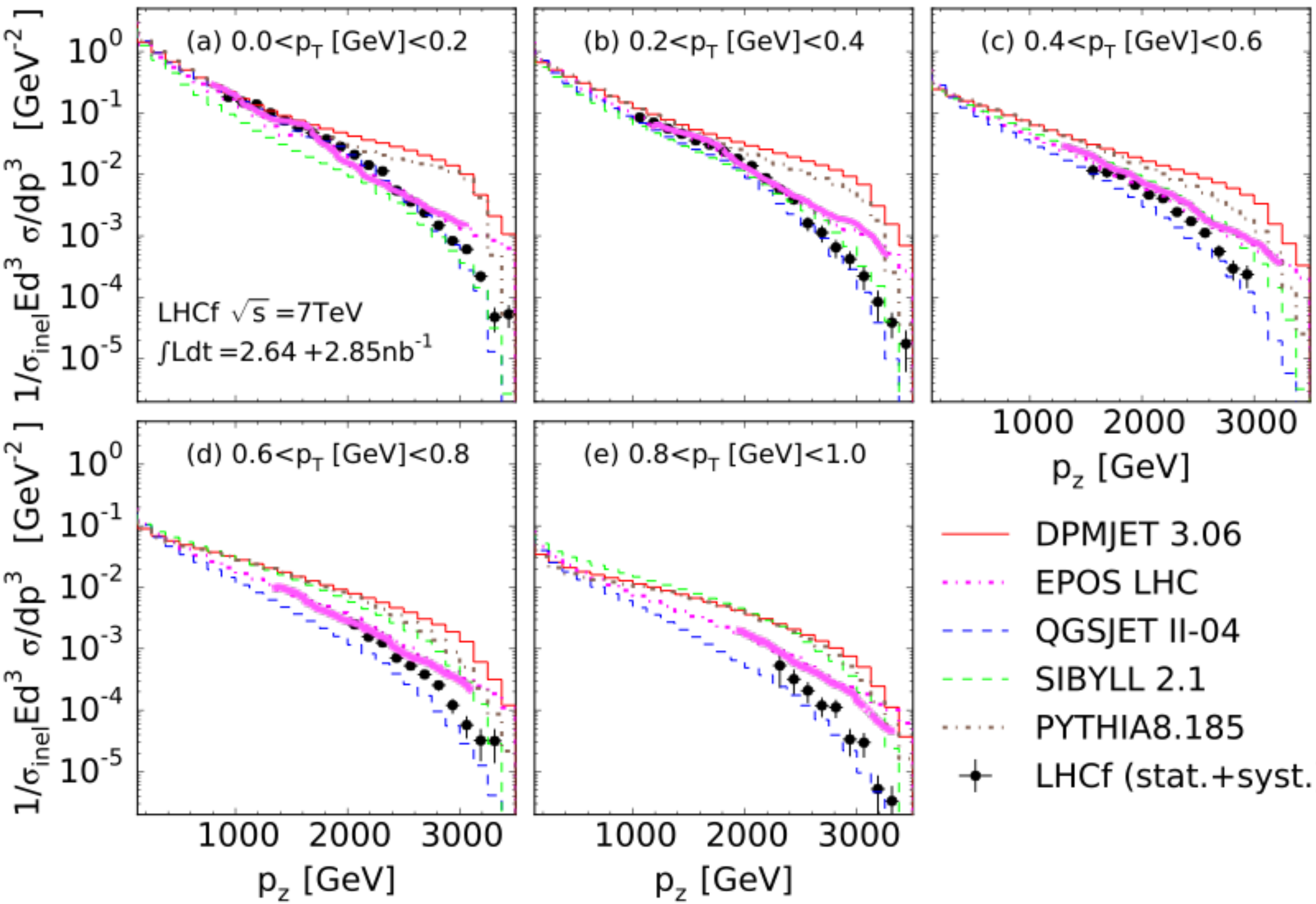

- Very good agreement at mid-energy (large cross-section range)
- Slightly overestimate at higher energy (small cross-section range)

LHCf @ pp 7 TeV: π^0 p_Z spectra QGSJET II-04

PRD 94 (2016) 032007

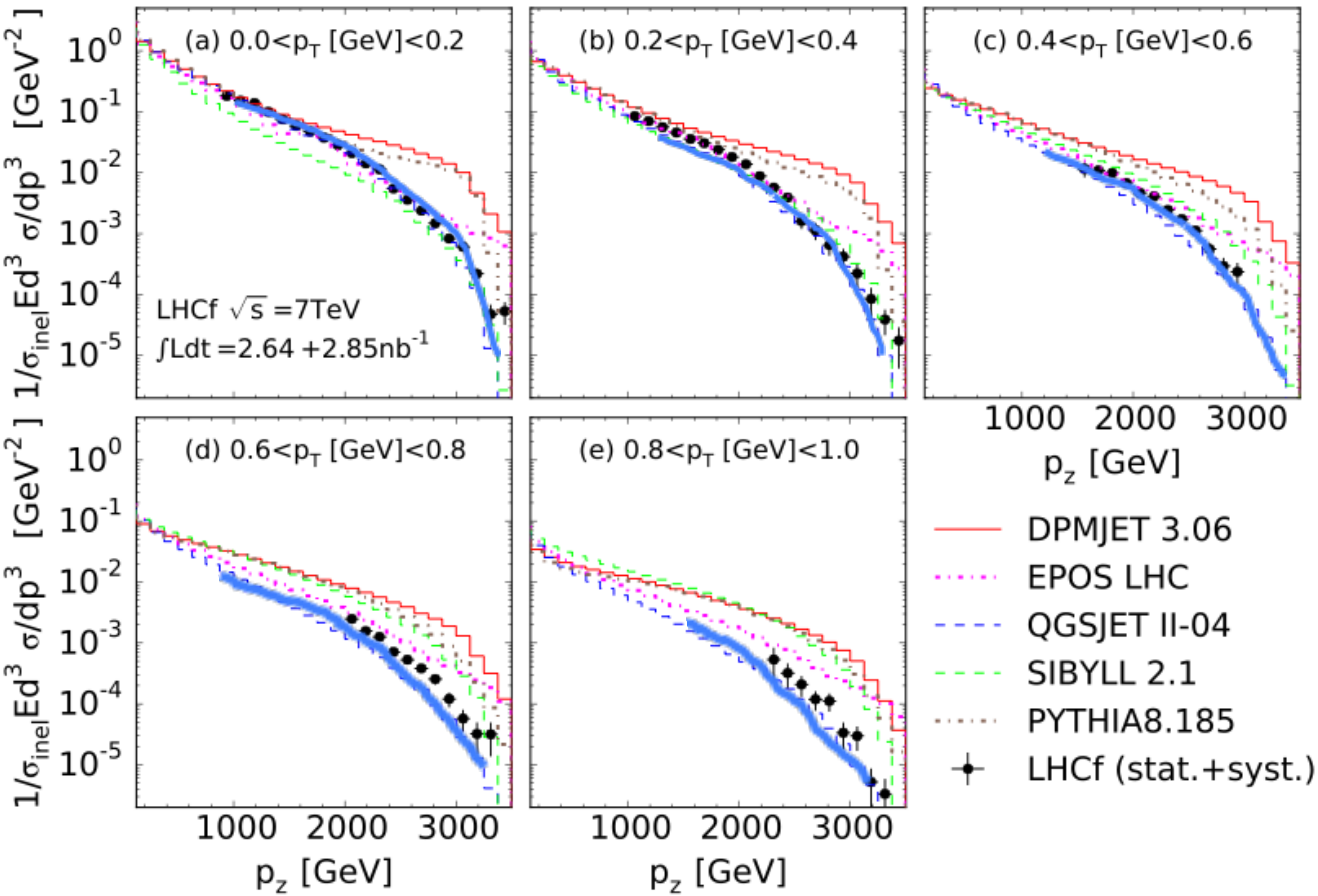

- Very good agreement in shape, slightly underestimate at high p_T
- Totally slightly underestimate

LHCf @ pp 7 TeV: π^0 data vs models

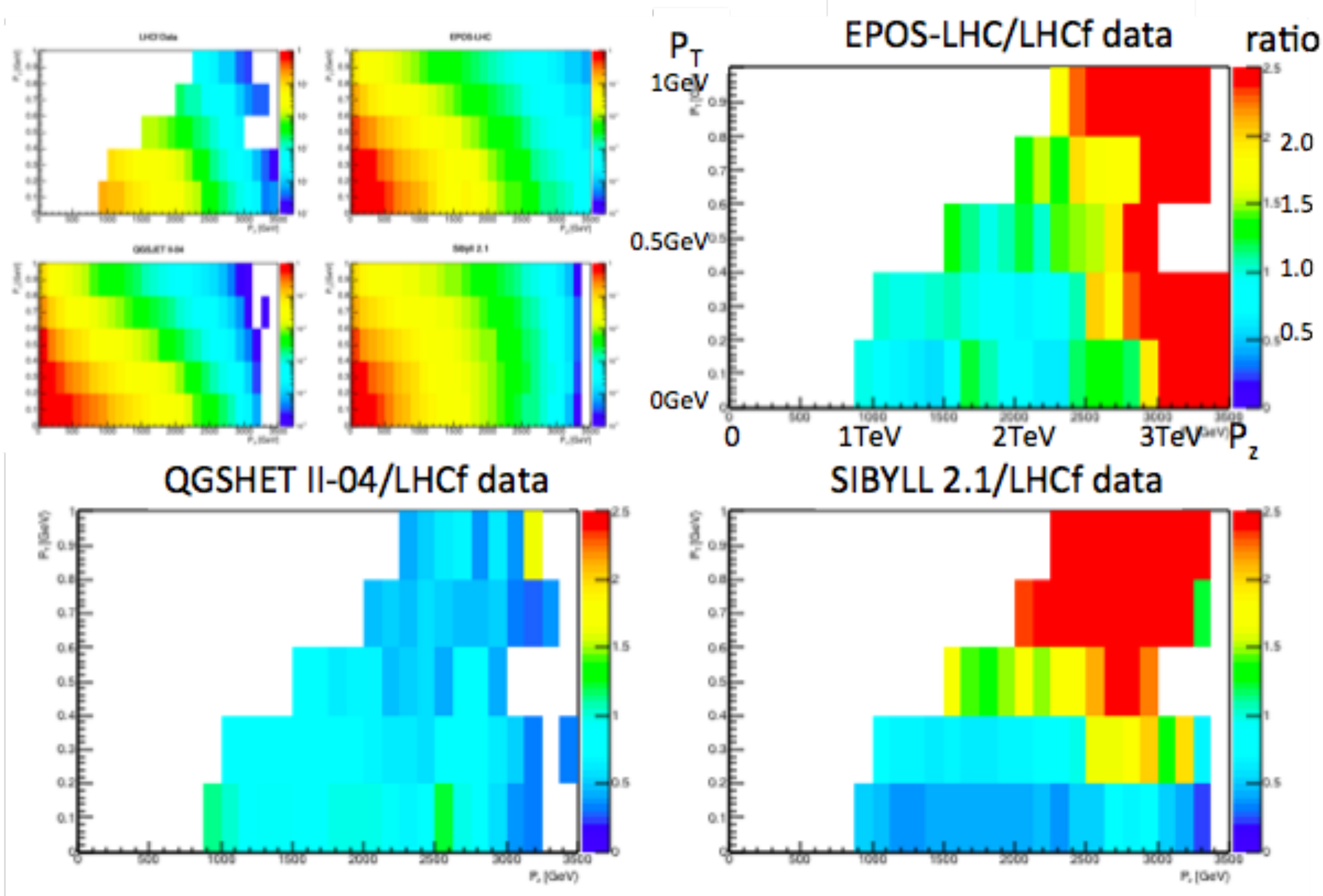

LHCf @ pp 7 TeV: neutron analysis

Motivations:

Inelasticity measurement $k=1-p_{leading}/p_{beam}$

Muon excess at Pierre Auger Observatory

- cosmic rays experiment measure PCR energy from muon number at ground and florescence light
- 20-100% more muons than expected have been observed

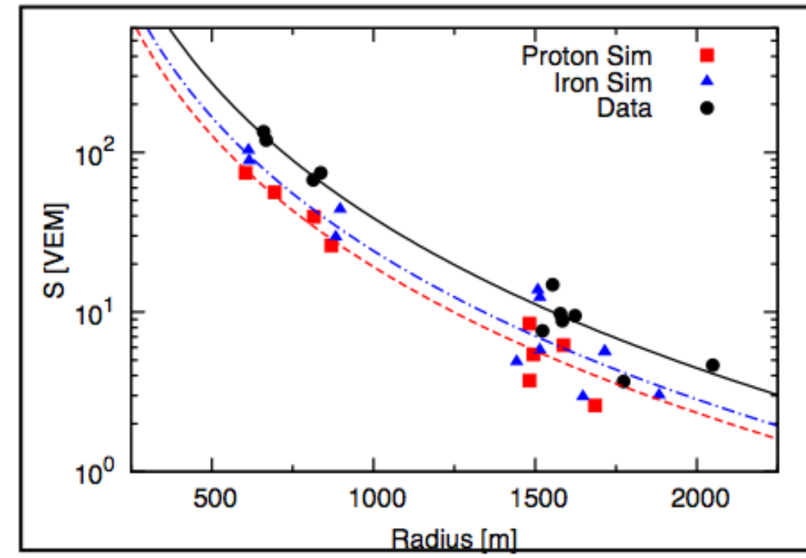

[J.Allen, et al. ICRC2011 Proceedings]

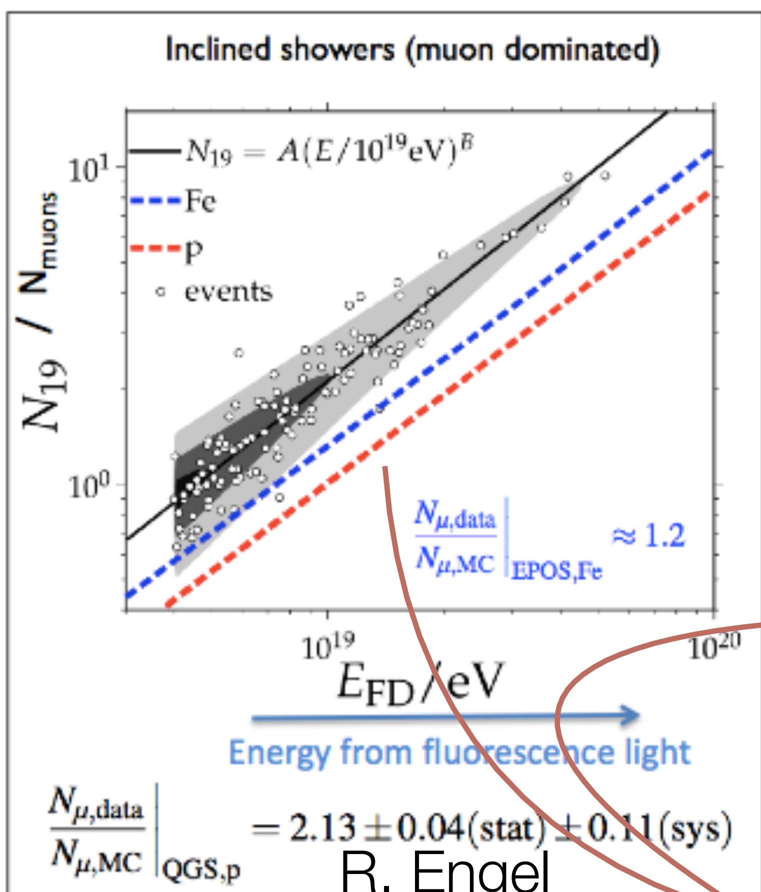

Number of muons depends on the energy fraction of produced hadron

Muon excess in data even for Fe primary MC

EPOS predicts more muon due to larger baryon production

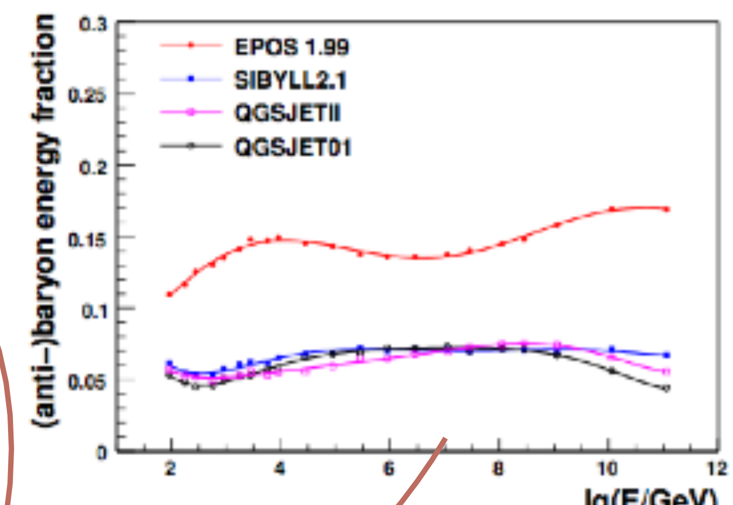

Neutron spectra predicted by interaction models

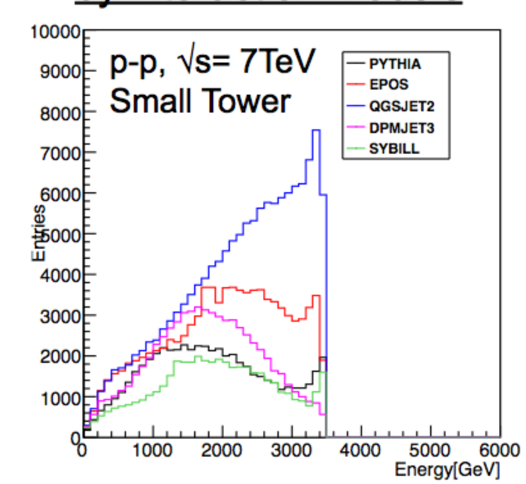

importance of baryon measurement

LHCf @ pp 7 TeV: neutron spectra

PLB 750 (2015) 360-366

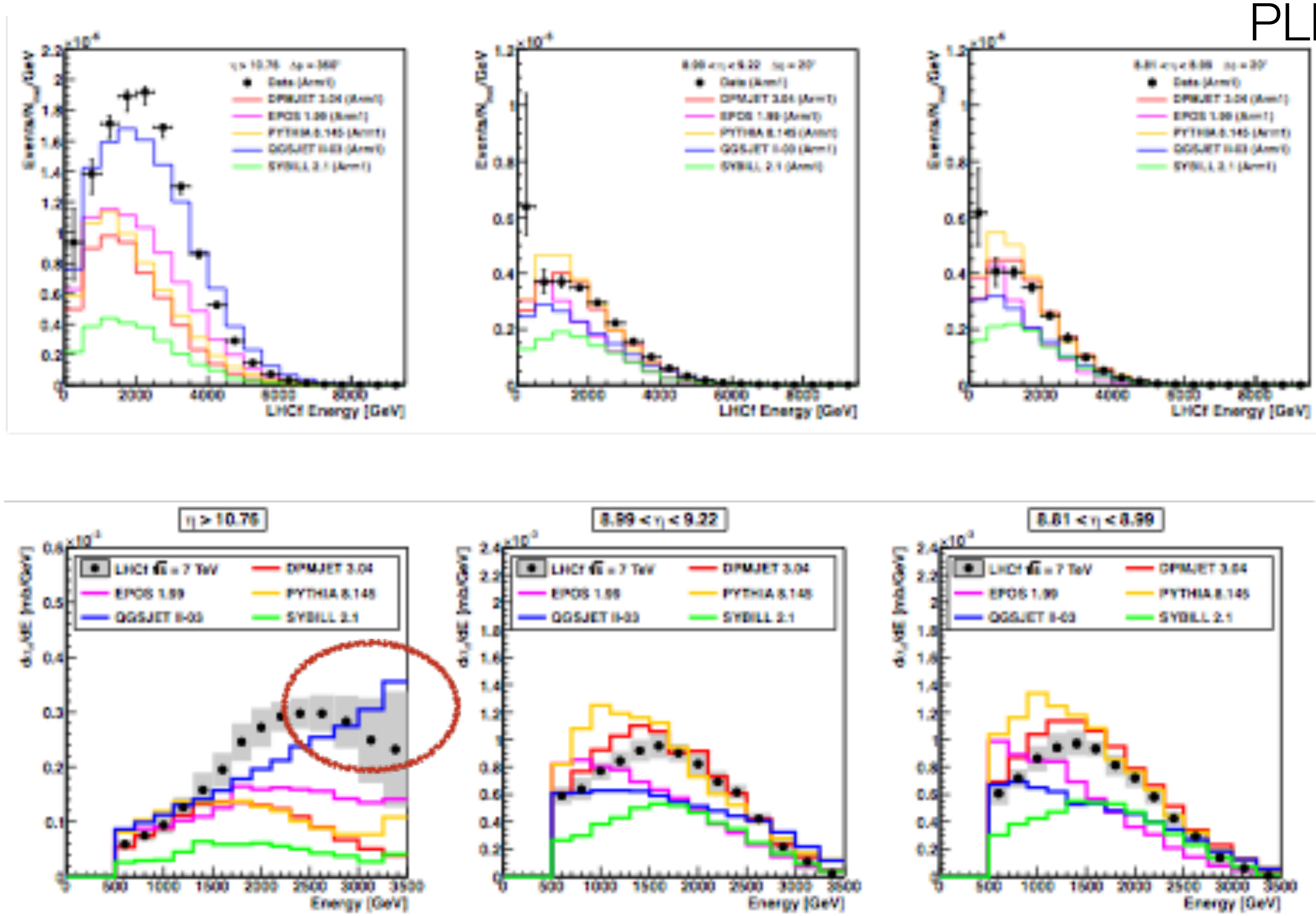

- LHCf Arm1 and Arm2 agree with each other within systematic error, in which the energy scale uncertainty dominates.
- In η>10.76 huge amount of neutron exists. Only QGSJET2 reproduces the LHCf result.
- In other rapidity regions, the LHCf results are enclosed by the variation of models.

LHCf @ pp 7 TeV: neutron spectra SIBYLL 2.1

PLB 750 (2015) 360-366

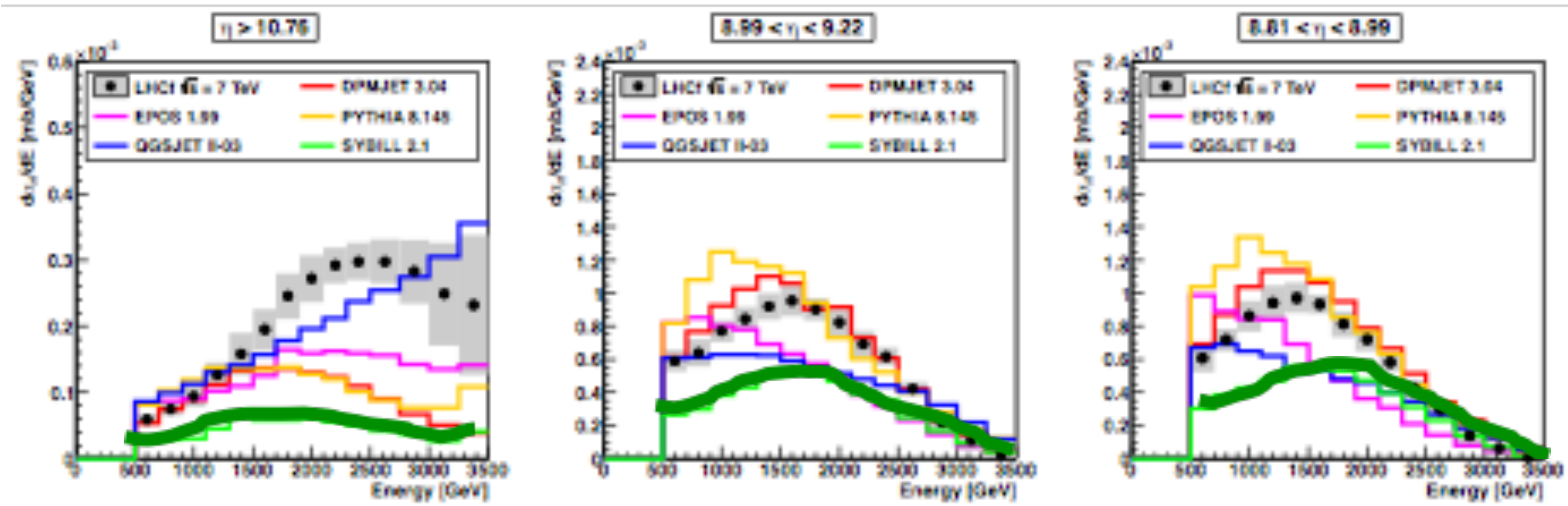

- Lowest neutron yield, especially at zero degree

LHCf @ pp 7 TeV: neutron spectra QGSJET II-03

PLB 750 (2015) 360-366

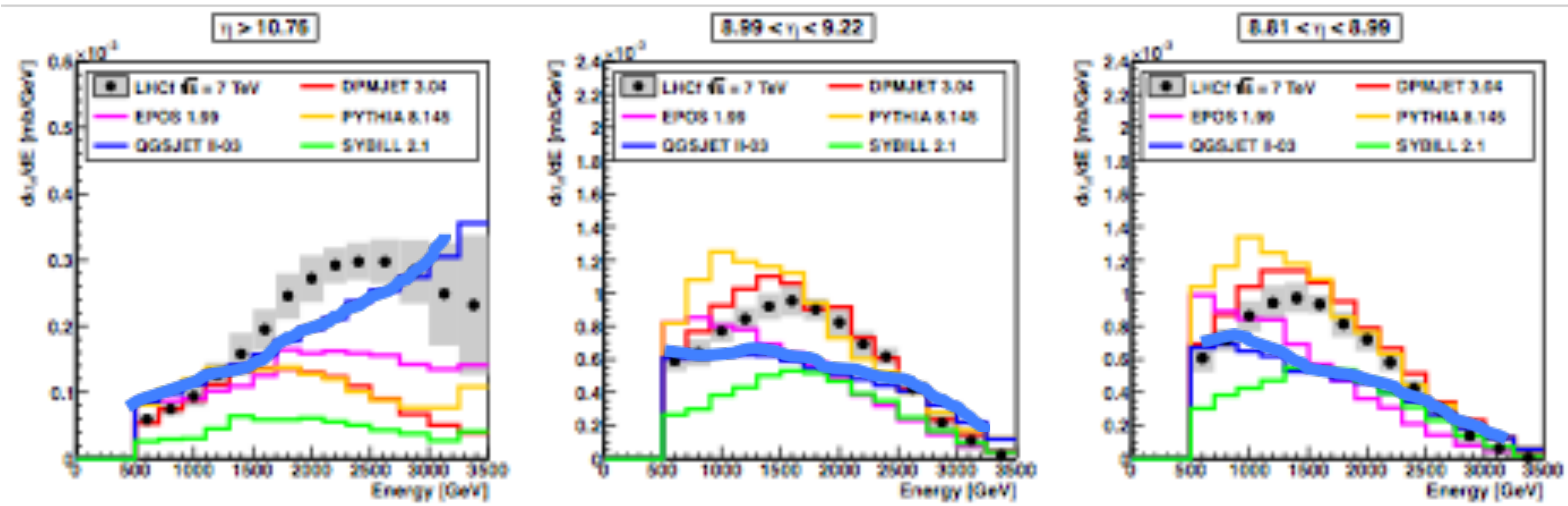

- Qualitatively nice agreement, only model, at zero degree
- Lower yield at non-zero angle

LHCf @ pp 7 TeV: neutron spectra EPOS 1.99

PLB 750 (2015) 360-366

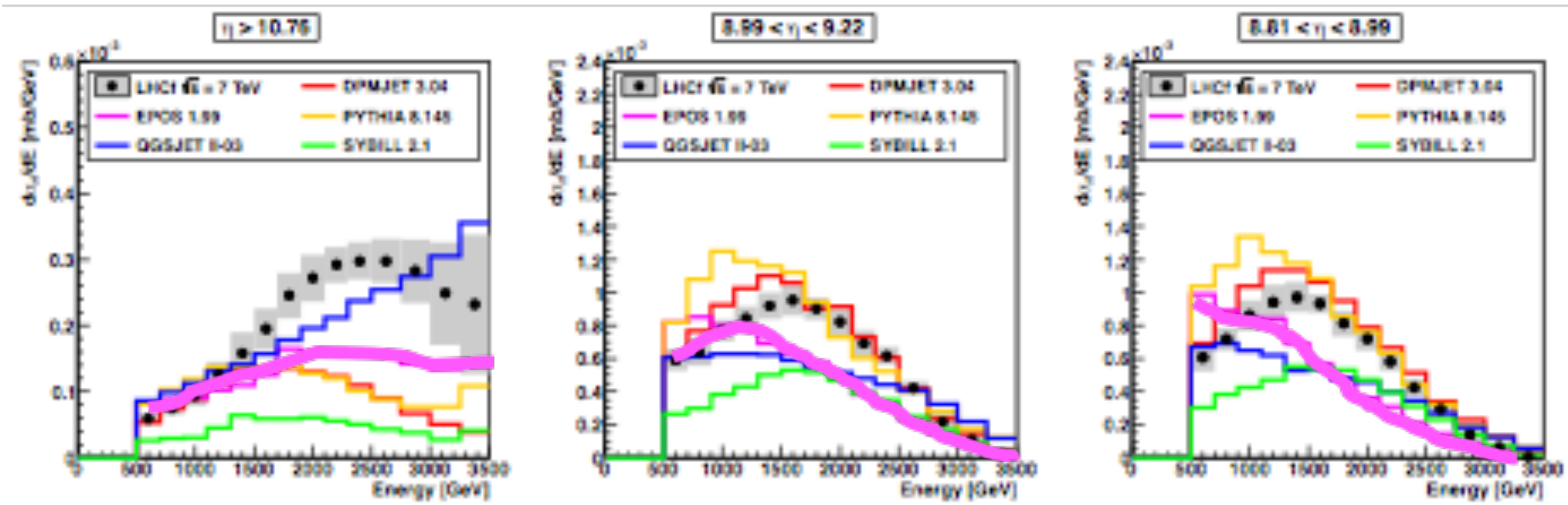

- Generally lower yield

Preliminary ARM2 unfolded neutron spectra @ 13 TeV

Differential production cross section

$$d\sigma_n/dE = \frac{dN(\Delta\eta,\Delta E)}{E}\frac{1}{L}\times\frac{2\pi}{d\varphi}$$

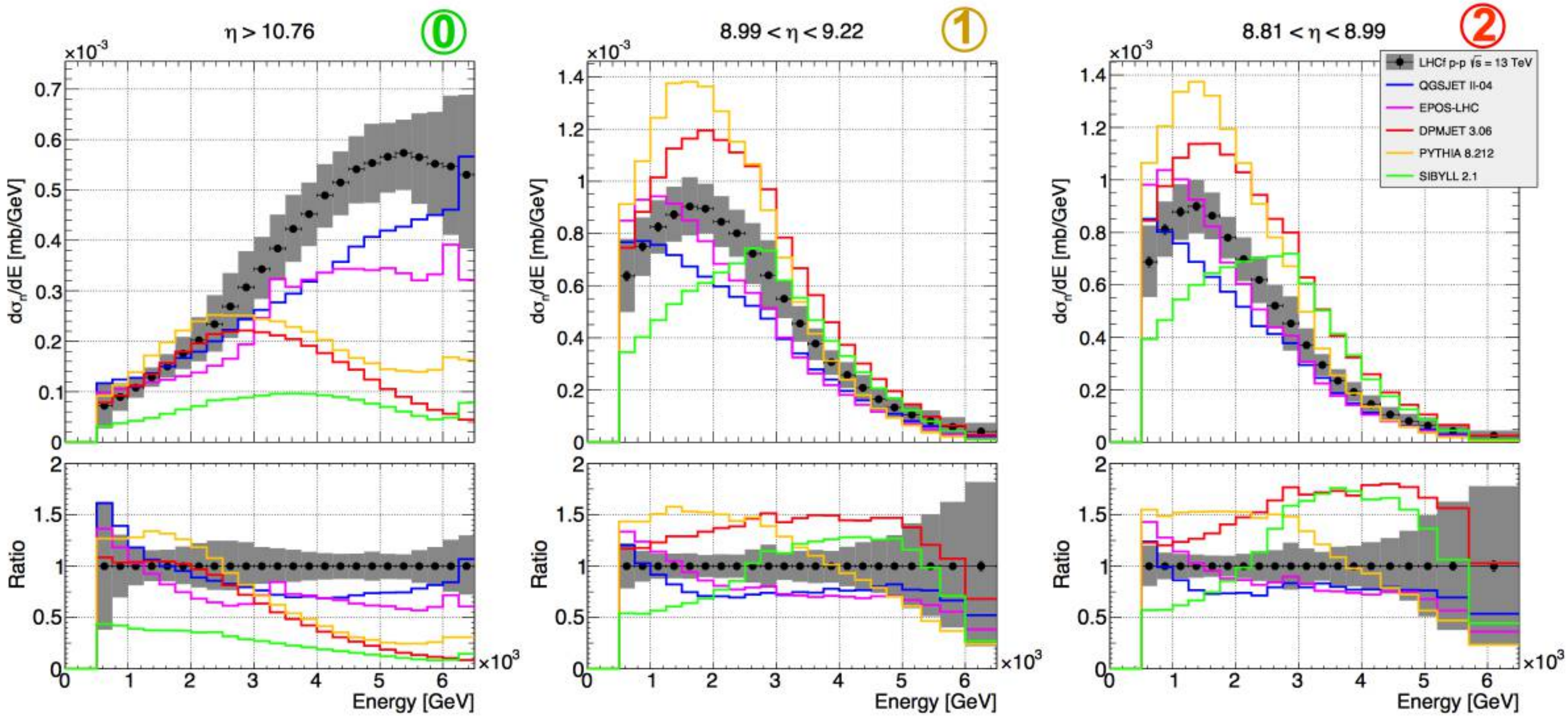

Only **QGSJET II-04** qualitatively reproduces behavior of data in $\eta > 10.76$
EPOS-LHC has similar shape in $8.81 < \eta < 9.22$, but lower yield

Measurement of interesting quantities for CR Physics

Inelasticity VS θ

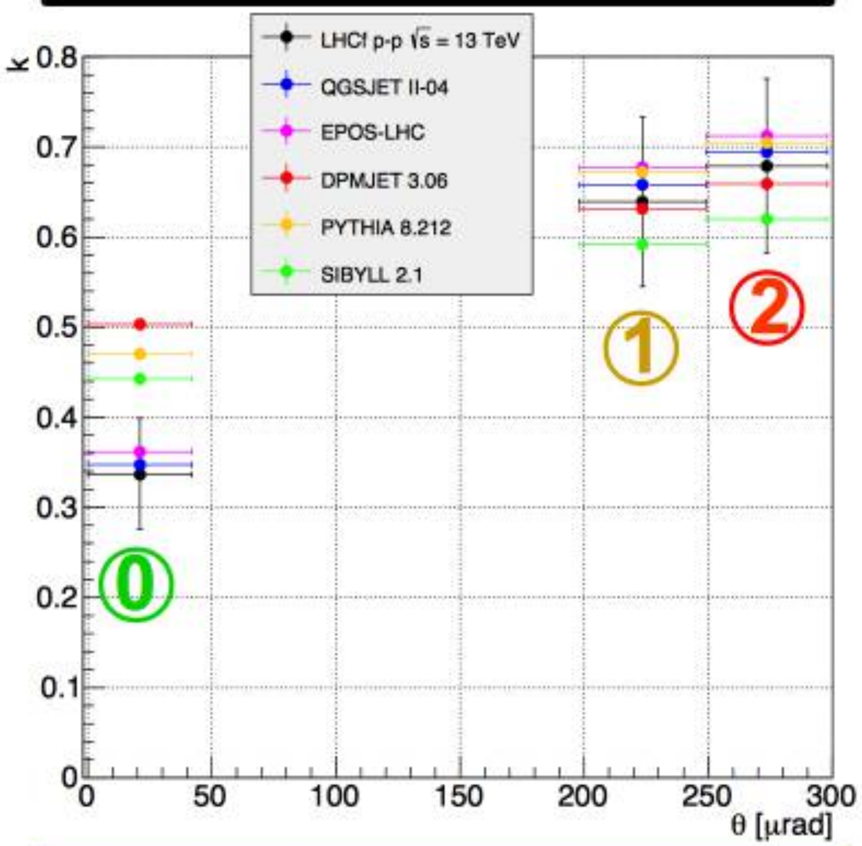

All models overestimate inelasticity in the most forward region even if **QGSJET II-04** and **EPOS-LHC** are consistent within the error bars

dσ/dη VS η

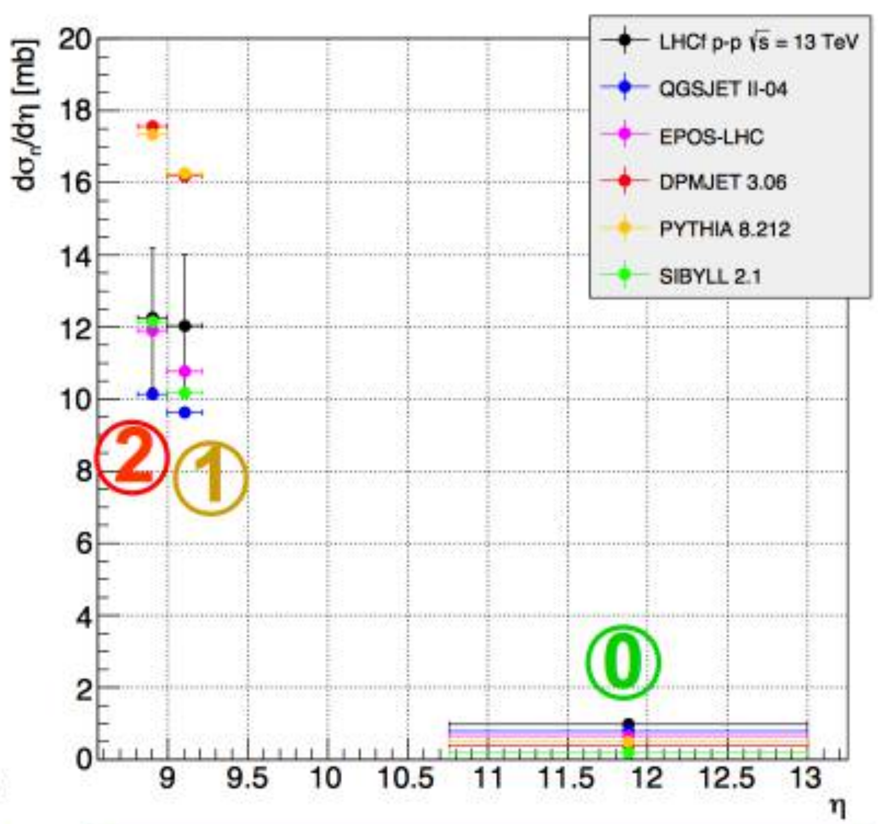

EPOS-LHC and **SIBYLL 2.1** reproduce enough well the measured total differential cross section except in the most forward region

dE/dη VS η

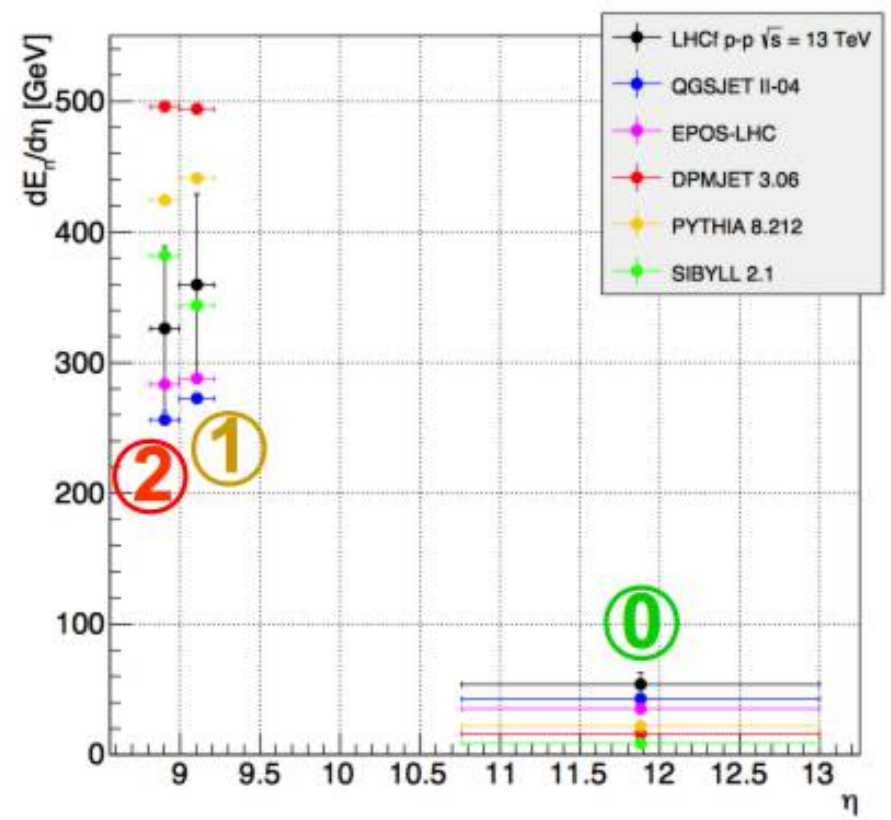

Where the energy flux is high, the agreement between experimental measurements and **SIBYLL 2.1**/**EPOS-LHC** is quite good

Very preliminary overview of the p-Pb run

- **5 TeV**
  - Fills 5007 and 5010 (100_200ns_702p_548Pb_81_389_54_20inj)
    - 26M common events (LHCf-ATLAS)

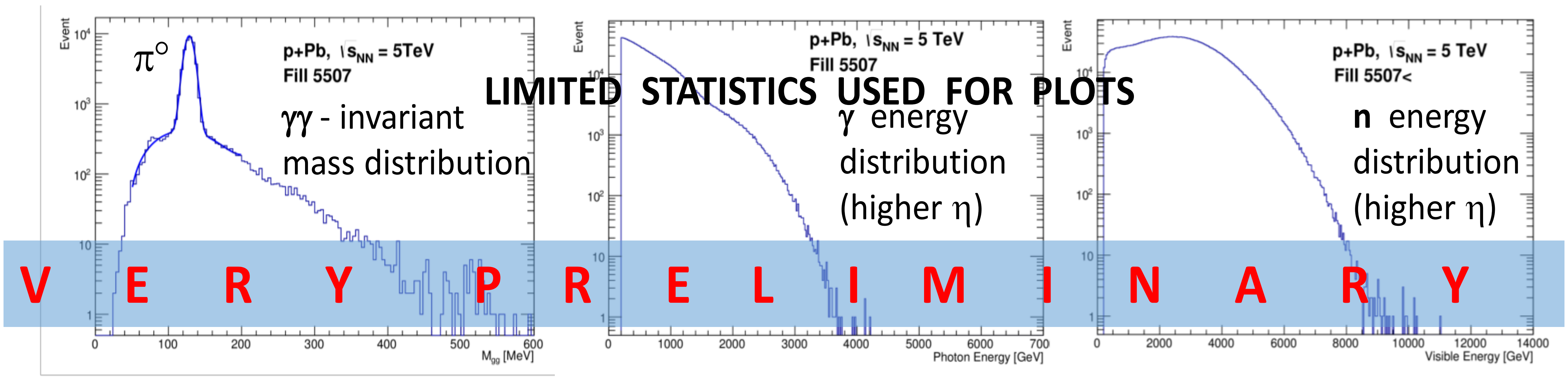

- **8 TeV**
  - Fill 5519 (Single_20p_20Pb_10_10_9_1non_coll) → 5.5M events (LHCf-ATLAS)
  - Fill 5538 (100_200ns_684p_540Pb_432_427_89_20inj) → 15M events (LHCf-ATLAS)

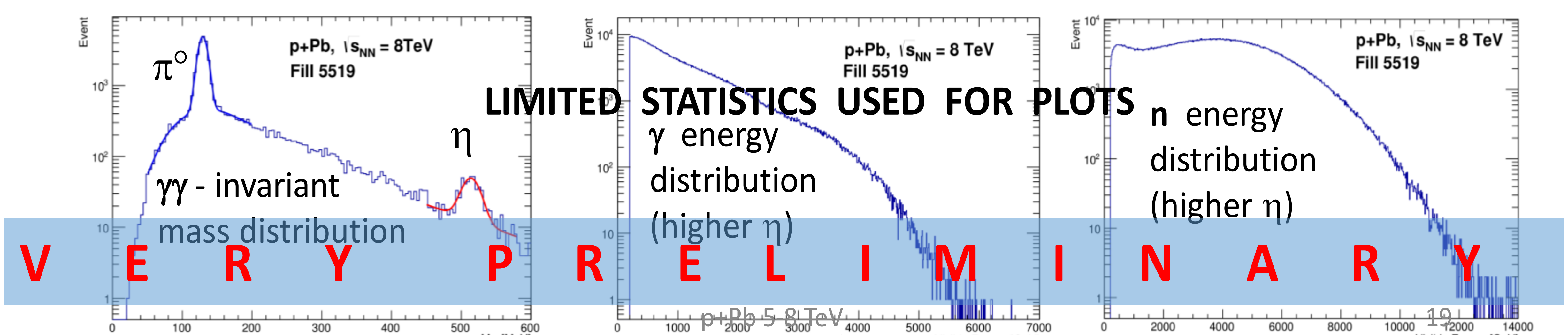

Physics cases with ATLAS joint taken data

- In p+p collisions
  - Forward spectra of Diffractive/ Non-diffractive events
  - Measurement of proton-π collisions

Both are important for precise-understanding of CR air shower development

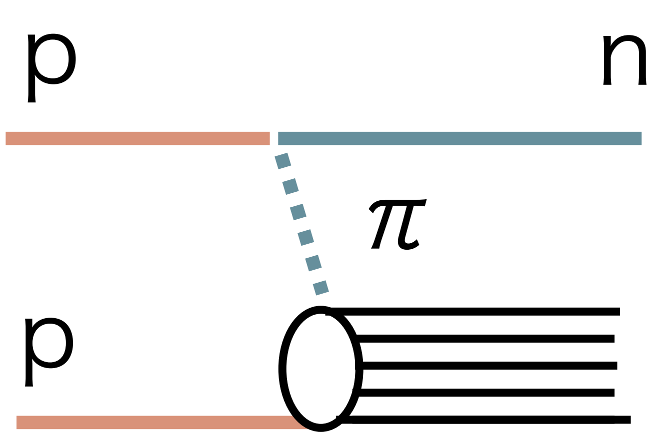

p-π measurement at LHC

Leading neutron can be tagged by LHCf detectors
-> total cross section
multiplicity measurement

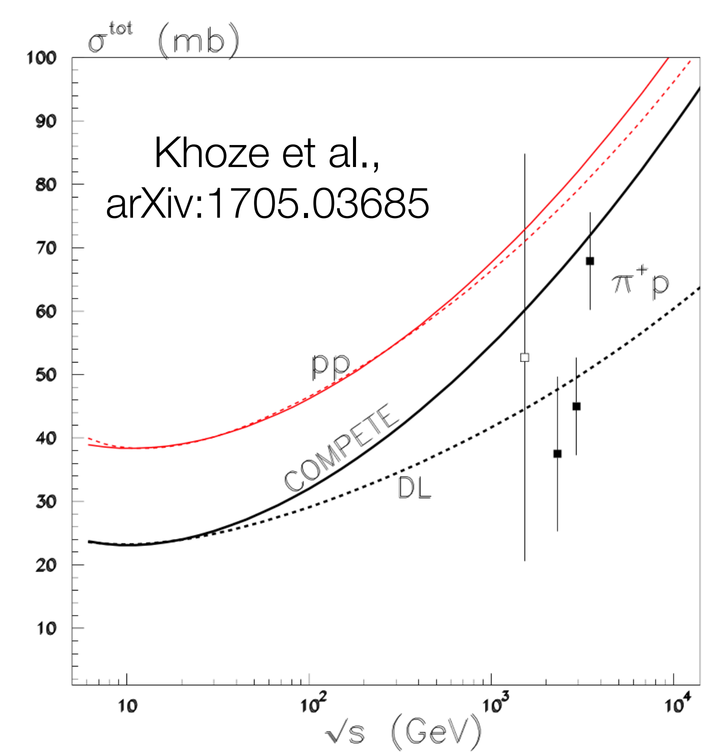

- In p+Pb collisions
  - Measurement of UPC in the forward region.

ATLAS-LHCf combined data analysis

- Operation in 2013
  - p+Pb, $\sqrt{s_{NN}}$ = 5TeV
    - → about 10 M common events.
- Operation in 2015
  - p+p, $\sqrt{s}$ = 13TeV
    - → about 6 M common events.
- Operation in 2016
  - p+Pb, $\sqrt{s_{NN}}$ = 5TeV
    - → about 26 M common events
  - p+Pb, $\sqrt{s_{NN}}$ = 8TeV
    - → about 16 M common events

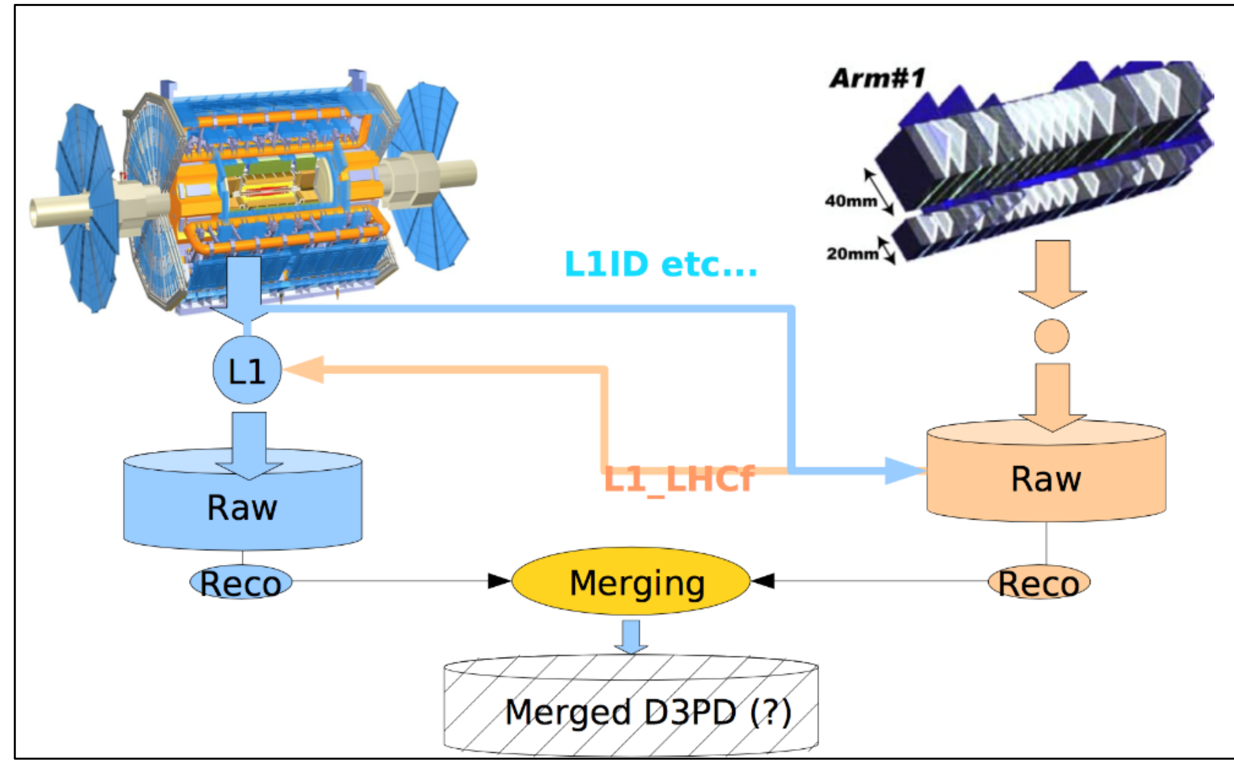

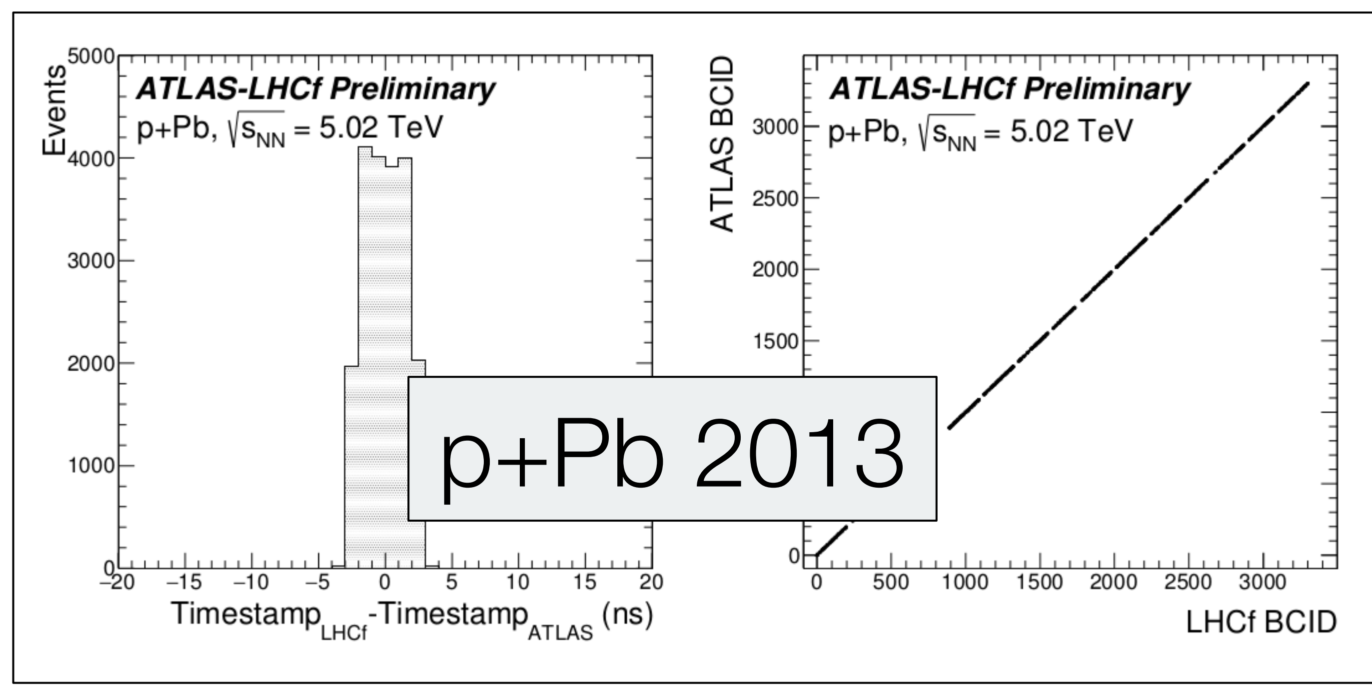

Off-line event matching

Important to separate the contributions due to diffractive and non-diffractive collisions

WG active meeting every 2 weeks

Diffractive studies

- MC studies
  - Contributions on forward photon/neutron spectra from diffractive/ non-diffractive collisions.

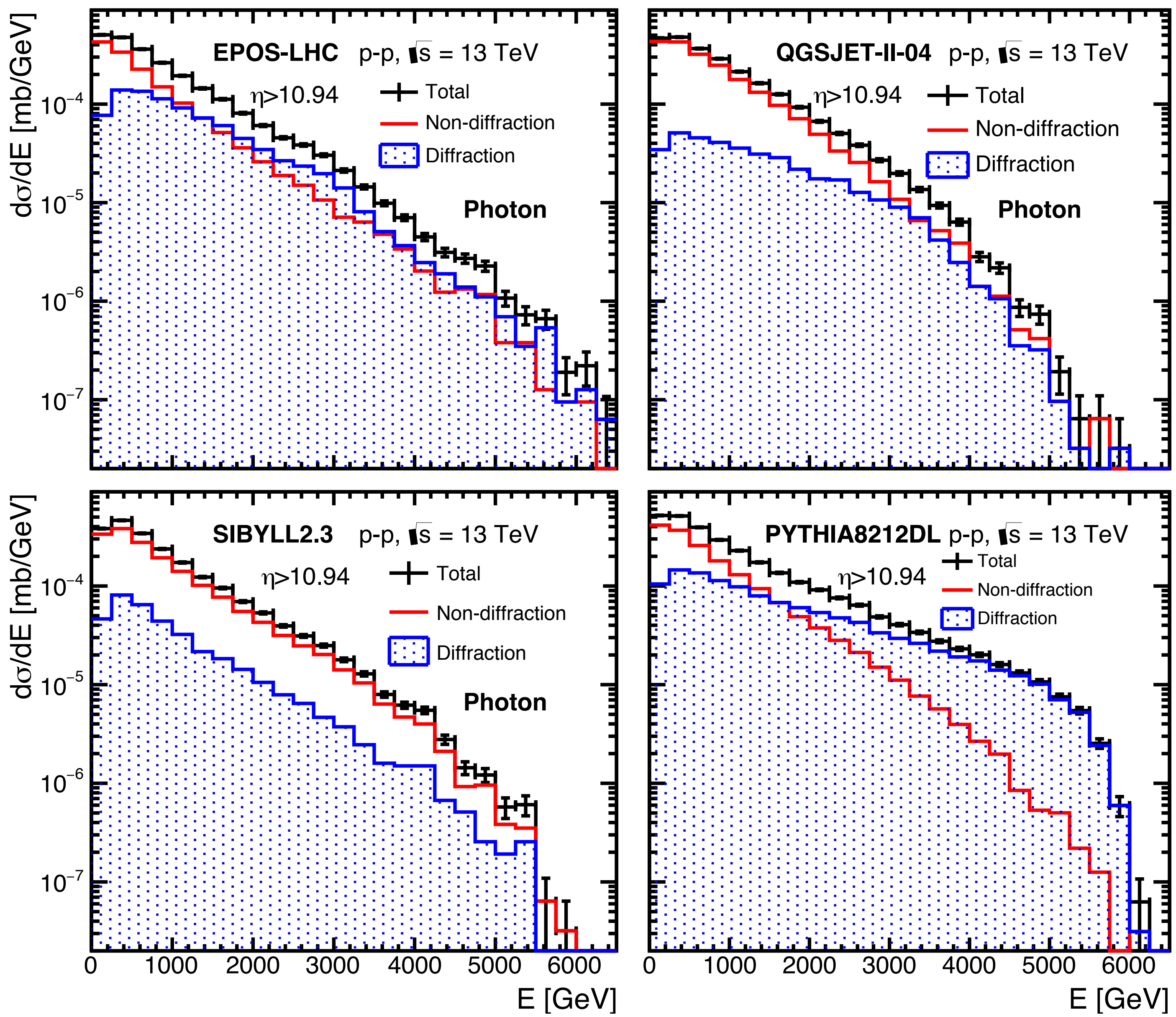

Very forward photon energy spectra predicted by four models with **total**/ diffractive/non-diffractive

- Total: Very similar spectra in EPOS,QGSJET and SIBYLL (LHCf alone)
- Diffractive/Non-diffractive: Very big difference between models (ATLAS-LHCf)

Diffractive studies

- Event selection for Diffractive/ Non-diffractive by using $N_{charged}$ with p_T>100MeV in |η|<2.5

By using ATLAS-tracker information, We can separate diffractive/non-diffractive contribution with high efficiency and purity

Expected efficiencies

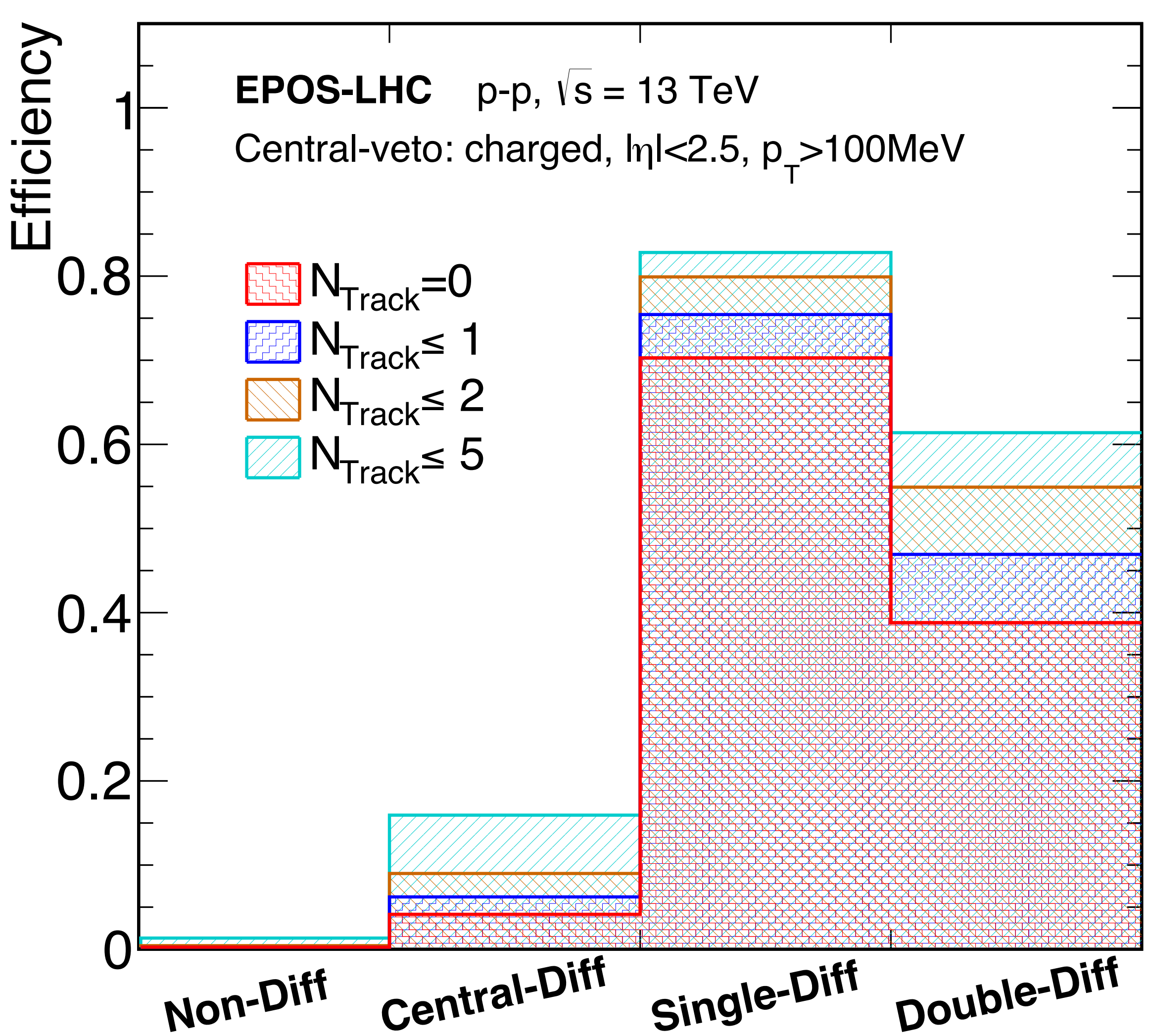

Forward neutron spectra

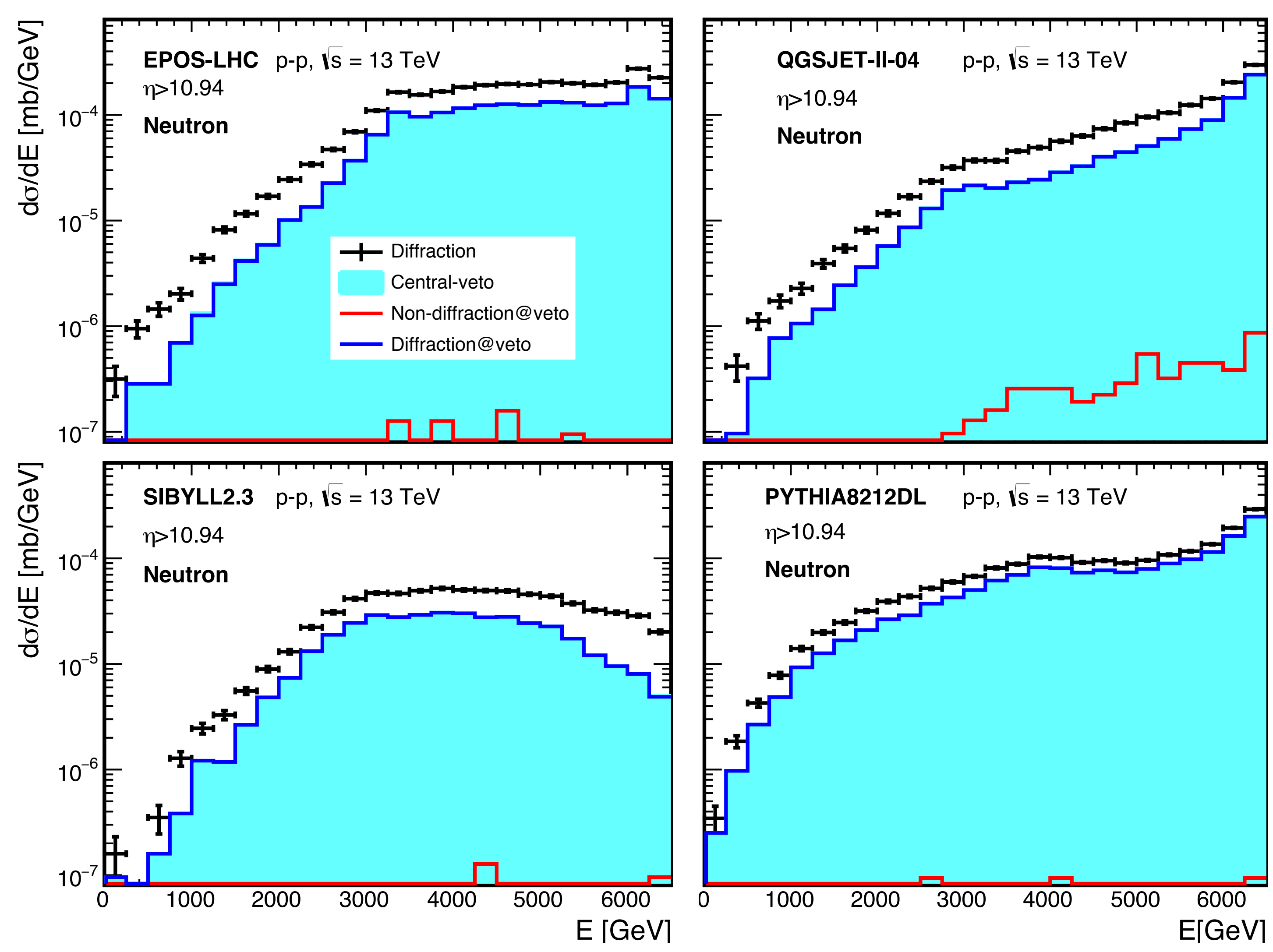

From the LHC to RHIC

LHCf Arm2 detector in the LHC tunnel

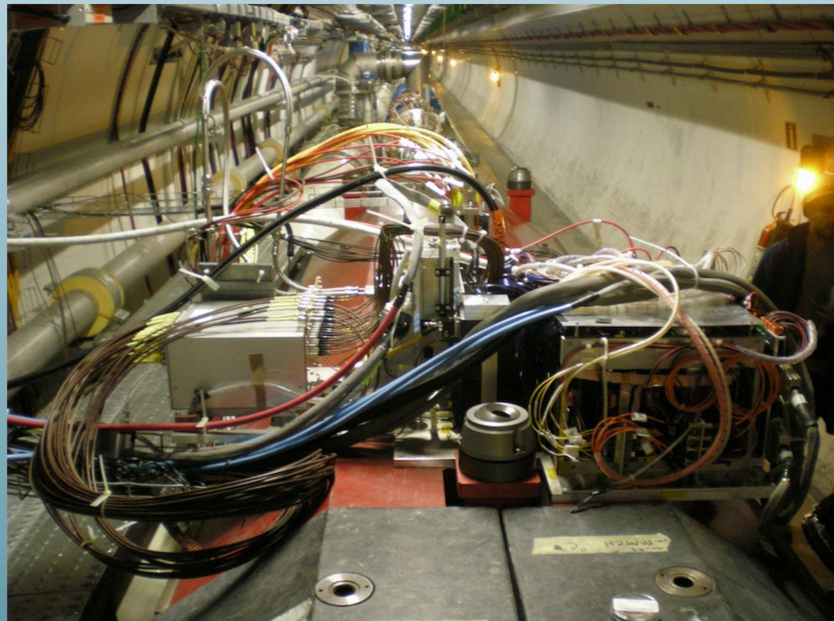

Schematic view of the RHICf installation

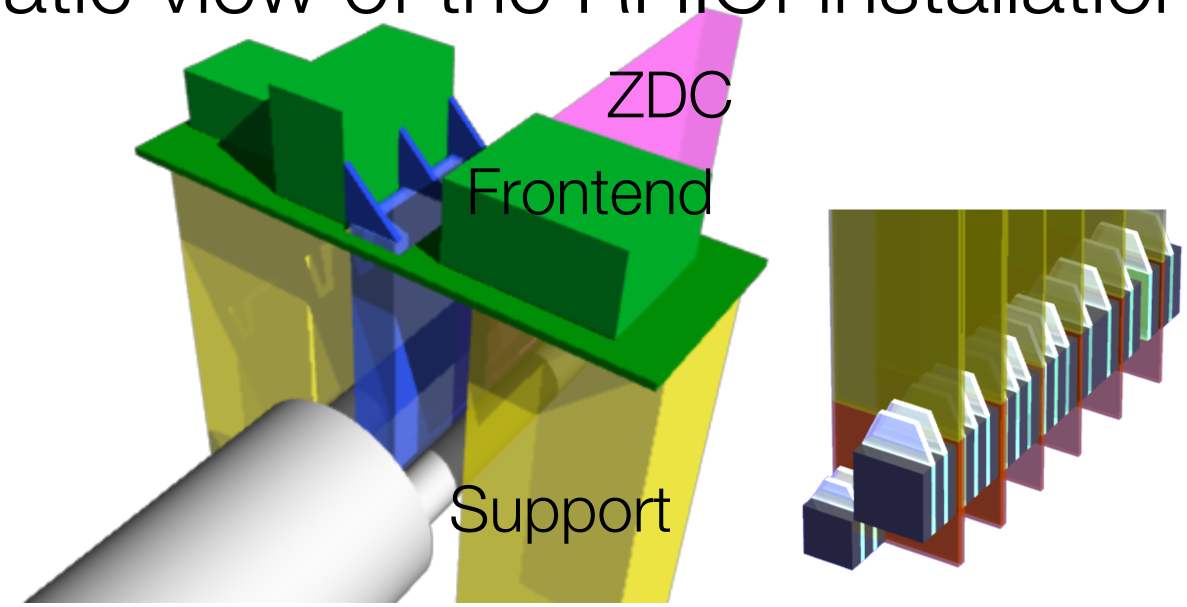

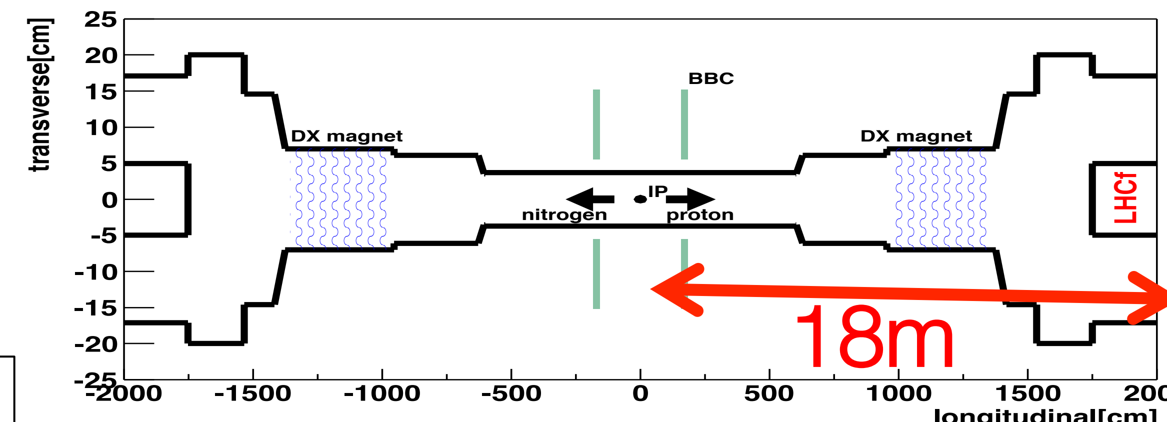

Acceptance in E-p_T phase space

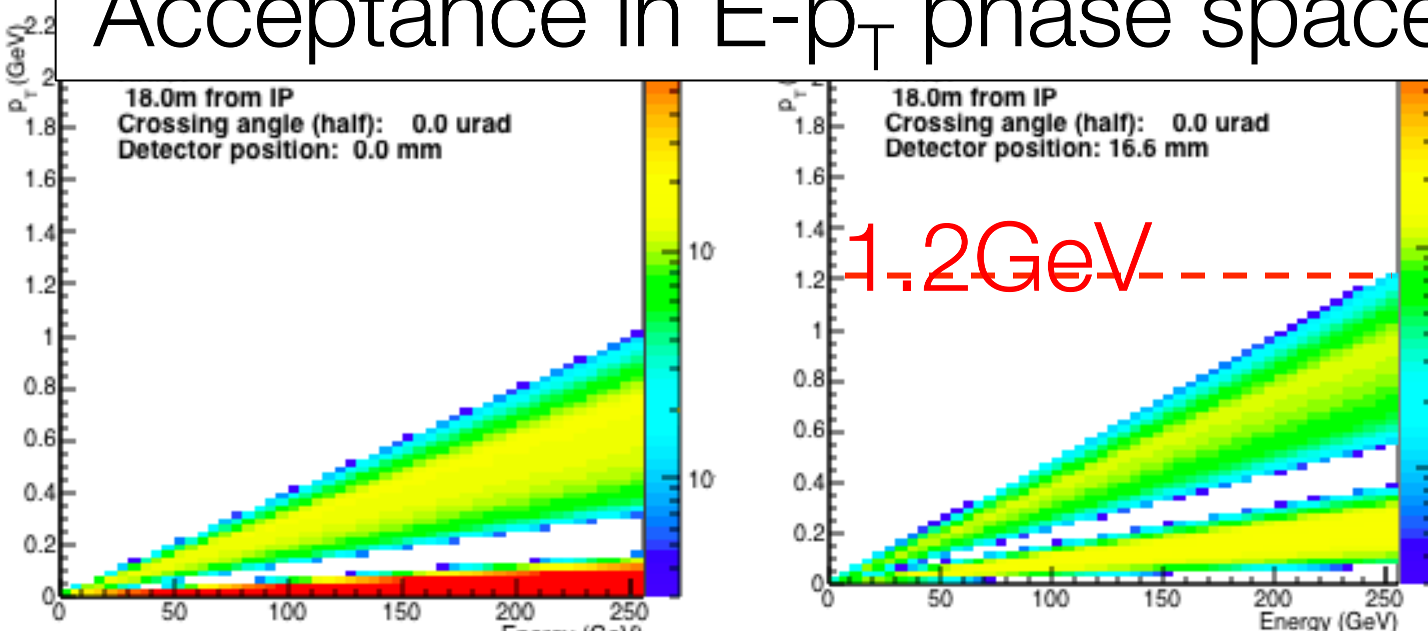

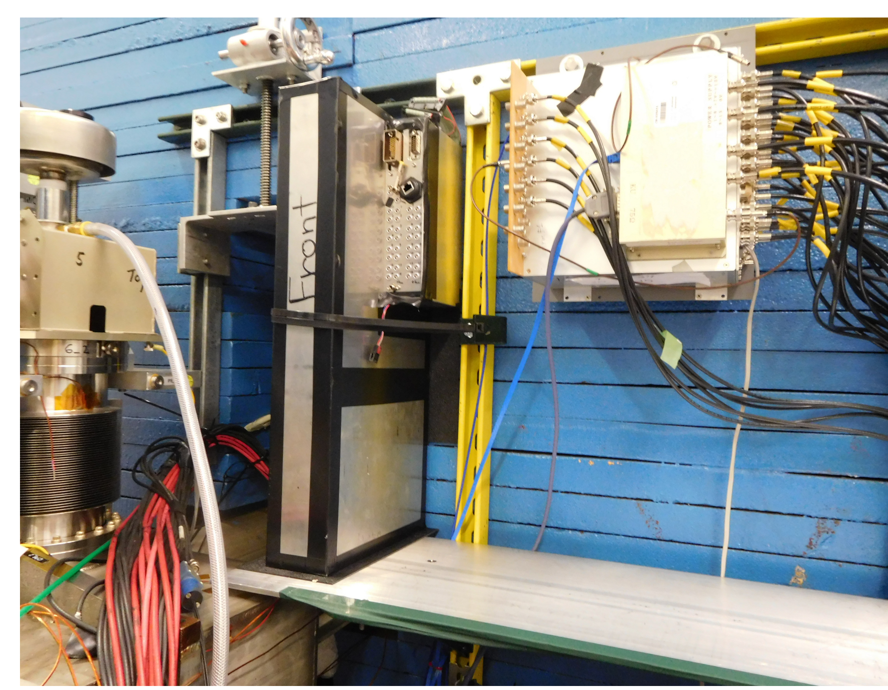

√s scaling, or breaking?

LHCf 2.76TeV and 7TeV data
shows scaling of forward π^0

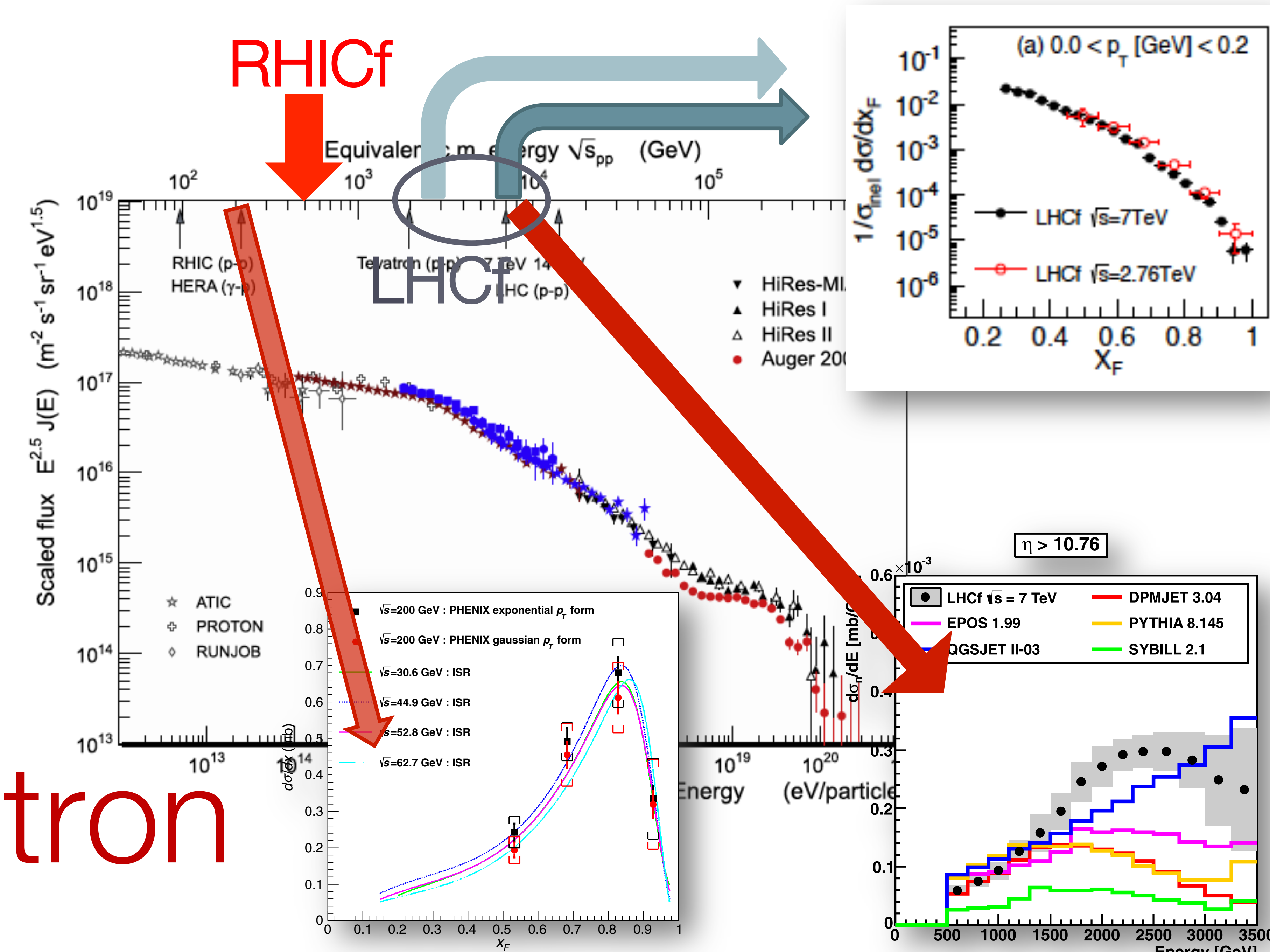

π^0

neutron

ISR (30-60GeV), PHENIX (200GeV) and LHCf (7TeV)
data indicate scaling ***breaking*** of forward neutrons

Very preliminary overwiew of the RHICf run

24 June 2017!!!

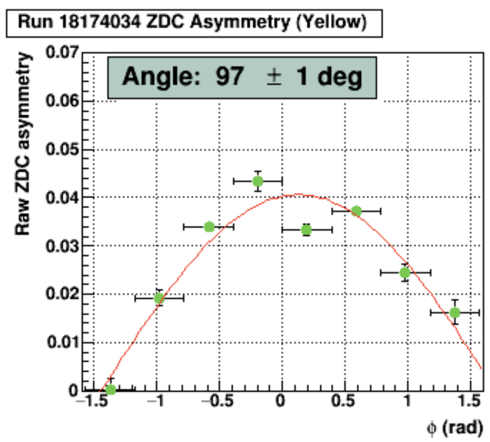

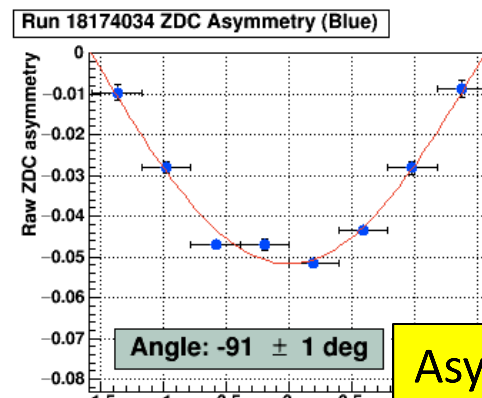

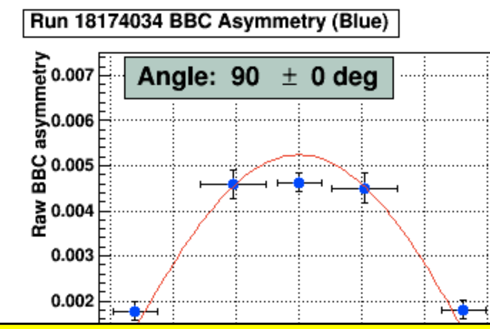

Asymmetry by STAR ZDC scaler
Radial polarization GOOD!!

Hadron shower hitmap
0 degree well defined!

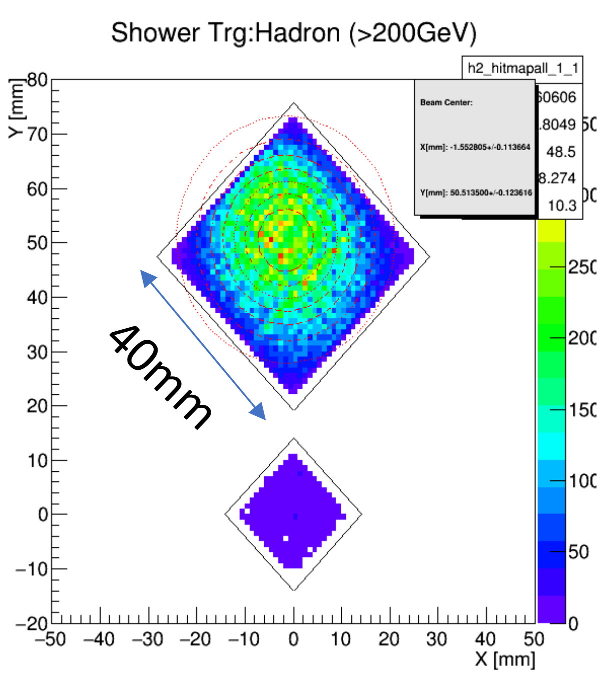

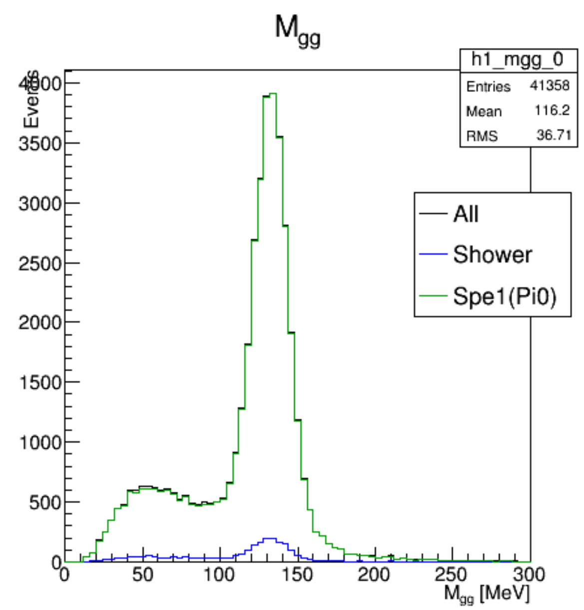

Invariant mass of 2γ
Peak by π^0 !!

Energy (anti) correlation
with ZDC west

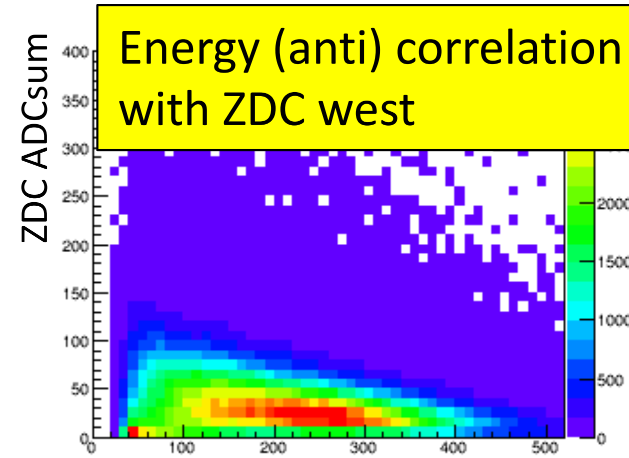

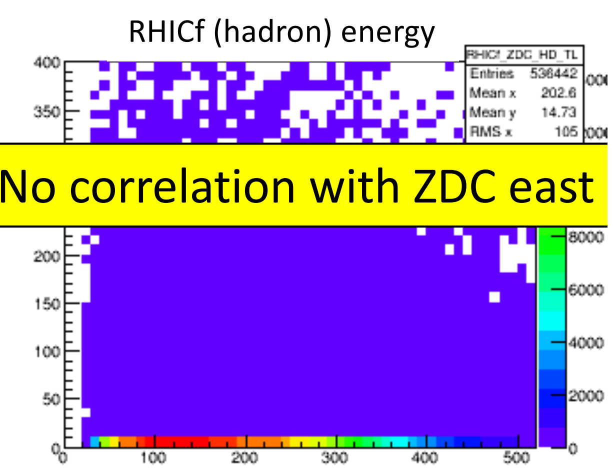

No correlation with ZDC east

The Near-Far Future at LHC

- The most promising future at LHC for LHCf involve the proton-light ion collisions
- To go from p-p to p-Air is not so simple….
- Comparison of p-p, Pb-Pb and p-Pb is useful, but model dependent extrapolations are anyway necessary
- Direct measurements of p-O or p-N could significantly reduce some systematic effects
- Still make sense to take data if intermediate ion (like Ar) will be available

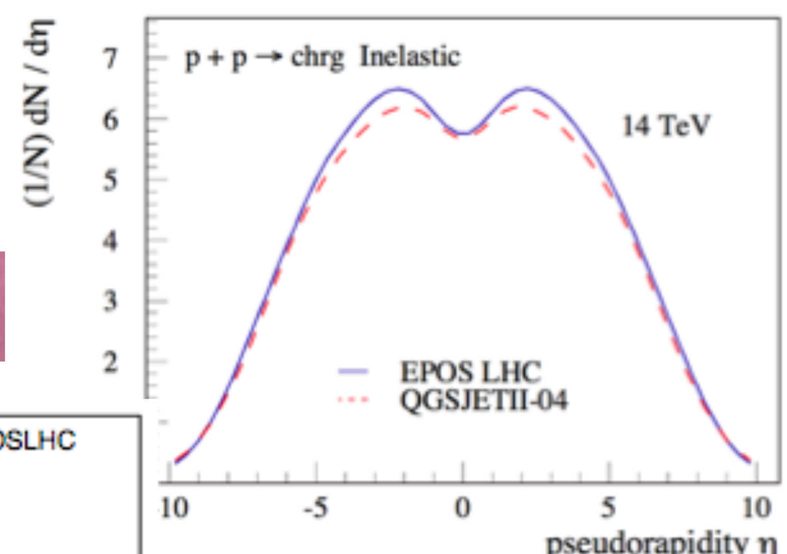

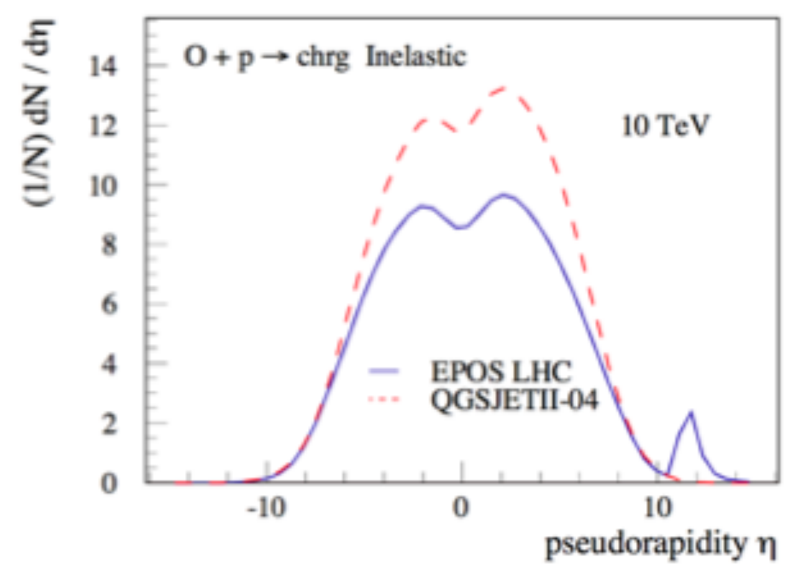

Photon spectra p-p vs. O-O

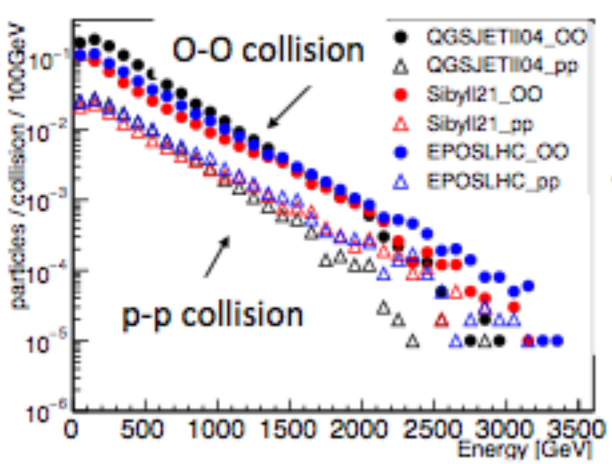

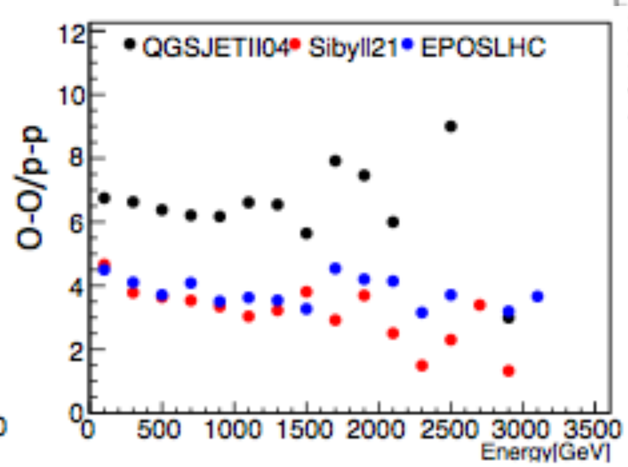

Y. Okuno, Master thesis
Nagoya university (2016)

Slide back-up

Analysis of hadron production in p-p collisions at 13 TeV

Data set

12 July 2015, 22:32-1:30 (3 hours)

Fill # 3855

$\mu = 0.01$

$\int L dt = 0.19\ nb^{-1}$

$\sigma_{ine} = 78.53$ mb

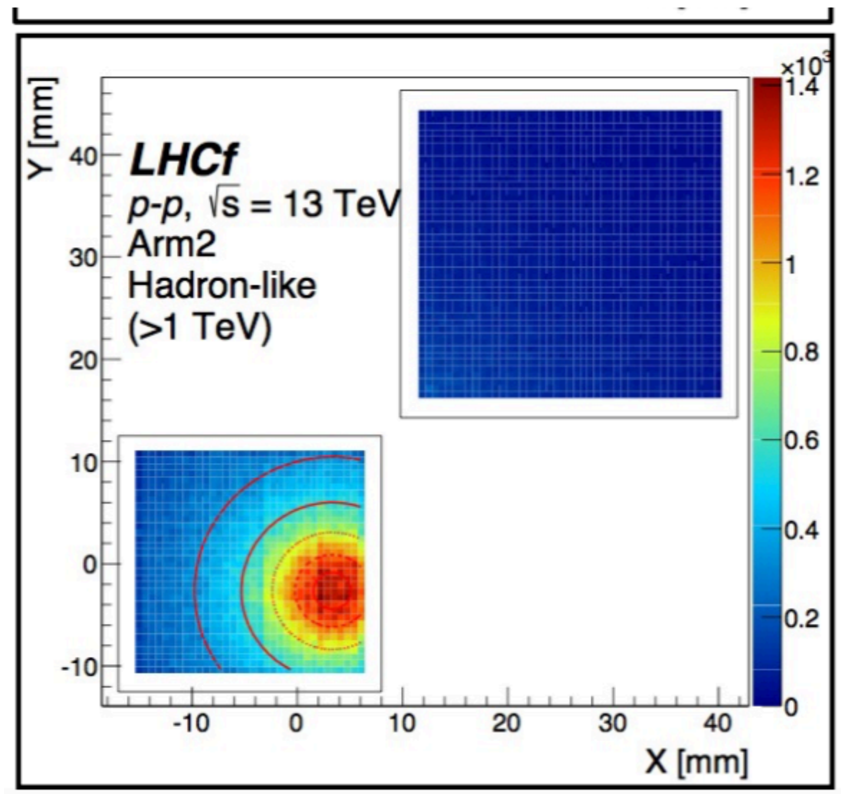

Beam Center

Estimated using 2D fit on high energy hadron hitmap distribution

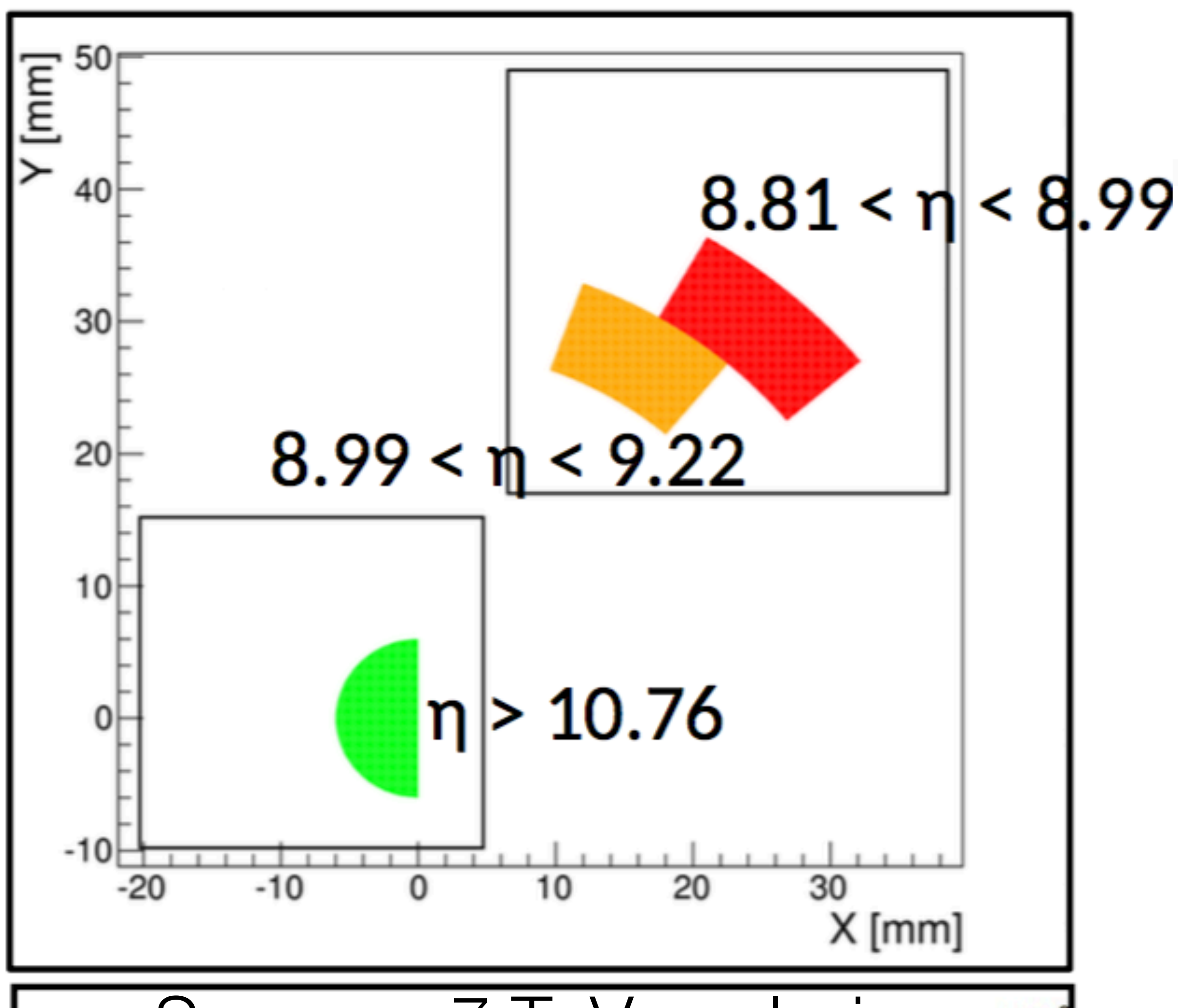

Same as 7 TeV analysis

PLB 750 (2015) 360-366

Event selection criteria:

software trigger

at least 3 consecutive layers with deposit above threshold $dE > dE^{thr}$

PID selection

$L_{2D} > L_{2D}^{thr}$ where L_{2D} is a variable related to shower longitudinal profile

pseudorapidity acceptance

3 different pseudorapidity regions

Reconstructed ARM2 hadron energy spectra

Events / N_{ine} / dE

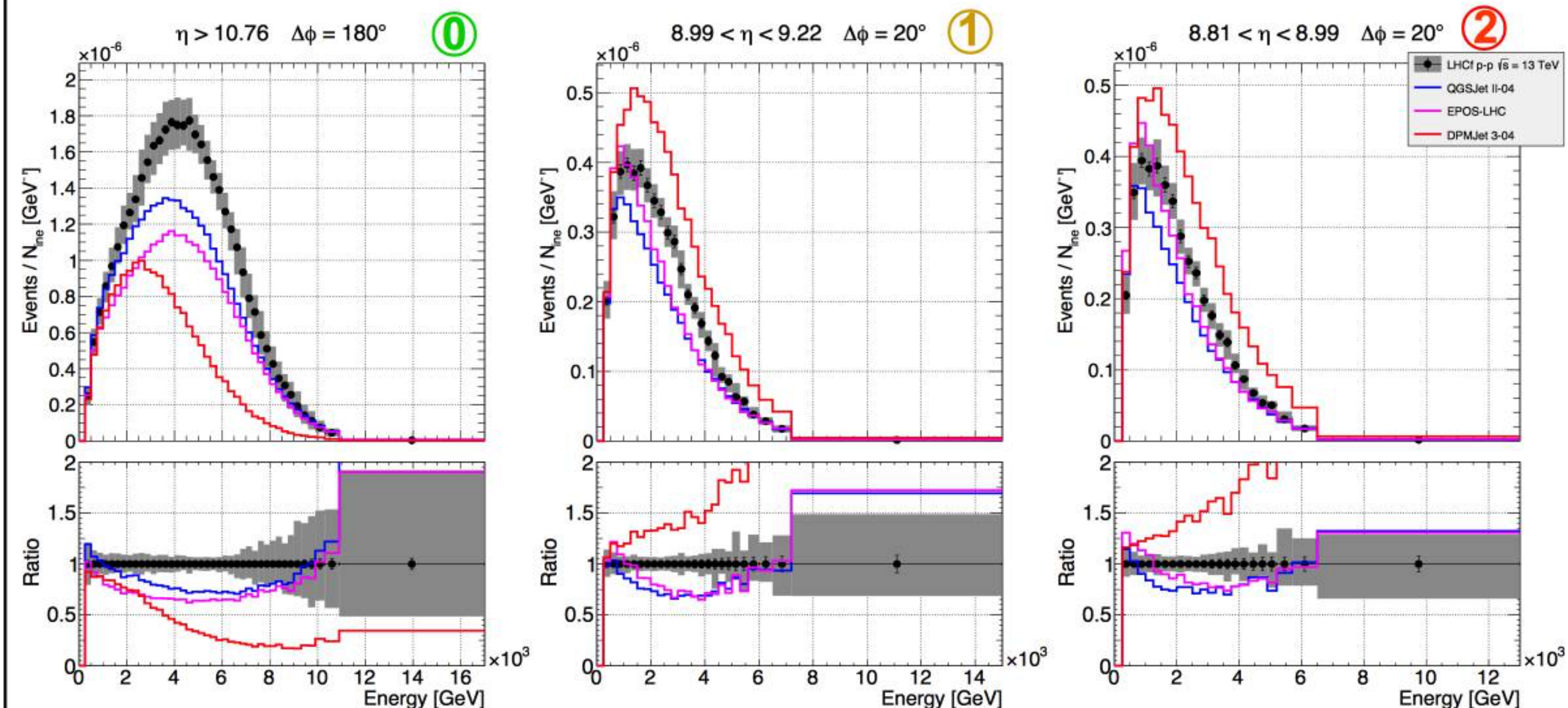

QGSJET II-04 and **EPOS-LHC** have similar shape but lower yield

DPMJET 3.04 have very different shape and yield

Feynman scaling in neutron production cross-section

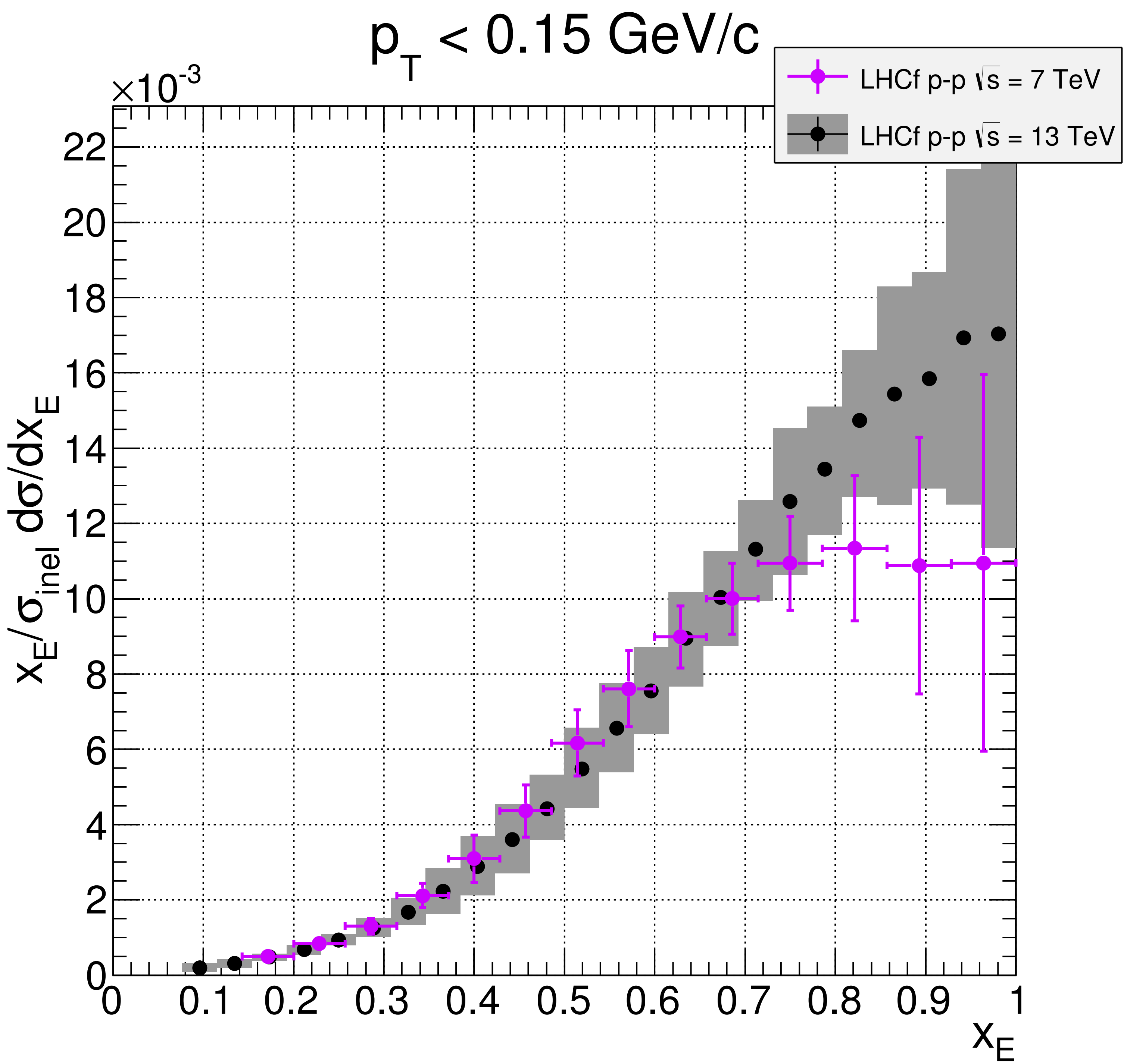

Feynman scaling hypothesis holds within the error bars

Consistency is good especially in the region $0.2 < x_F < 0.75$

LHCf @ pPb 5.02 TeV: π^0 p_T spectra

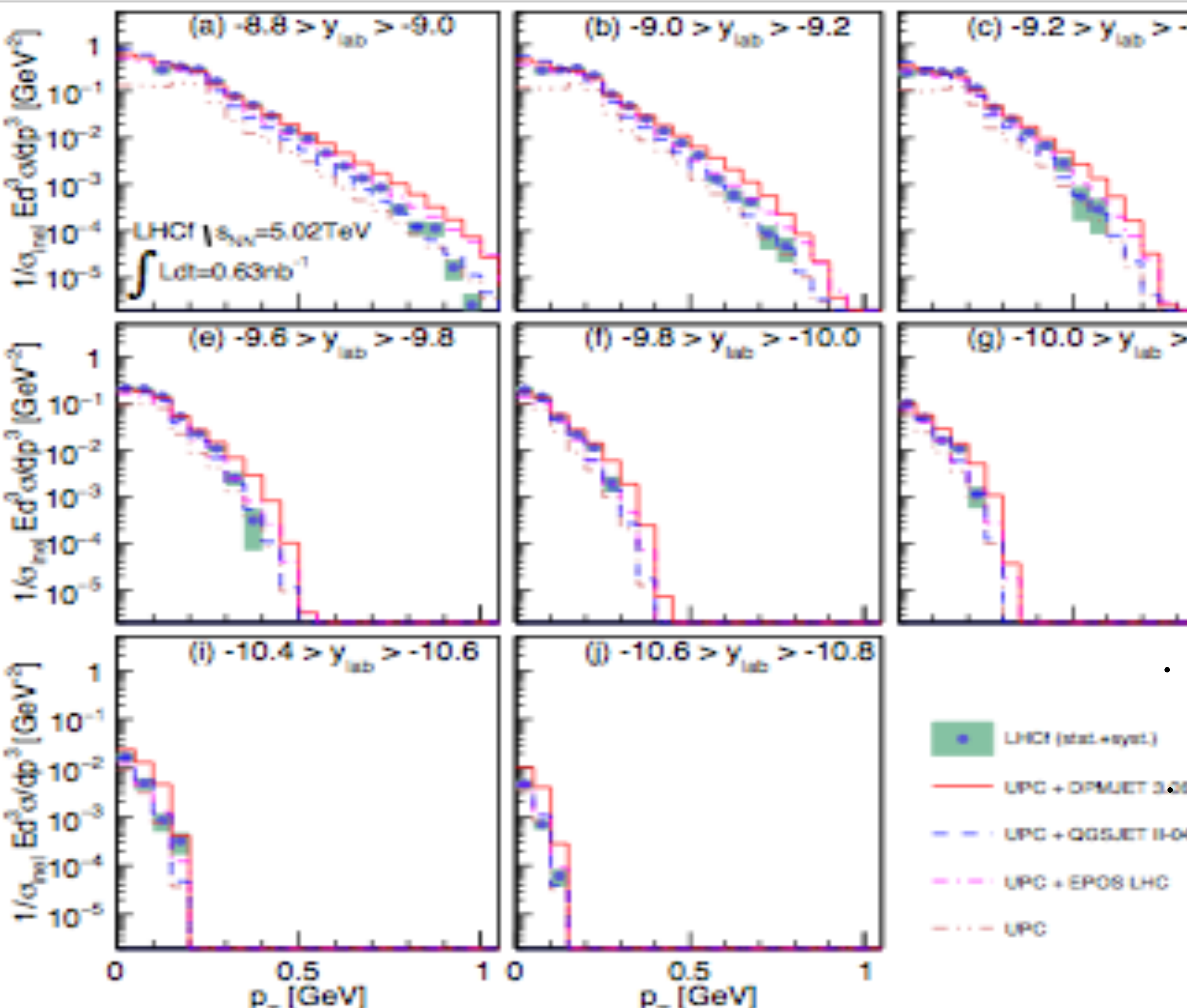

- QGSJETII-04 and EPOS-LHC: similar, good agreement for pT>0.4 GeV
- DPMJET: good agreement for $-8.8 > ylab > -10.0$ and $p_T < 0.3$ GeV
- Characteristic bump at $y > -9.6$ and $p_T \sim 0.2$GeV: Ultra Peripheral Collisions

LHCf @ pPb 5.02 TeV: Nuclear modification factor

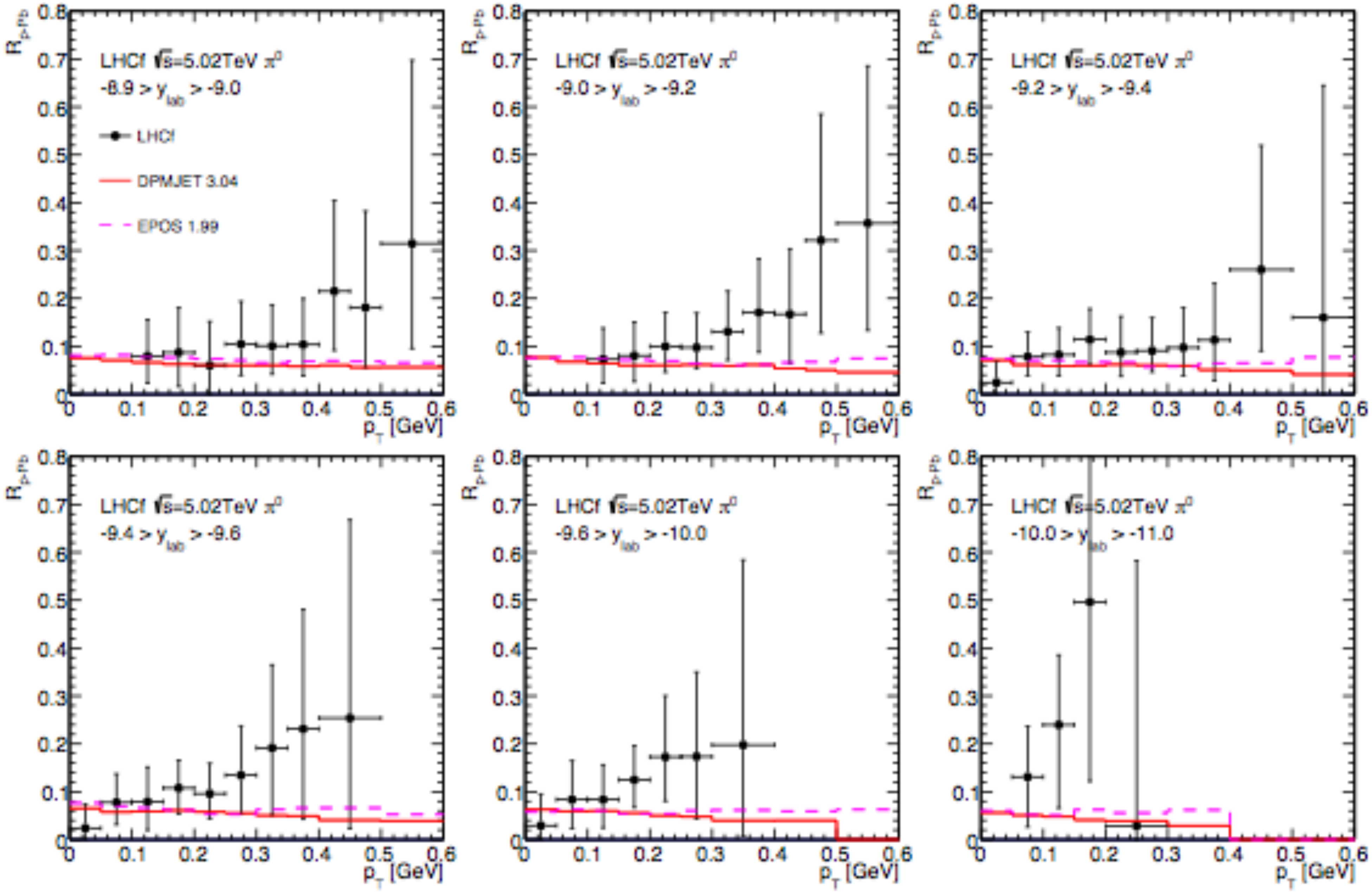

$$R_{\mathrm{pPb}}(p_{\mathrm{T}}) \equiv \frac{d^2N^{\mathrm{pPb}}_{\pi^0}/dydp_{\mathrm{T}}}{\langle N_{\mathrm{coll}}\rangle d^2N^{\mathrm{pp}}_{\pi^0}/dydp_{\mathrm{T}}}$$

$\langle N_{\mathrm{coll}} \rangle = 6.9$

Both LHCf and MCs show strong suppression
But LHCf grows as increasing p_T, understood by the softer p_T spectra in p-p at 5TeV than those in p-Pb.

LHCf @ pPb 5.02 TeV vs RHIC:
Nuclear modification factor

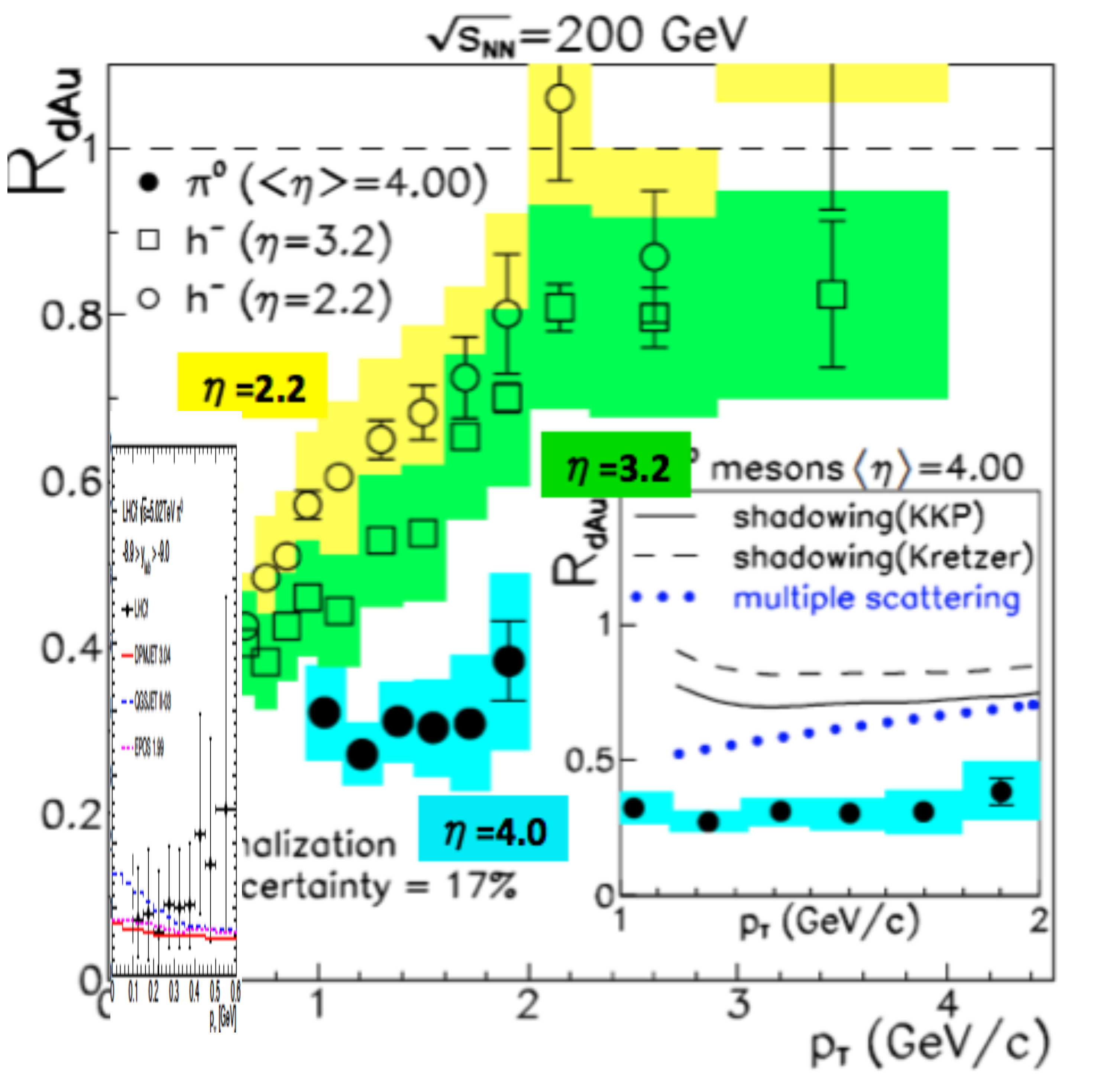

π^0 average p_T for different cm energies

p_T spectra vs best-fit function

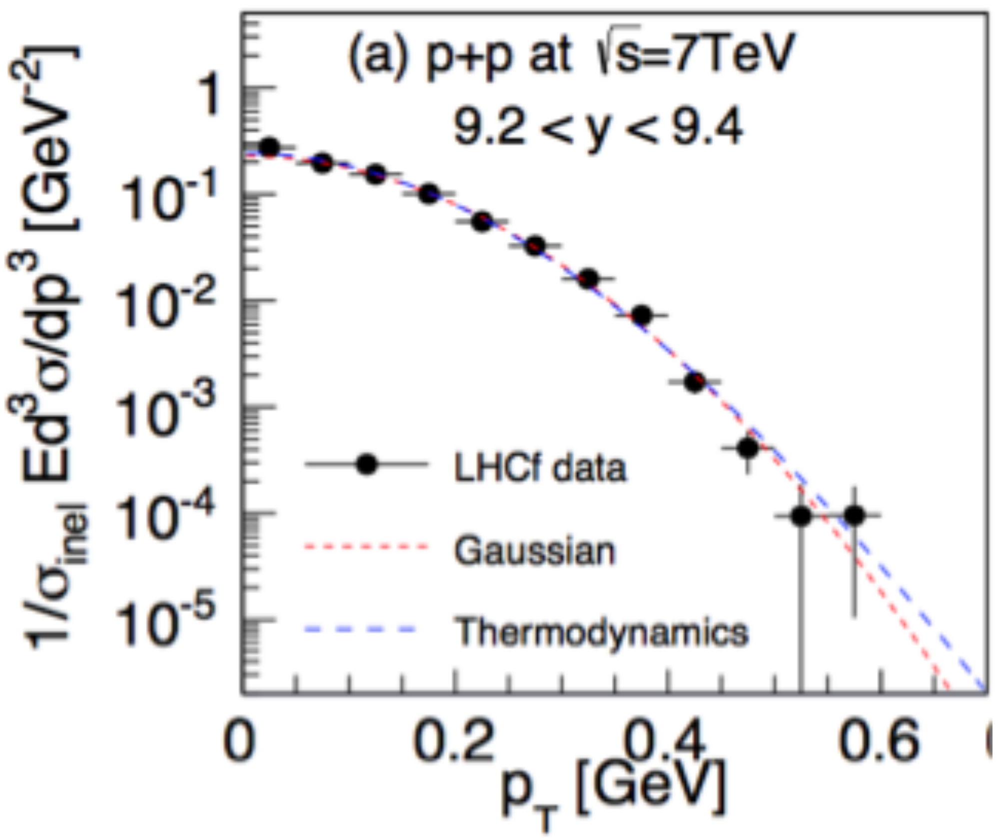

Average p_T vs y_{lab}

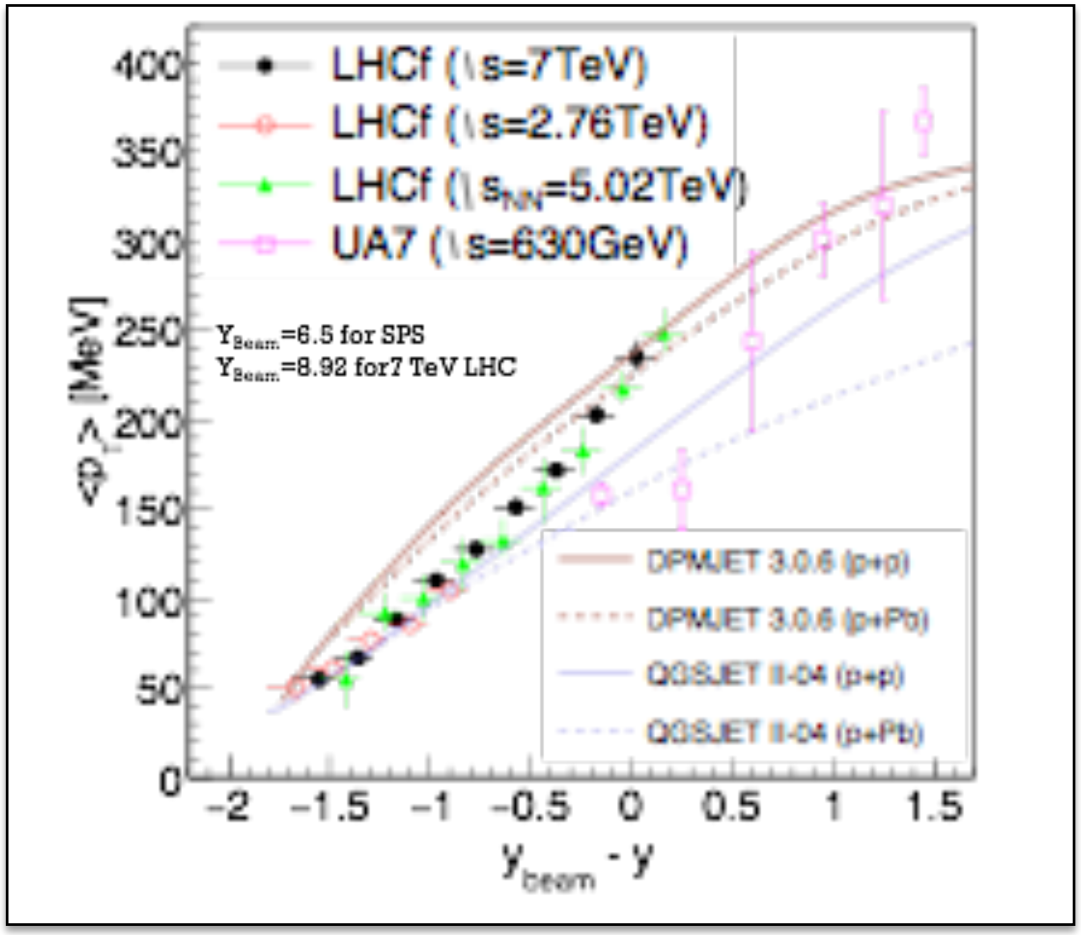

<p_T> is inferred in 3 ways:

1. Thermodynamical approach
2. Gaussian distribution fit
3. Numerical integration up to the histogram upper bound

From scaling considerations (projectile fragmentation region) we can expect that <p_T> vs rapidity loss should be independent from the c.m. energy

Reasonable scaling can be inferred from the data

Limiting fragmentation in forward π^0 production

Limiting fragmentation hypothesis: rapidity distribution of the secondary particles in the forward rapidity region (target's fragment) should be independent of the center-of-mass energy.

This hypothesis for π^0 is true at the level of ±15%

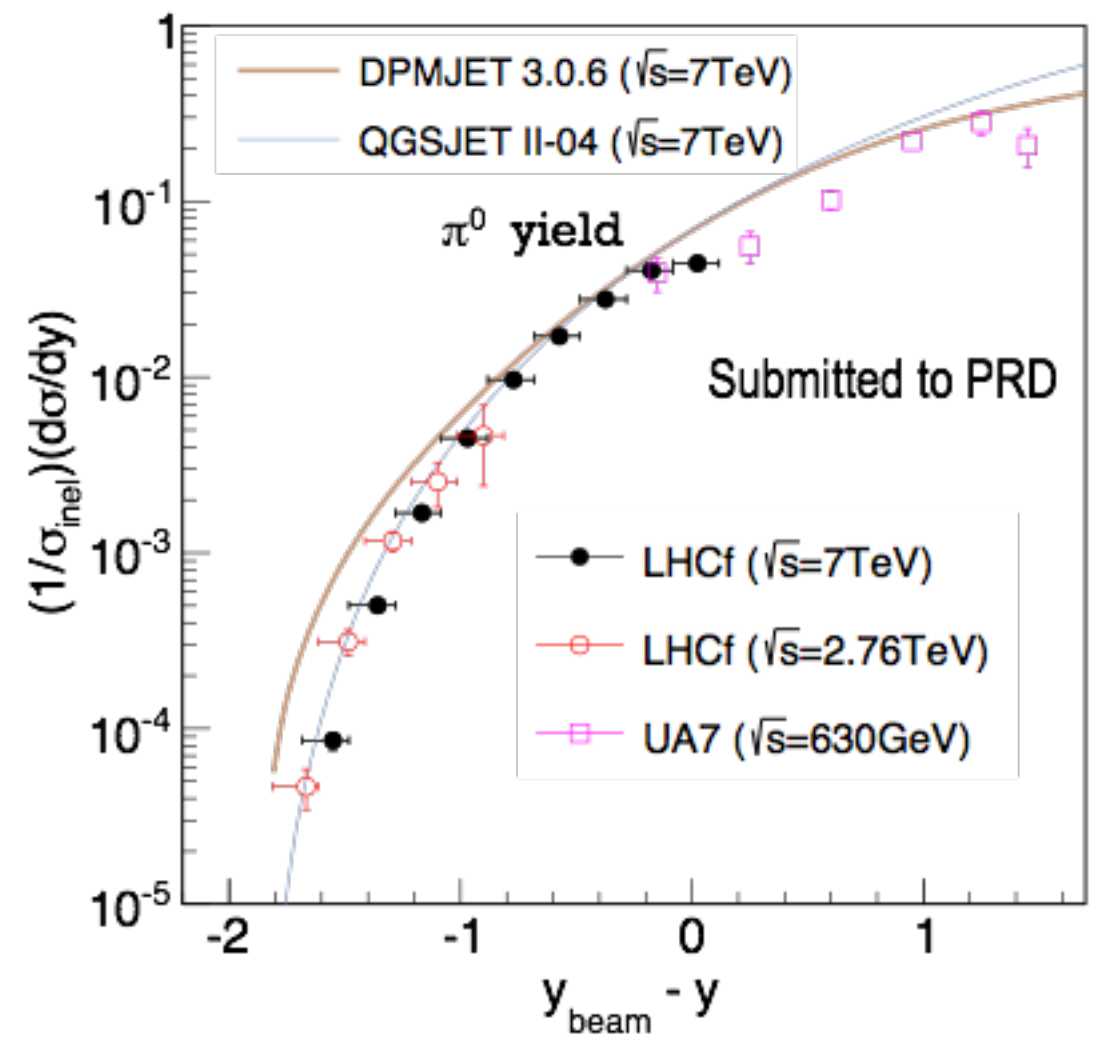

Feynman scaling in forward π^0 production

Feynman scaling hypothesis: cross sections of secondary particles as a function of $x_F \equiv 2p_z/\sqrt{s}$ are independent from the incident energy in the forward region ($x_F > 0.2$).

This hypothesis for π^0 is true at the level of ±20%

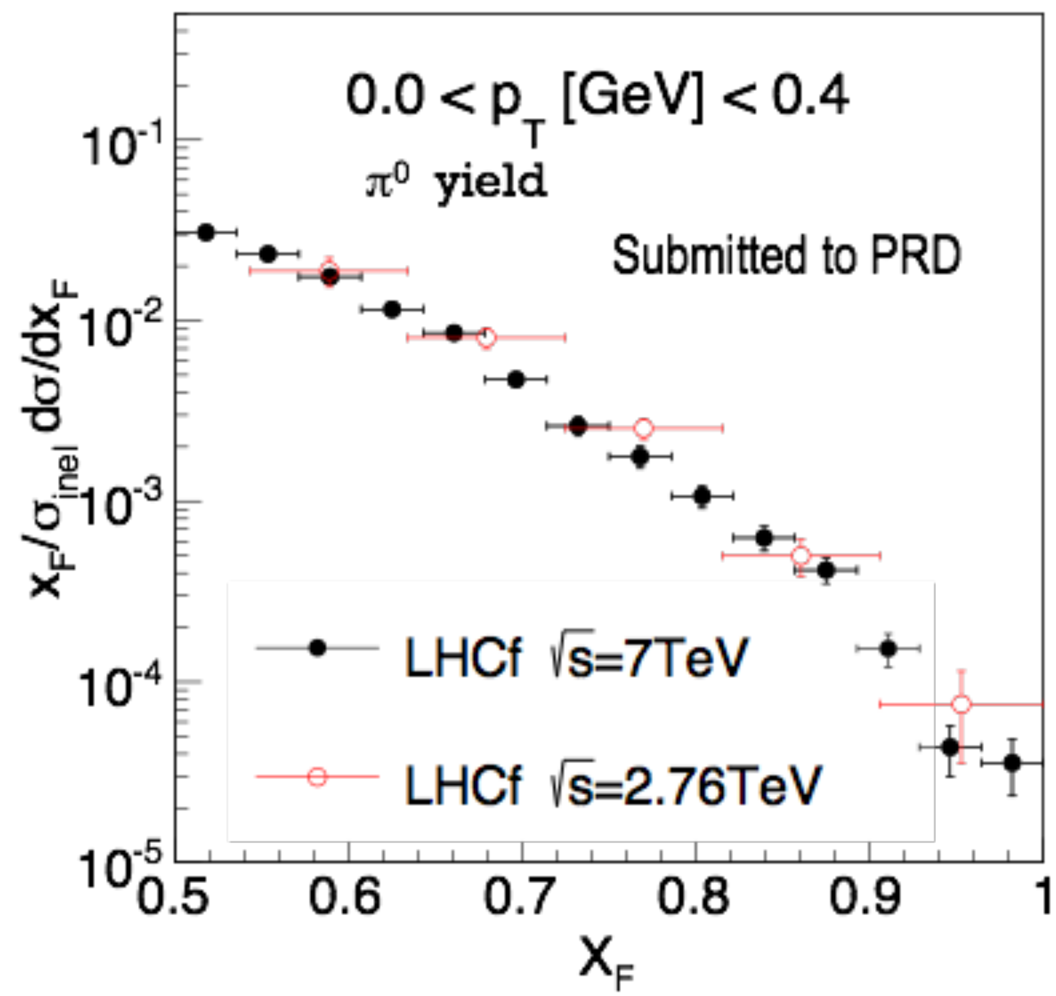

LHCf @ pp 7 TeV: neutron spectra

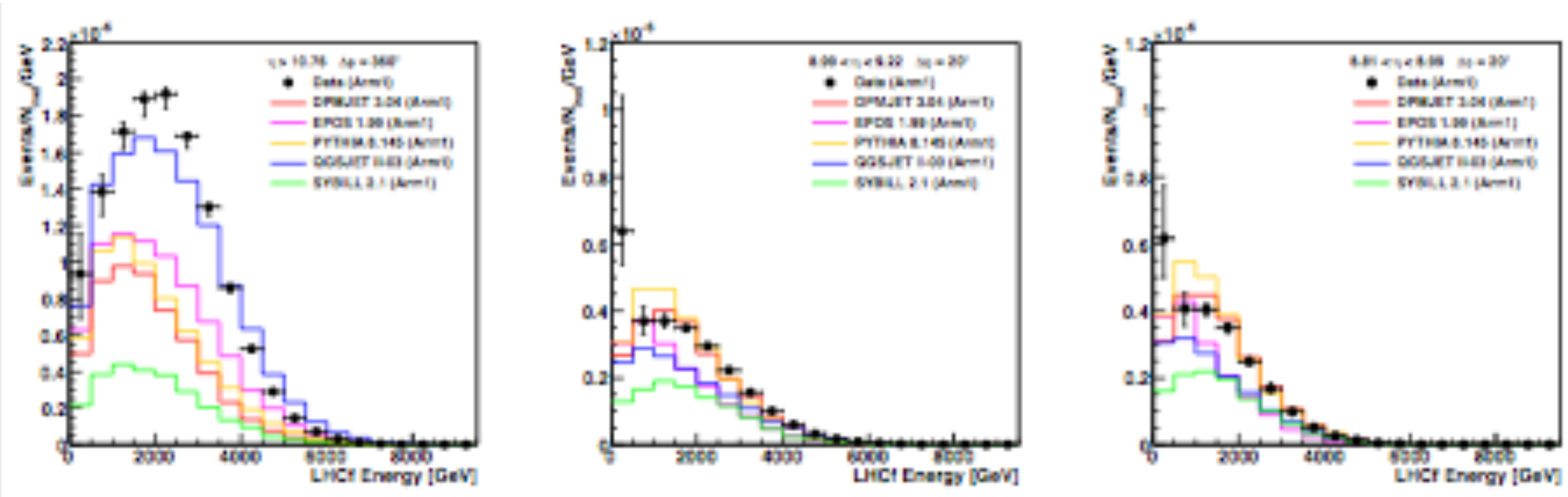

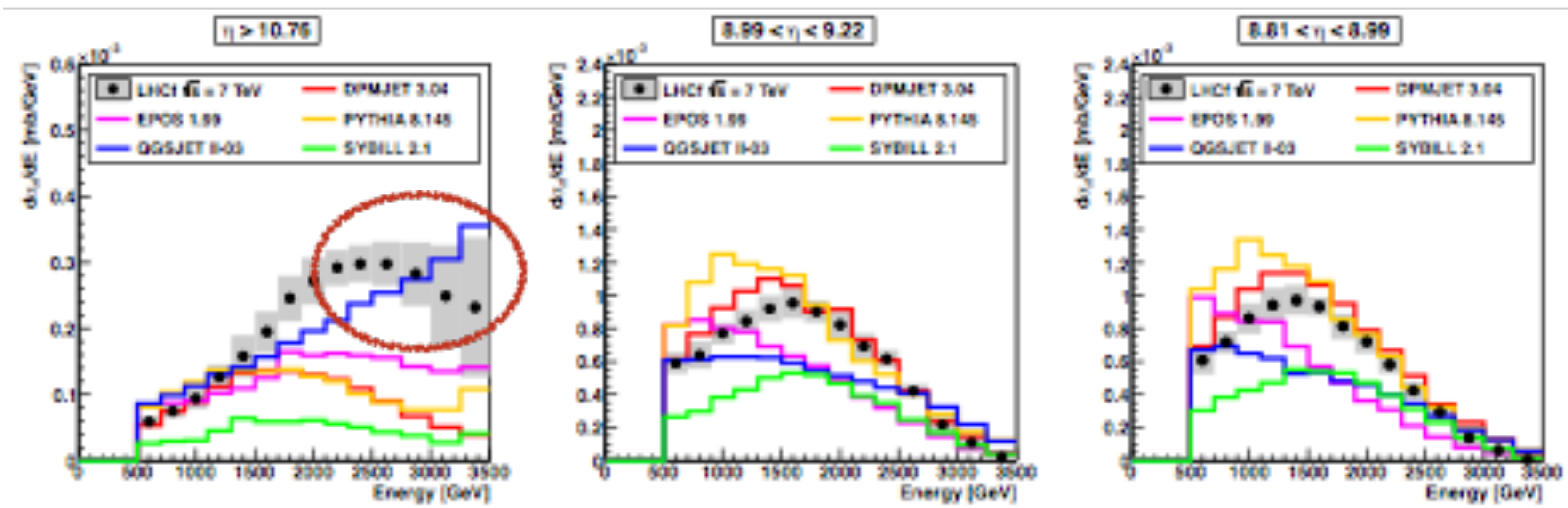

n/γ ratio

Data (η>10.76)	3.05±0.19
DPMJET3.04	1.05
EPOS 1.99	1.80
PYTHIA 8.145	1.27
QGSJET II-03	2.34
SYBILL 2.1	0.88

Data (8.99<η<9.22)	1.26±0.08
DPMJET3.04	0.76
EPOS 1.99	0.69
PYTHIA 8.145	0.82
QGSJET II-03	0.65
SYBILL 2.1	0.57

- LHCf Arm1 and Arm2 agree with each other within systematic error, in which the energy scale uncertainty dominates.
- In η>10.76 huge amount of neutron exists. Only QGSJET2 reproduces the LHCf result.
- In other rapidity regions, the LHCf results are enclosed by the variation of models.

LHCf spectra in p-Pb collisions with Atlas tagging on tracks

Nsel:
number of good charged ATLAS tracks

- $p_T > 100$ MeV
- vertex matching
- $|\eta| < 2.5$.

Significant UPC contribution in the very forward region with $N_{sel}=0$

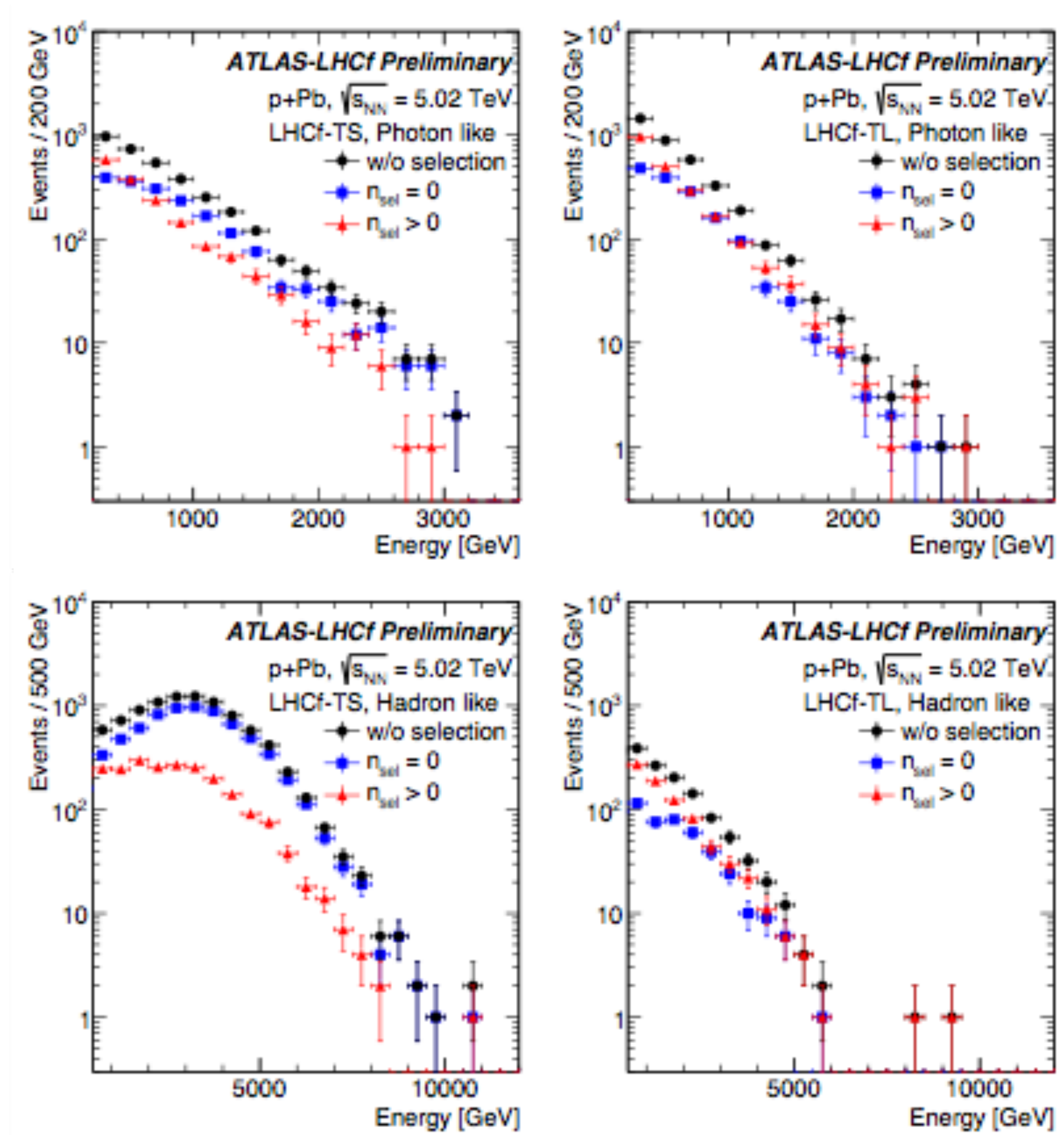

Impact of common ATLAS-LHCf trigger

PYTHIA MC study @ 14 TeV. Diffractive event selection efficiency and purity:dropping events with (PT > 100 MeV/c & Nch>1 in Iηl<2.5) @ATLAS

All events

in MC true,
Non-diffractive
Diffractive

w/ event selection (not ND)

For diff. events,
35-40% efficiency
99 % purity

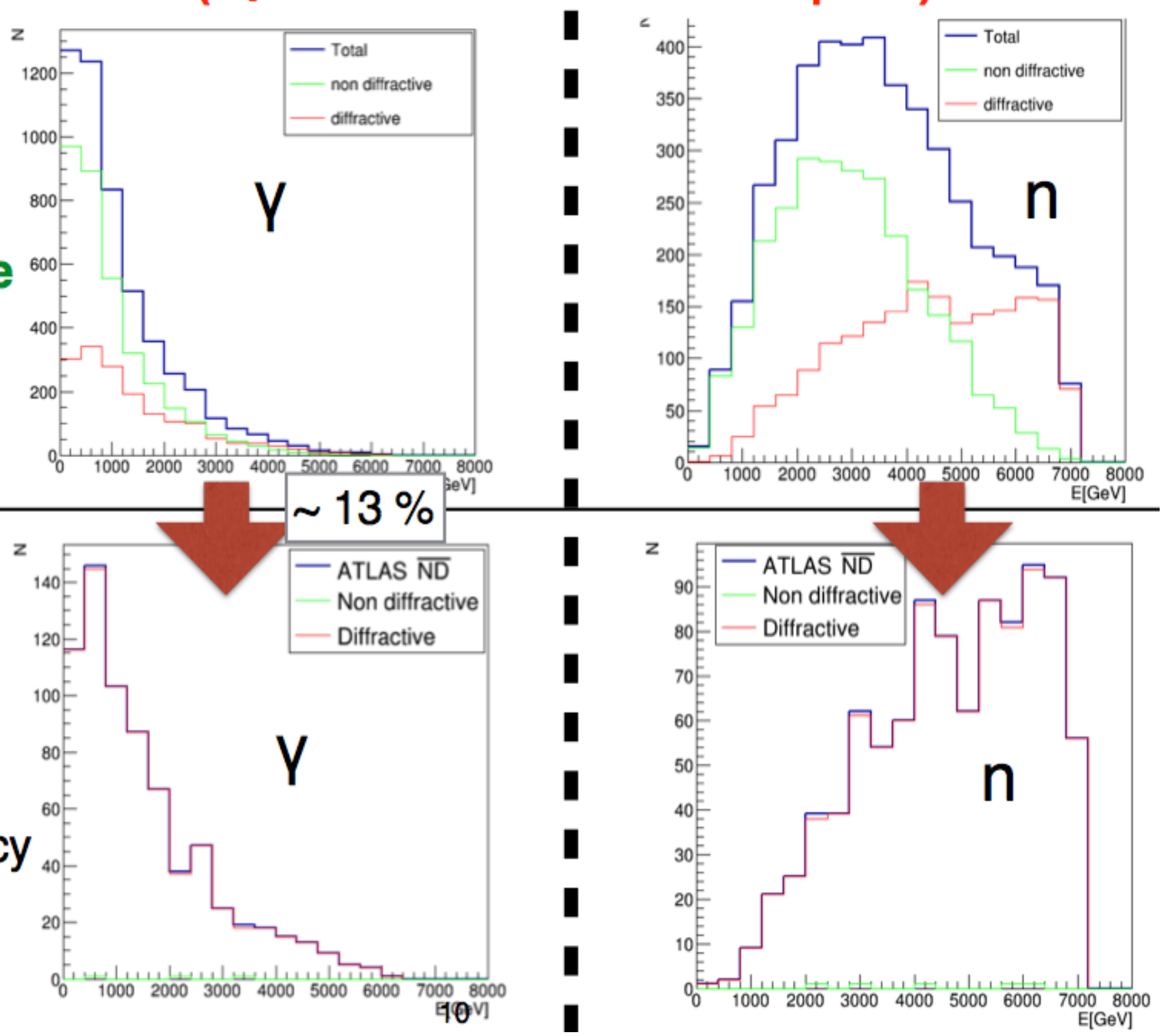

key: low mass diffraction (Ostapchenko)

Use neutron tag in LHCf to measure π+p in ATLAS

From R. Engel / T. Pierog

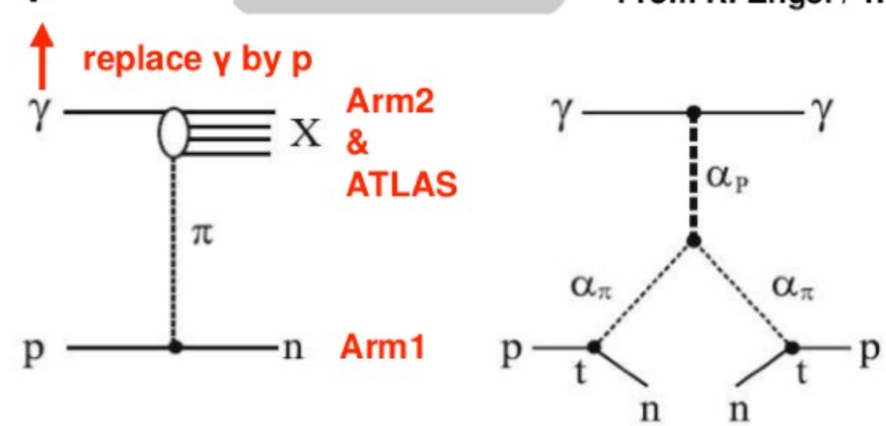

Physics discussed in detail for HERA (H1 and ZEUS) measurements
(see, for example, Khoze et al. Eur. Phys. J. C48 (2006), 797 and Refs. therein)

Diffractive vs. non diffractive at η>8.2 with √s=510GeV p+p collisions

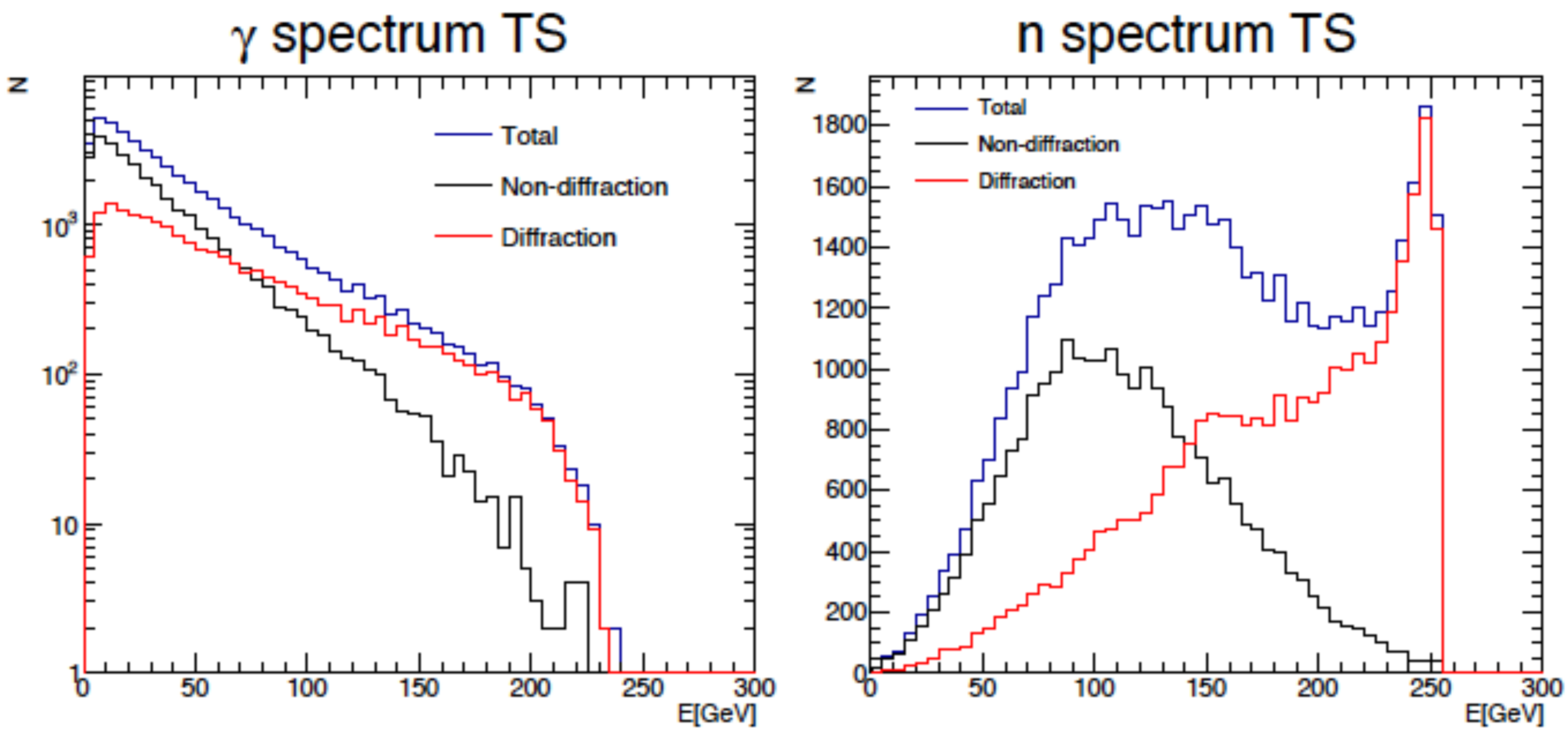

PYTHIA 8 simulation

BLUE: inclusive spectra expected by RHICf only

RED: diffractive only (“RHICf + no central track in STAR” will be similar => TBC)

BLACK: non diffractive (“RHICf + >=1 central track in STAR” => TBC)